REPORT

Improving inundation simulation by adapted roughness and bed profile implementation in a Flood Hazard Mapper

Case study: Ayeyarwady River in Myanmar

Jelmer Dijkstra s1367404
Master Thesis Water Engineering and Management
University of Twente

Date: 19 July 2019

Supervised by:
dr.ir. M.J. Booij University of Twente
dr.ir. D.C.M. Augustijn University of Twente

ir. H.G. Nomden Royal HaskoningDHV
ir. R.J.M. Huting Royal HaskoningDHV

UNIVERSITY OF TWENTE.

Royal HaskoningDHV
Enhancing Society Together

Preface

This thesis is the final result of the master program Civil Engineering and Management at the University of Twente. The research is part of the development of a Flood Hazard Mapper for river basin scale flood analysis by Royal HaskoningDHV. I am glad I got the chance to work and be supervised for this thesis at Royal HaskoningDHV.

My interests in river engineering, particularly modelling water levels and flood inundation maps, forms the basis of this thesis subject. After the course ‘River dynamics’, I recognised my interest in the morphology of a river and the importance of reliably estimating water levels in a model. I wanted to learn more about hydraulic modelling of rivers and the roughness of the riverbed and floodplain. This thesis is about gaining insight into the effects of the application of roughness of a floodplain and the importance of river profile shape in the Flood Hazard Mapper tested with local datasets from the Ayeyarwady River in Myanmar.

I would like to express my gratitude towards my thesis committee, Martijn Booij and Denie Augustijn from the University of Twente and Harm Nomden and Ric Huting from Royal HaskoningDHV, who guided me towards this final product. Their knowledge and insightful comments on river engineering, data analysis and research methods helped me to improve myself and this thesis report. Without them, I would not have been able to bring this thesis towards a successful end. Finally, I want to thank my parents, siblings, friends and girlfriend for their support during my study and this thesis.

Summary

The quick scan Flood Hazard Mapper (FHM) is developed to generate flood inundation maps for river basins based on open source Digital Elevation Models (DEMs). The Flood Hazard Mapper consists of separate modules for hydrology (generation of water available for runoff), flow routing (discharge through networks) and flood inundation mapping.

The Flood Hazard M is developed to identify flood prone areas along rivers for which limited data is available like in developing countries. The flood inundation maps can be used for spatial planning and planning flood protection measures. This research focuses on improving the Flood Hazard Mapper with application to the Ayeyarwady River in Myanmar. The Ayeyarwady is one of the most rapidly changing rivers in the world, due to fine soil materials especially present in the central part of Myanmar. The river transports enormous quantities of sediment during annual floods leading to erosion and sedimentation of the navigation channel, bars, islands and riverbanks. These constant profile changes make it difficult and expensive to measure river cross-sections. The DEMs used in the Flood Hazard Mapper are measured during low discharges, a large part of the river's cross-section is already shown on satellite images.

First the available discharge and water level data were analyzed and combined to useful data series. Two aspects of the Flood Hazard Mapper were looked at (1) the shape of the bed profile and (2) the implementation of roughness.
The cross-section of the river below the water surface at the moment the satellite images were taken from which the DEM is derived is unknown. The shape of the bed profile has a significant influence on the simulated water levels. Three profile shapes are compared to find the best fit between simulated and measured water levels. Based on the results for the Lower Ayeyarwady River, the trapezoidal profile gave the best results.
In the current version of the Flood Hazard Mapper a Manning roughness coefficient between 0.030-0.035 s $m^{-1/3}$, depending on the slope, is used for both the riverbed and floodplains of the Lower Ayeyarwady River. In the new approach a distinction is made between the Manning coefficient for the riverbed and the floodplains. Based on literature values between 0.030-0.033 s $m^{-1/3}$ were used for the river bed and between 0.045-0.058 s $m^{-1/3}$ for the floodplains which are significantly rougher than the river bed due to vegetation and obstructions.
The results show that the use of a trapezoidal shape of the river bed and a separated Manning coefficient for the river bed and floodplains, with a higher value for the floodplains, reduced the root mean square error between the measured and simulated water levels compared to the current model, suggesting that more accurate flood inundation maps are produced for the Ayeyarwady River in Myanmar.

Table of Contents

1 Introduction

In this chapter, the motivation for this research is presented in section 1.1, followed by the state of the art on flood inundation modelling in regions where data is limited in section 1.2. The research gap is described in section 1.3, the research objective and research questions are described in section 1.4. At last, the structure of the report is included in section 1.5.

1.1 Motivation

Floods are the most common natural disasters that affect people around the world. An UN report "The Human Cost of Weather Related Disasters", revealed that between 1995 and 2015 around 157,000 people have died as a result of floods. According to this report, floods accounted for 47% of all weather- related disasters between 1995 and 2015, affecting 2.3 billion people, the majority of whom (95%) live in Asia (UN Office for Disaster Risk Reduction, 2015). In Asia, urbanization and deforestation have significantly increased rainfall runoff, where recurrent flooding of agricultural land has taken a heavy toll in terms of lost food production (UN Office for Disaster Risk Reduction, 2015).

"Vulnerable farmers in Myanmar are still recovering from the major floods that swept through rural areas between July and October this year humanitarian needs remain and longer-term recovery work must be expanded to help farmers rebuild resilient livelihoods" (Food and Agriculture Organisation of the United Nations, 2015). "Experts say time will be short to replant ahead of the traditional November to December harvests paddy fields in Myanmar's main rice growing areas such as Sagaing and Ayeyarwady regions were particularly hard-hit by the floods" (Myanmar Times, 2015).

The flood in 2015 was considered an exceptional flood, but in 2016 a similar flood affected the population living along the Ayeyarwady River. The floods were brought on by heavy monsoon rains coupled with high winds and heavy rain from Cyclone Komen. The affected population by flooding in 2015 and 2016 of the Ayeyarwady River in Myanmar is shown in Table 1-1 and Figure 1-1 for 2016. People living along the Ayeyarwady River could benefit from reliable flood maps on the long term, by urban planning and flood protection for these areas.

Table 1-1 Summary of affected people in 2015 and 2016 by flooding of the Ayeyarwady River in Myanmar

State/ Region	Affected population in 2015[1]	Affected population in 2016[2]
Ayeyarwady	498,759	74,989
Bago (West)	177,315	53,357
Magway	63,694	204,365
Mandalay	18,977	107,200
Sagaing	473,365	27,996
Total:	**1,232,110**	**467,907**

[1](International Federation of Red Cross and Red Crescent Societies, 2017), [2] (Davies, 2016)

The World Resources Institute (2015) stated that Myanmar has an annual expected population affected by river floods of 0.4 million, which is mainly caused by flooding of the Ayeyarwady River. Along the river basin of the Ayeyarwady lives most of the population of Myanmar and the risk of flooding is of great importance, as the affected population of the most recent flood in 2016 shows in Figure 1-1.

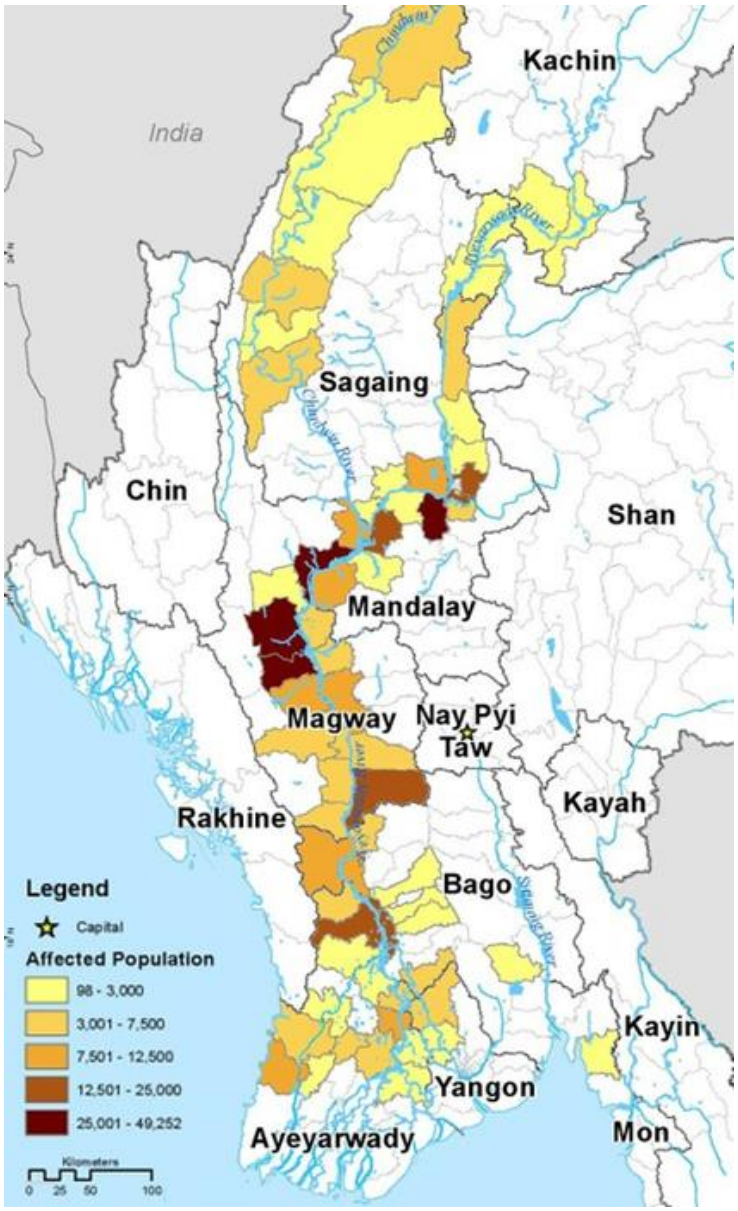

Figure 1-1 Affected population from the monsoon flooding of 2016, Myanmar (MIMU, 2016)

Flood inundation maps could help, as it is important that the government has knowledge of the areas with high risks of flooding to minimize new urban development and protect or warn people living in these areas. However, despite recent advancements in computational techniques and availability of high-resolution topographic data, flood inundation maps are still lacking in many countries (Samela et al., 2018). These flood maps are especially relevant for developing countries, since most suffer from weak coping strategies and inefficient mechanisms for disaster management. This can mainly be attributed to limited resources for flood protection, which causes that not all areas along the river can be protected against floods.

Traditional modelling approaches to generate flood maps need more input and are therefore time consuming and costly, making them unaffordable for developing countries (Samela et al., 2018). Therefore, there is a need in countries where data is limited to look for efficient and less expensive ways to generate flood maps, since flood maps are an effective tool for sustainable planning, protecting human properties, lives, and disaster risk reduction (Zin et al., 2018).

1.2 State of the art

There are different simulation models for generating flood maps, such as HEC-RAS (Hydrologic Engineering Center - River Analysis System), MIKE 21 HYDRO River and SOBEK (1D/2D) hydrodynamic modelling program (Patro et al., 2009; Sharma et al., 2018). The 2D simulation models generate directly inundation maps, while 1D models generate water levels, which need to be translated into flood maps. Flood inundation or hazard maps are an important source of information for land development planning in river basins (Verwey et al., 2017; Samela et al., 2018; Zin et al., 2018), which can show the intensity of floods and their associated exceedance probability (Baldassarre et al., 2010).

The model HEC-RAS is widely applied in many water resources studies with reliable outputs (Kim et al., 2015; Boulomytis at al., 2017). Maswood and Hossain (2016) used HEC-RAS for hydrodynamic modelling and observed that the use of Shuttle Radar Topography Mission (SRTM) elevation data to determine river bed slope and a hydrologic model for rainfall runoff transformation to model lateral flow can significantly improve simulation of river levels downstream. Zin et al. (2015) mentioned that studies in this area are significant for countries where data is limited, because of lack of climate and hydrological datasets, as well as a topographic dataset to develop flood maps.
Recent studies show that using Digital Elevation Models (DEMs) to represent topography in flood modelling is becoming common practice (Saleh et al., 2013; Luo et al., 2017; Sharma et al., 2018; Notti et al., 2018). Further, Ettritch et al., (2018) described that DEM data is beneficial to enable flood-risk modelling within regions where data is limited, because DEM data is open source and can be used to determine the slope and estimate the local drainage direction for each cell in hydraulic models (Van Huijgevoort et al., 2016). In 2018, Samela et al. mentioned that in order to advance this field of research, an automated DEM-based procedure exhibited in a GIS (Geographic Information System) environment is needed, which has high accuracy and reliability in identifying the flood-prone areas.

Flood inundation modelling is commonly performed with flood propagation models, which are often complex and expensive models or simplified and consider only one channel roughness parameter value to be calibrated (Schumann et al., 2007). Nomden (2018) developed a quick scan Flood Hazard Mapper, a 1D model that generates water levels which are then translated into flood maps. The Flood Hazard Mapper uses open source Digital Elevation Models (DEMs) for the creation of flood maps for complete river basins, the river deltas excluded. He found that existing hydrological models are either conceptual with low resolution or give highly detailed results based on detailed input data, physics and computer power. The Flood Hazard Mapper includes separate modules for hydrology (generation of water available for runoff), flow routing (discharge through networks) and water level mapping.

The goal of the Flood Hazard Mapper is to return to the basics of hydrology and estimates both discharges and associated water depths using a limited number of parameters and local and regional characteristics. For accomplishing this goal, the Flood Hazard Mapper is further developed, since all the parameters in a hydraulic model, water levels are generally considered most sensitive to roughness coefficients (George et al., 1989; Berends et al., 2018). This research focuses on improving the implementation of roughness and determining the shape of the bed profile of the river.

The current version of the quick scan Flood Hazard Mapper water level module estimates the water level at each location in the river network. In hydrodynamic computations, hydraulic roughness is one of the main sources of uncertainty (Warmink et al., 2012). Hydraulic roughness is a measure for the frictional resistance water experiences when passing over an object. The spatial distribution of roughness elements in natural rivers is generally heterogeneous. In the main channel, roughness often comes from bed material, bed forms or structural elements. Whereas, floodplains are generally more diverse, with various vegetation species, hedges, pools and other structural features (Berends et al., 2018). In the Flood Hazard Mapper, the roughness coefficient of Manning is used for the frictional resistance of the water. The Manning formula is

used extensively around the world for estimating flow velocities of rivers (Chow, 1959; Ghani et al., 2007; Luo et al., 2017). The Manning roughness coefficient in rivers reflects the resistance to water flows and is determined by many factors, such as roughness of the riverbed and floodplain, vegetation, the cross-section of the channel (Luo et al., 2017).

1.3 Research gap

The main difficulty in using a specific model for generating flood maps is primarily related to the amount of data and parameters required by these models. This is especially relevant for the river profile shapes used in these models. These river profiles often need to be adjusted manually and need many measurements to determine the profile shape of the river. This requires a high amount of input data, which is hard and expensive to obtain, especially for developing countries. Besides, the constant morphological change of some rivers makes measuring of river profile shape expensive and time-consuming. Therefore, there is a need for models with less detailed input data to generate reliable water levels. Instead primarily open source data is used, since detailed input data is not available in many countries.
Warmink et al. (2012) describes that uncertainty due to bed form roughness in the main channel and vegetation roughness in the floodplains has a major contribution to the uncertainty in water levels. As observed by Kim et al. (2010), the roughness coefficient has an extensive effect on flow simulation of a river, including computation of the water level and therefore its accurate estimation is important for prediction of the water levels especially during flooding.

The Flood Hazard Mapper needs to be further developed before it gives reliable analysis of flood inundation for a river basin. Like other simulation models, the Flood Hazard Mapper has some uncertainties, as shown in Figure 1-2. Knowledge of the type of uncertainties is crucial for a meaningful interpretation of the model outcomes and their usefulness in decision making (Warmink et al., 2012). These uncertainties need to be addressed and if possible reduced, so that the Flood Hazard Mapper can be implemented succesfully in studies for river basins.

Sources of uncertainties in hydrodynamic modelling:

- **Cross-section**: River cross-sections change over time, after each flood the river profile shape changes due to erosion and deposition of sediment. For an almost free flowing sandy river, this is especially the case, since these rivers are under constant morphological change, which makes it more difficult to understand and model.
- **Roughness:** In hydrodynamic modelling, roughness is often determined on an event-based calibration. The morphology of a river and vegetation on the floodplain change, so different roughness coefficients occur for instance in summer time compared to winter time or dry to wet season, because the height of the vegetation is the most important of roughness in the floodplain.
- **Discharge:** The uncertainty in discharge is related to the meteorological data and hydrological modelling and the quality of local data used. The discharge used influence on the water levels.
- **Digital Elevation Model:** Another important uncertainty in flood mapping is the Digital Elevation Model used. DEMs are becoming better, but the spatial resolution is still 90x90 meter for most countries and errors can occur in DEMs especially in dense vegetated and urban areas. It is one of the limitations of current free satellite data, since the high spatial resolution is indeed a key factor for flood mapping (Notti et al., 2018).

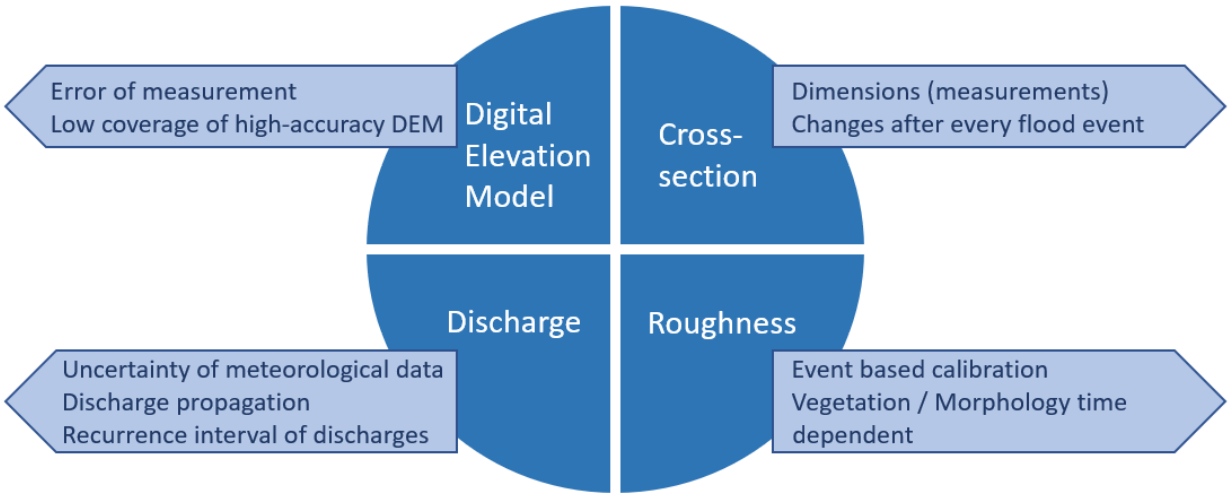

Figure 1-2 Sources of uncertainties in hydrodynamic modelling (adjusted from Disse, 2018)

A sensitivity analysis by Sharma et al. (2018) revealed that a model used for flood inundation mapping is most sensitive to Manning's roughness value compared to other input parameters, which is followed by the sensitivity to errors in the DEM. Accurate estimation of Manning's roughness coefficient is essential for the computation of the flow rate (Ghani et al., 2007), as it represents the resistance to flows in channels and floodplains. The channel roughness can vary with water depth, as the effect of riverbed resistance on river flow generally declines with increasing water depth (Luo et al., 2017). If the water depth increases, the water at the surface experiences less resistance from the riverbed. Due to the high sensitivity to roughness, the determination and understanding of roughness is important for the further development of the Flood Hazard Mapper. The riverbed and floodplain have clearly distinguishable roughness coefficients, depending on bed material, bed patterns, vegetation, season, etc. Furthermore, the shape of the bed profile in the current approach is assumed a rectangular shape under all conditions. In practice, the river profile does not have a rectangular shape and is normally a combination of a riverbed and a floodplain.

1.4 Research objective and research questions

The Flood Hazard Mapper is developed to estimate both discharges and associated water depths using several parameters and local and regional characteristics. Accurate estimation of discharges and water levels are essential for determining areas that are in danger of flooding. Hydrodynamic models are used for the prediction of water levels to support flood safety and are often applied in a deterministic way. However, the modelling of river processes involves numerous uncertainties, with main sources as roughness and determination of the river cross-section.
Eventually, the goal for the Flood Hazard Mapper is to be used for developing flood maps for various river systems, where the model is used to carry out quick scan assessments of large areas in the field of flood risks. The flood inundation maps can be used for spatial planning and planning flood protection measures.

The objective of this research is to improve the Flood Hazard Mapper water level output. this research focusses on determining the wetted cross-section, separate implementation of roughness for the riverbed and floodplain in the Flood Hazard Mapper. This is done by comparing outcomes to analysed datasets with observed water levels and implementing different roughness coefficients for the riverbed and floodplain on the Ayeyarwady River, as well as determining the shape of the bed profile. Thus, the Flood Hazard Mapper will be further developed by reducing the uncertainties in modelling roughness and in determining the shape

of the bed profile. The Flood Hazard Mapper is tested on the Ayeyarwady River in Myanmar, by comparing model outcomes to measured water levels with using representative discharges.

The research questions provide the themes and direction of this study.

Main question: Can the Flood Hazard Mapper, for basin scale river flood risk analysis, be improved by implementing roughness for the riverbed and floodplain and/or by determined bed profile shape for the Ayeyarwady River in Myanmar?

The following sub-questions will help to find an answer to the main question:

1. Based on local datasets on water levels and derived discharges, which representative discharges through the river system of the Ayeyarwady River can be used?

2. What is the influence of the profile shape of the unknown bed profile of the river cross-section?

3. Which representative Manning's roughness coefficients for the riverbed and floodplain should be used for the Lower Ayeyarwady River?

4. What is the effect of different roughness coefficients for the riverbed and floodplain on generated water levels and flood inundation maps by the Flood Hazard Mapper?

1.5 Outline thesis

The outline of this thesis follows the research questions as described in the previous section. In chapter 2, the study area, data and the current Flood Hazard Mapper are described. The methods to answer the research questions are shown in chapter 3. In chapter 4, the data analysis to determine representative discharges are presented. In chapter 5, the results of the shape of the unknown bed profile and the different roughness coefficients for the riverbed and floodplain are described. Chapter 6 discusses the methods and results of this research. At last, the conclusion and recommendations for further research are given in chapter 7.

2 Study area, data and model

In this chapter, the study area, the obtained data from gauging stations in Myanmar and the current state of the Flood Hazard Mapper are described.

2.1 Study area

Myanmar is a country that has been closed off for the world by the militarily regime from 1962 till 2010. The river management of the Ayeyarwady River kept mainly unchanged in those years. In recent years the Ayeyarwady River experiences increasing pressure of human development, similar to many other rivers in Asia (Furuichi et al., 2009). Myanmar's population is currently listed at 52 million of which 77% live in the rural areas (Aung et al., 2017). When it comes to river flooding, Myanmar is the 8th country with the largest population exposed to river floods in the world, which is mainly due to flooding of the Ayeyarwady River (Luo et al., 2015). Myanmar is about 676,600 square kilometres and the drainage basin of the Ayeyarwady in Myanmar is about 404,200 square kilometres, which means that around 60% of Myanmar is covered by the drainage basin of the Ayeyarwady River. For over 1200 years the river forms an important lifeline for the country, many cities including former capital Mandalay are located near the river. Like many of the large rivers in Asia, the Ayeyarwady River arises from the Tibetan plateau in the Himalayan mountain range.

Myanmar has a tropical climate, which is characterized by strong monsoonal influences. The country has a considerable amount of sun hours, a high rate of rainfall and high humidity. The seasonal rainfall is concentrated in the hot humid months of the southwest monsoon from May till October (AQUASTAT, 2011). The northwest monsoon from December till March is relatively cool and almost entirely dry. The monthly distribution of river flows closely follows the pattern of rainfall, which means that about 80% flows during the wet monsoon season (May-October) and 20% in the dry season (November-April).

The Ayeyarwady River is the largest river in Myanmar with a length of 2170 km and has been described as the heart of the nation. Other main rivers in Myanmar are the Chindwin, Sittaung and Thanlwin. The Ayeyarwady River flows from north to south through Myanmar, with the Chindwin River as largest tributary. The Ayeyarwady is the country's largest river and most important commercial waterway, which flows through a large part of the country before running through the Ayeyarwady Delta into the Andaman Sea (Chavoshian et al., 2007). The main river is navigable for 1,280 km from the Andaman Sea, opening a vast highway deep into the interior of the basin (ICEM, 2018).

The Ayeyarwady is one of the most rapidly changing rivers in the world, with its river profile changing after every flood event. The river transports enormous quantities of sediment during annual floods leading to erosion and sedimentation of the navigation channel, bars, islands and riverbanks (ICEM, 2018). The discharge of the Ayeyarwady River in the wet monsoon season can be larger than ten times the discharge during the dry season, which causes large differences in water levels. These seasonal variations in discharge and water level alter the river morphology of the Ayeyarwady during a single season.

The annual rainfall in Myanmar, comes mainly from the southwest monsoon from May to October and is shown in Figure 2-1. The central part of Myanmar, also called the dry zone, experiences less rainfall than the rest of the country. At this dry zone in Myanmar mainly fine sand is present, erosion and deposition of sediment creates sandbars, which causes the cross-section of the Ayeyarwady River to change rapidly through time. The drainage network of the Ayeyarwady River displayed in Figure 2-1 also includes the gauging stations.

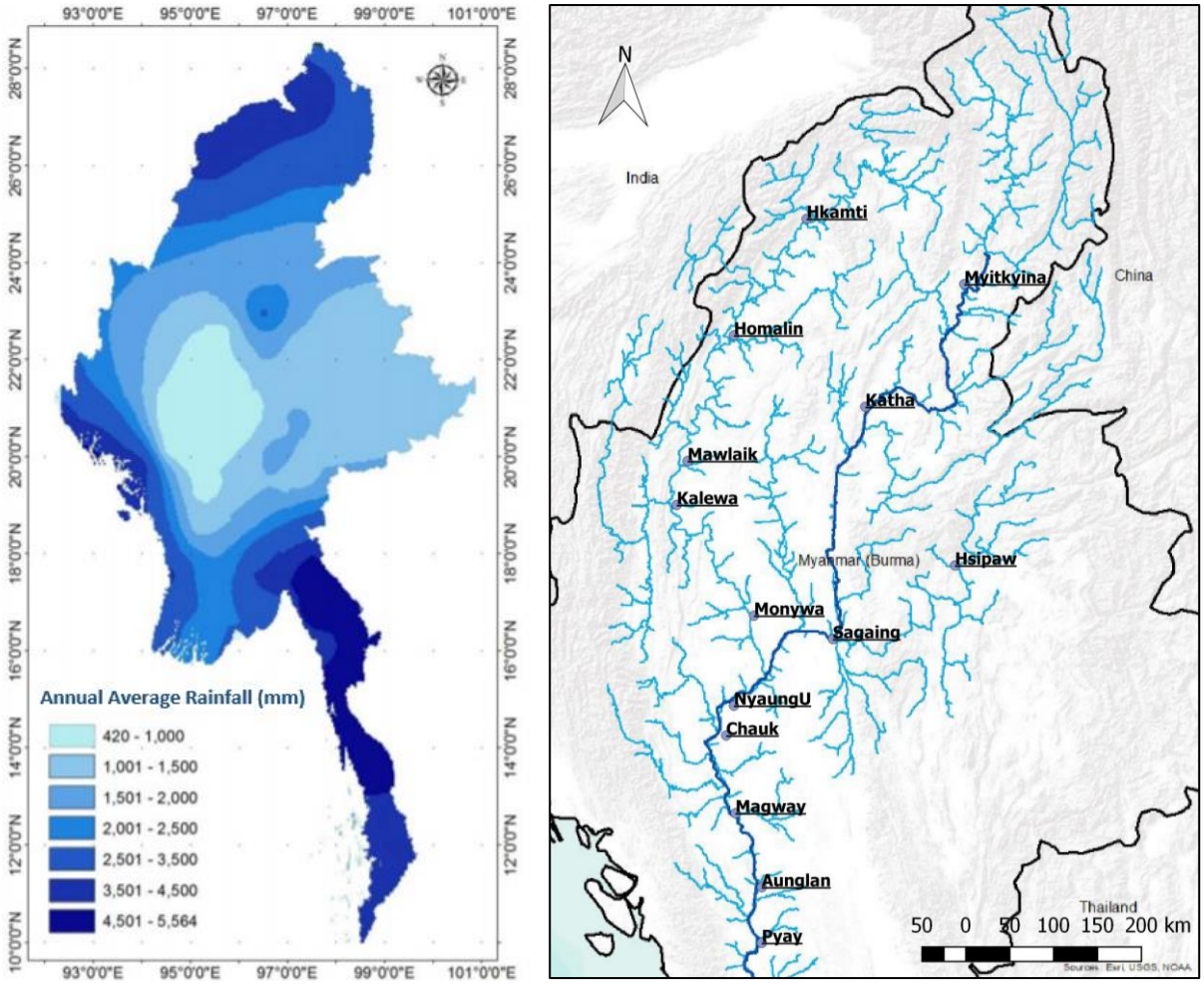

Figure 2-1 Annual average rainfall from 1966-2014 in Myanmar (left) (Than, 2012). Drainage network of the Ayeyarwady River (dark blue) and the Chindwin tributary including gauging stations (right)

The study area is the Ayeyarwady River modelled from the upstream part at the Tibetan plateau until the downstream located city Pyay. The river discharge changes are extreme per seasons, where the Ayeyarwady upstream at Myitkyina station in the dry season has an average discharge of 1700 m³/s and in the wet season 8500 m³/s. Downstream at the Pyay station the average discharge 2600 m³/s in the dry season and in the wet season 26000 m³/s.

2.2 Data

For this research, the available water level and discharge records are used to derive the relation between discharge and stage (Q-H relations) and understanding the river system. The water level and discharge records that are used in this research are derived from two local datasets. The first dataset was obtained from the Directorate of Water Resources and Improvement of River Systems (DWIR) in Myanmar with water level records from 1966 to 1986 and discharge series from 1966 to 2010. The second dataset was obtained from the Irrigation and Water Utilization Management Department (IWUMD) in Myanmar with water level records from 1980 to 2017 and discharge series from 1980 to 2014. All water level and discharge records have been obtained locally, where some data records from DWIR have even been recovered from floppy disks (A. Commandeur, local expert RHDHV).

A schematisation of the gauging stations along the Ayeyarwady River upstream from station Pyay is displayed in Figure 2-2. Upstream of station NyaungU, the Chindwin River flows into the Ayeyarwady River. The Ayeyarwady River is therefore divided into three sub-basins: Upper Ayeyarwady, Lower Ayeyarwady and Chindwin.

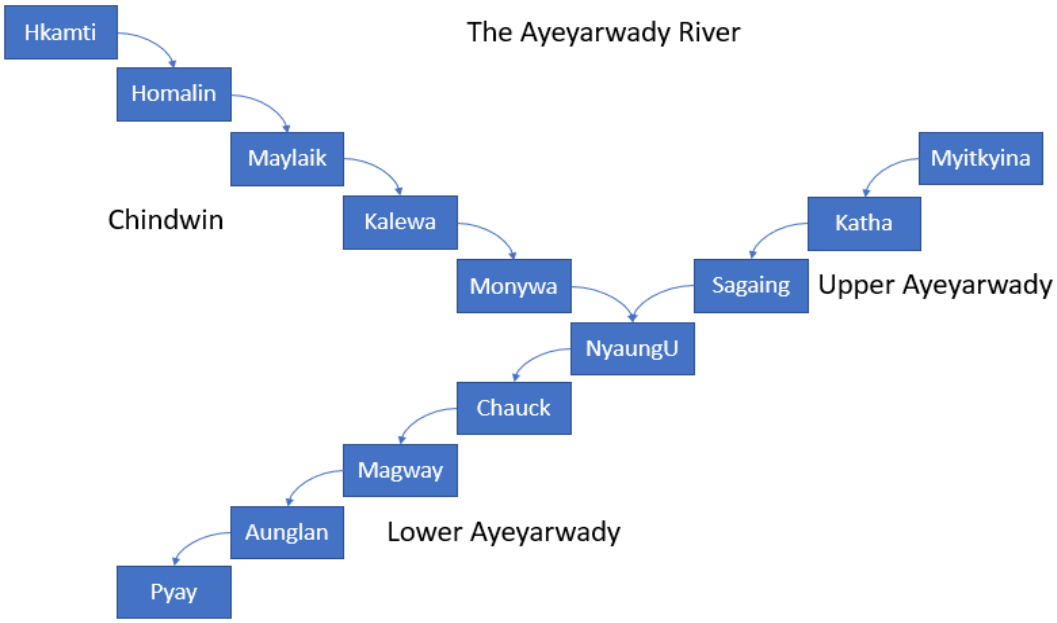

Figure 2-2 Schematisation of the gauging stations along the Ayeyarwady River and the tributary the Chindwin River

The manual gauges are located near villages and towns, where water levels are read daily at 12:30. A disadvantage of manually read gauges and equipment is that it does not give continuous records of the water levels. Furthermore, the data is as good as the reliability of the reader and in addition demands manual input to be saved on a computer. At first, for some gauging stations measurements are missing or incomplete, but since the datasets are from different recording periods and have overlapping record periods the record can be improved. The total available record periods of the combined datasets (DWIR and IWUMD) are shown in Table 2-1. Secondly, water level records are based on local measured water levels, not with respect to Mean Sea Level (MSL). Because of these factors, some errors occur in the water level measurements and discharge series, since discharge series are almost exclusively determined by measuring the water level and converting it into discharge by means of an estimated stage–discharge relationship (Petersen-Øverleir, 2006). Although the datasets from DWIR and IWUMD contain some uncertainties the water level records and discharge series are still valuable and show interesting findings on the behaviour of the Ayeyarwady throughout the recorded history.

Discharge data is available for the gauging stations, but water level records upstream of Monywa station on the Chindwin River are missing. The discharge series are almost exclusively obtained by daily measurement of the stage and subsequently converting it into discharge by the stage–discharge relationships.

Table 2-1 Dataset at hydrological stations from DWIR and IWUMD from upstream the Ayeyarwady and Chindwin until station Pyay

River	Station	Danger Level (m)	Discharge		Water level		Lat	Long
			From	To	From	To	Location as in Discharge data	
Ayeyarwady	Myitkyina	12.00	1999	2014	1966	2017	22'00'	97'21'
	Katha	10.40	1966	2014	1966	2017	24'10'	96'20'
	Sagaing	11.50	1966	2014	1966	2017	21'86'	95'98'
	NyaungU	21.20	1991	2014	1966	2017	21'12'	94'91'
	Chauk	14.50	1973	2014	1976	2017	20'54'	94'50'
	Magway	17.00	1994	2014	1994	2017	20'08'	94'55'
	Aunglan	25.50	1987	2014	1976	2017	19'22'	95'13'
	Pyay	29.00	1966	2014	1980	2017	18'48'	95'13'
Chindwin	Hkamti	13.60	1968	2010			26'00'	95'04'
	Homalin	29.00	1968	2010			24'52'	94'54'
	Mawlaik	12.30	1972	2010			23'38'	94'25'
	Kalewa	15.50	1967	2010			23'12'	94'18'
	Monywa	10.00	1966	2014	1966	2017	22'06'	95'08'

The drainage area upstream of gauging stations is displayed in Table 2-2, for both the area given by the local datasets of the DWIR and the Flood Hazard Mapper. The differences between the drainage area found in the datasets of the DWIR and the drainage area from the DEM in the Flood Hazard Mapper (HAND method) are small, where most differences stay within the 5% range. Only the first gauging station shows a significant difference, which could be explained by the difficulty to determine the drainage area around the origin of the Ayeyarwady River at the border with China in the Himalayas.

Table 2-2 Drainage area upstream of a measurement station along the Ayeyarwady and Chindwin river

STATION	DRAINAGE AREA (KM^2)		
	Field (DWIR)	Model (HAND)	Sub drainage area
UPPER AYEYARWADY RIVER			
MYITKYINA	41,803	48,108	48,108
KATHA	77,942	84,292	36,184
SAGAING	120,193	124,912	40,620
END UPPER AYEYARWADY	-	195,717	70,805
CHINDWIN RIVER			
HKAMTI	27,420	27,408	27,408
HOMALIN	43,124	43,269	15,681
MAWLAIK	69,339	69,860	26,591
KALEWA	72,848	73,299	3,439
MONYWA	110,350	103,028	29,729
END CHINDWIN	-	110,810	7,728
LOWER AYEYARWADY RIVER			
NYAUNGU	309,248	306,527	4,453
CHAUK	323,630	315,082	8,555
MAGWAY	335,567	332,532	17,450
AUNGLAN	340,390	342,616	10,084
PYAY	346,225	352,287	9,671

2.3 Model description

The separate modules used in the Flood Hazard Mapper by Nomden (2018) are described, followed by the overall general methods and programs used. In section 2.3.2 the approach for determining the roughness and the bed profile shape as implemented currently in the Flood Hazard Mapper is explained.

2.3.1 The Flood Hazard Mapper

The Flood Hazard Mapper includes separate modules for hydrology (generation of water available for runoff), flow routing (discharge through networks) and water level mapping. The Flood Hazard Mapper uses the following modules:

Hydrological module: The Flood Hazard Mapper uses a spatially distributed rainfall-runoff model named Wflow to calculate water volumes available for runoff. Wflow is an open source distributed hydrological modelling platform developed by Deltares, with the use of a set of Python scripts that run and perform hydrological simulations (Schellekens, 2018). The rainfall-runoff model Wflow also considers the shape of upstream catchments, where the instantaneous unit hydrograph is applied. This unit hydrograph can be used as a transfer function for modelling the transformation of rainfall into surface runoff (Rai et al., 2009). Furthermore, Wflow is based on raster data with a grid size of 2x2 km and uses daily rainfall data with a grid size of 27x27 km based on the European Centre for Medium-Range Weather Forecasts (ECMWF) metrological datasets as model input.

Discharge module: Instantaneous discharges at every possible location within the network are based on flow routing by PCRaster. PCRaster is a modelling language developed to free the modeller from problems with data input and output by providing a large range of basic primitive operators at the level of understanding of the researcher (Utrecht University, 2018). The instantaneous unit hydrograph is used to calculate available runoff upstream of each location in the network. The water depth calculation is based on discharge and local upstream characteristics.

Water level module: Estimation of water level and flood extent mapping is based on instantaneous discharge and local parameters such as: slope, representative profile, roughness and Height Above Nearest Drainage (HAND). Furthermore, the module uses Digital Elevation Models (DEMs) to represent topography, which at present is commonly used in modelling (Nobre et al., 2011; Luo et al., 2017; Sharma et al., 2018). However, in remote regions where data is limited, high resolution DEMs are often not available or are costly to obtain (Sichangi et al., 2016). The DEM data allows the Flood Hazard Mapper to calculate and predict water levels and river discharges.

The Flood Hazard Mapper uses Multi-Error-Removed Improved-Terrain (MERIT) DEM as input for topographic data obtained from the Shuttle Radar Topography Mission (SRTM) in February 2000. For the case study in Myanmar this is in the middle of the dry season, where much of the river profile can be observed. The MERIT DEM was developed by removing multiple error components (absolute bias, stripe noise, speckle noise, and tree height bias) from the existing space borne DEMs (Yamazaki et al., 2017). It represents the terrain elevations at a 3 second resolution, which corresponds to 90 x 90 meter at the equator and covers land areas between 90N-60S, referenced to EGM96 geoid. High-accuracy coverage of DEM data (e.g., with elevation errors less than 1 m) is limited, hydrologic modelling at regional or larger scales uses DEM data obtained by space borne sensors, which are of lower accuracy coverage.

DEM data has been widely used for hydrologic modelling (Luo et al., 2017). The SRTM uses the observation data from two viewpoints (satellites) to generate three-dimensional images to generate elevation maps. Unfortunately, the DEM does not always filter for houses standing in elevated areas, where the roof height

can be taken as mistake instead of the ground elevation (Yamazaki et al., 2017), which can cause some uncertainty in urban areas. Sharma et al., (2018) describes that topographic data plays a major role in determining the accuracy of hydraulic modelling and flood inundation mapping. DEM data is used to determine the cross-sectional shape and slope between cells and estimate the local drainage direction for each cell (Van Huijgevoort et al., 2016).
The Flood Hazard Mapper uses a quantitative topographic algorithm, called HAND (Height Above Nearest Drainage), based on DEM data (Daleles et al., 2008). For a DEM represented by a grid, the simplest and most widely used method for determining flow directions is designated D8, which uses eight flow directions. In this method, the flow from each grid point is assigned to one of its eight neighbours, towards the steepest downward slope as shown in Figure 2-3. The result is a grid called LDD (Local Drain Directions), whose values clearly represent the link to the downhill neighbour (Daleles et al., 2008; Nobre et al., 2011). Spatial variation in elevations results in gradients of potential energy, which is the main physical driver of water flow on and through rough terrain (Nobre et al., 2011).

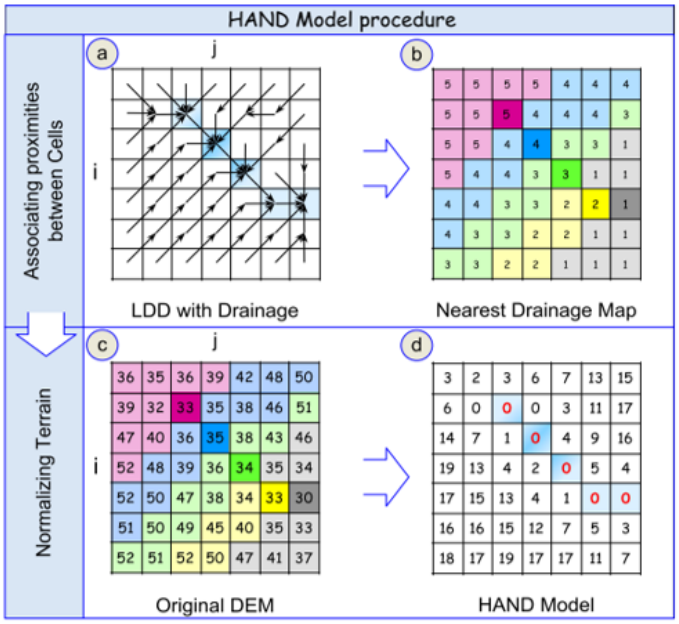

Figure 2-3 Procedure to generate a HAND model: (a) the coherent local drain direction grid (LDD) with the drainage network is used in the generation of (b) the stream order is determined, then (c) the original DEM is processed using the HAND operator and the nearest drainage map, which results in (d) the HAND model, where each number represents the difference in level to its respective nearest drainage cell (Nobre et al., 2011).

The Flood Hazard Mapper is a conceptual model calculating inundated areas based on HAND as described by Nobre et al. (2011). The drainage areas are characterized in terms of the hierarchy of stream ordering, where the order of the basin is the order of its highest stream order. The first order is defined as the streams that receive water entirely from overland surface flow and do not have any tributaries. The junction of two first order streams forms the second order stream, the two second order streams join together forms the third order streams, and so on. This scheme of stream ordering is referred to as the Strahler ordering scheme (Strahler, 1957; Rai et al., 2009).
Finally, the Wflow 1D model and the Flood Hazard Mapper are run by Python scripts and the results are loaded into an open source geographic information system (QGIS) that supports viewing, editing and analysis of geospatial data to generate flood inundation maps. In the following section the current approach to determine roughness and bed profile in the Flood Hazard Mapper are described.

2.3.2 Current approach to determine roughness and bed profile

The current version of the Flood Hazard Mapper water level module estimates the water depth at each location in the river network based on the Manning formula. To apply the Manning formula, first the dimensions of the representative cross-sections were roughly estimated. Currently, the representative width of the cross-sections has been estimated by:

$$W = [\ \alpha * (\ \alpha + 2\ )^{2/3}\ ]^{3/8} * Q^{3/8} * S^{-3/16} * n^{3/8} \quad (1)$$

With river width *W* (m), width-to-depth ratio *α*, discharge *Q* (m^3/s) provided by the discharge module, local slope *S* and roughness *n* (Manning). Calculated river width is translated into water depth using the width-to-depth ratio α. Values for the roughness coefficient *n* ($s\ m^{-1/3}$) and width-to-depth ratio α have been estimated based on the local characteristics (slope) according to Table 2-3.

Table 2-3 Relation between slope and bed material with corresponding width-to-depth ratio and roughness used within the first version of the Flood Hazard Mapper.

Slope (m/m)	Bed material	α	Manning's coefficient n ($s\ m^{-1/3}$)
0.0001	Gravel	59	0.030
0.001	Cobble	21	0.035
0.01	Boulder	9	0.040
0.1	Bedrock	5	0.050

In Table 2-3, the width-to-depth ratio depends primarily on the bed material, according to the research of Finnegan (2005, see Figure 2-4), which relates low values of α (narrow rivers) to rough bed material like bed rock (α=5) or boulder (α=9) and higher values to cobbles (α=21) or gravel (α=59). This relation is also roughly used within the Wflow model. Further, rougher bed material is expected to be found more in the upstream/mountain areas with steeper slopes, while finer material can be found more in the downstream river reaches with shallower slopes. In the Flood Hazard Mapper, it is stated that these relations should be more or less valid in general.

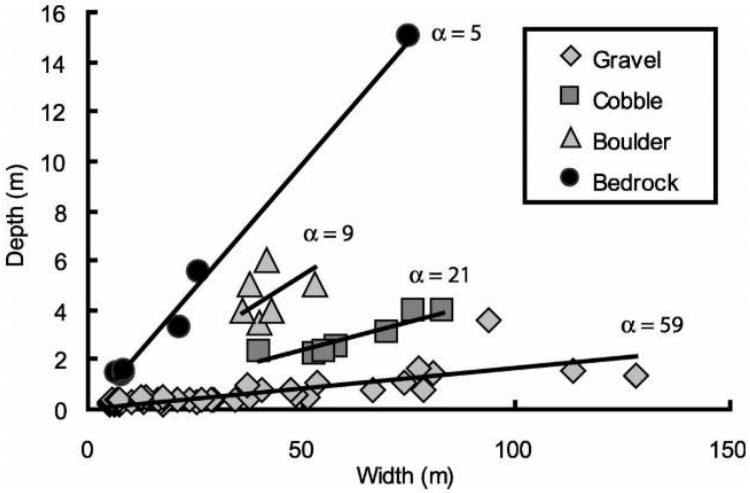

Figure 2-4 Width-to-depth ratio α for different dominant channel substrates (Finnegan et al., 2005). Gravel data are from Yellowstone River, Wyoming (Leopold and Mattock, 1953), and largest bedrock width data points is from LiWu River, Taiwan (Hartshorn et al., 2002). Other data are from field surveys in Cascades of Washington State. While gathered from various locations, all bedrock data are from channels incised in high-grade metamorphic or granitic rocks.

Based on the local slope, the roughness value and the width-to-depth ratio of the rectangular bed profile shape can be found through interpolation between Manning n-values of 0.030 s $m^{-1/3}$ (downstream) till 0.050 s $m^{-1/3}$ (upstream) depending on the slope. This results in the estimated river dimensions and subsequently into the local water depth. The estimated water depth at each river cell is projected on the DEM and all adjacent cells with a lower HAND-value. A small correction has been made to the calculated water depth to consider the water depth at the date of measuring the DEM (water surface area is mapped within the DEM).

Main disadvantages of this approach as described in the research gap are:

- Profile shape: The Flood Hazard Mapper assumes under all conditions a rectangular shape with a specific width-to-depth ratio. In practice, the river profile does not have a rectangular shape and is normally a combination of a riverbed and a floodplain.
- Roughness: riverbed and floodplain have clearly distinguishable roughness coefficients, depending on bed material, bed patterns, vegetation, season, etc.

3 Method

In this chapter, the research method is explained and what data is used to answer the research questions. First the research method is discussed, then the approach to determine representative discharges from the data analysis is explained. Further, the new approach to determine inundation levels, including the method for comparing the simulated and observed water levels is discussed. At last, the approach to generate flood inundation maps is shown.

3.1 Overview

For the prediction of water levels in the Flood Hazard Mapper (FHM) an accurate estimation of roughness is important, especially during flood events. The simulated water levels from the current approach and the new approach will be compared to observed water levels for representative discharge values derived from duration curves. Before the roughness of the riverbed and floodplain is determined, first the best fitting shape of the bed profile is determined.
The flow diagram in Figure 3-1 shows the research question used to compare the simulated and observed water levels along the Ayeyarwady River for representative discharges. The water level output of the Flood Hazard Mapper depends on both the roughness of the riverbed and floodplain, as well as the cross-sectional shape of the river. To be able to understand the influence of the implementation of roughness, the effect on water levels at gauging stations is tested for the Lower Ayeyarwady River.

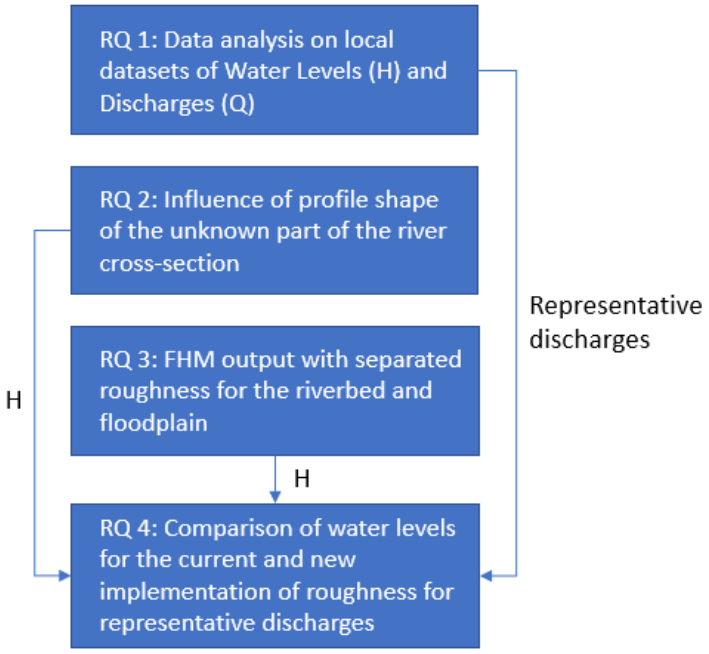

Figure 3-1 Flow diagram of the research questions (RQ): Comparison of water levels (H) with representative discharges for the current and new approach for roughness and bed profile in the Flood Hazard Mapper (FHM) at gauging stations along the Ayeyarwady River

3.2 Approach to determine representative discharges

For the first research question, the available water level and discharge records are used to derive the Q-H relations and duration curves to better understand the river system of the Ayeyarwady River and determine representative discharges. Before the Q-H relations are derived from the data, first the quality and availability of the data records is considered. The quality of records is improved with use of overlapping data records from DWIR and IWUMD. Discharge records for gauging stations are generally computed by applying a Q-H relation for the site to a continuous or periodic record of water levels. Furthermore, duration curves are used to generate representative discharges used to simulate water levels. The simulated water levels of the different methods for roughness and bed profile are compared with observed water levels to eventually improve the output of the Flood Hazard Mapper.

3.2.1 Derivation of the Q-H relations

A Q-H relation or rating curve is established by making a number of concurrent observations of water level and discharge over a period of time covering the expected range of water levels at a river gauging station (Marg & Khas, 1999). The data is plotted versus the concurrent stage to define the rating curve for that gauging station, where most ratings relate discharge to stage (derived Q-H relation) only and are called simple rating curves (Braca, 2014). To determine the derived Q-H relation for each of the gauging stations, the recorded water levels are plotted against the discharge from the local datasets. The range of the Q-H relation is of importance to be applicable for extreme flow conditions. Discharge measurements are usually missing in the upper and lower end of the rating curve (Braca, 2014). However, most of the factors that affect the quality of a discharge record are either determined by natural conditions or costly to improve (Kennedy, 1984).
In alluvial sand-bed rivers as the Ayeyarwady River, the stage-discharge relation usually changes with time, either gradually or abruptly, because of moving sand dunes and bars and due to scour and silting in the channel (Marg & Khas, 1999). The extent and frequency with which a bed profile changes depends on the material size and the flow velocities (Marg & Khas, 1999). For sand-bed rivers the stage-discharge relationship varies not only because of the changing cross-section due to erosion and deposition, but also because of changing roughness due to different bed forms (Marg & Khas, 1999). The two types of algebraic equations commonly used for deriving rating curves are:

1. Power type equation which is most commonly used:

$$Q = c\,(H + a)^b \quad (1)$$

2. Parabolic type of equation

$$Q = c_2(H + a)^2 + c_1(H + a) + c_0 \quad (2)$$

where: Q = discharge (m^3/sec)
H = measured water level (m)
a = water level (m) corresponding to Q = 0
c = coefficients derived for the relationship corresponding to the station characteristics

For gauging stations located in a reach where the slope is very flat, the Q-H relation can be affected by hysteresis, which is the superimposed slope of the rising and falling limb of the passing flood wave (Marg & Khas, 1999; Petersen-Øverleir, 2006). During the rising stage the velocity and discharge are normally higher for a given stage (Mander, 1978; Marg & Khas, 1999). In the falling stage, when the flood peak passes into the reach downstream of the cross-section, the tail of the wave increases the backwater conditions and so reduces the velocity at a given discharge at the cross-section (Mander, 1978). The result is that, for the same stage, the discharge is higher during the rising stage than during the falling stage. In unsteady flow conditions affected by hysteresis, the stage-discharge relationship will be a slightly looped curve, which can

represent a challenge. However, the Q-H relations that are derived from the local datasets do not show different discharges for the same stage.

3.2.2 Duration curves

The representative discharge of the gauging station is determined by the flow duration curves. A flow duration curve relates the flow of a river to the percentage of the time that a certain discharge is exceeded in the record (Cole et al., 2003). A flow duration curve provides a comprehensive description of the hydrological regime of a catchment and its knowledge is fundamental for many water-related applications (Domeneghetti et al., 2018). The flow duration curve is used to describe the daily flow in the context of long-term planning (Vogel & Fennessey, 1994). The reliability of the discharge records determined by a stage-discharge relationship of high and low discharges is questionable. Therefore, the discharge records of the gauging stations are compared by the discharges for exceedance percentages to determine representative discharges. The stationary derived discharges are used as input for the Flood Hazard Mapper.
The exceedance percentages for the discharges used in the duration curve range from 0-100% and correspond to certain water levels in the derived Q-H relations. These water levels at the gauging stations are compared to water levels simulated for different shape of the bed profile and the roughness coefficients for the riverbed and floodplain.

3.3 Approach to determine inundation levels

The water levels in a river strongly depend on the resistance to flow and therefore depends on roughness coefficient and the shape of the bed profile. An increase in this roughness will cause a decrease in the velocity of water flowing across the riverbed. As described, Manning is in the current approach depending on the slope with the shape of the bed profile assumed rectangular. To simulate water levels in the Flood Hazard Mapper, first the different shapes of the bed profile are discussed.

3.3.1 Shape of the bed profile

For the second research question, the shape of the bed profile of the river during SRTM measurement in February 2000 is unknown and needs to be determined to estimate water levels, because dimensions of the river cross-sections are required to represent channel geometry in hydrodynamic models (Saleh et al., 2013). The unknown part of the river cross-section can be estimated as different cross-sectional shapes. First the equation of Manning is described, to understand the effect of hydraulic roughness on water levels of a river. The Manning formula is applied widely in engineering practice for calculating flows (Shaw et al., 2011; Luo et al., 2017).
In the Flood Hazard Mapper, the water-surface elevation is given with respect to the DEM, which is the water level of the river measured in February 2000. The cross-section of the river is in a constant morphological change, which makes hydrological modelling challenging. At a given station along the river, a cross-section profile is drawn in the direction perpendicular to the main flow direction (Julien, 2002), cross-sections that are not measured perpendicular to the flow direction will appear wider due to the sinuosity of a meandering river. The river planform is not measured below water surfaces in the DEM, causing the river profile shape and depth to be unknown. At regional or larger scale rivers, channel cross-sectional shape is usually simplified to be a rectangle or a trapezoid (Sichangi et al., 2016; Luo et al., 2017). The cross-sectional area for the Ayeyarwady River is tested for the rectangular, trapezoidal and channel as cross-sectional shape. The circular shape is not researched, since the channel width is much larger than depth ($W >> D$). The three profile shapes for the river cross-section, by Sichangi et al., (2016) are described below.

The Manning equation can be written as:

$$Q = V\,A \quad (1)$$

$$V = \frac{1}{n} R^{2/3} S^{1/2} \quad (2)$$

$$R = \frac{A}{P_{wet}} \quad (3)$$

$$Q = \frac{1}{n} A \left(\frac{A}{P_{wet}}\right)^{2/3} S^{1/2} \quad (4)$$

Where,
Q = discharge, m^3/s
A = cross-sectional area of flow, m^2
V = average velocity, m/sec
S = slope of the water surface, m/m
n = Manning roughness coefficient, $s/m^{1/3}$
R = hydraulic radius, m^2/m
Pwet = wetted perimeter, m
D = water depth, m
W = width, m

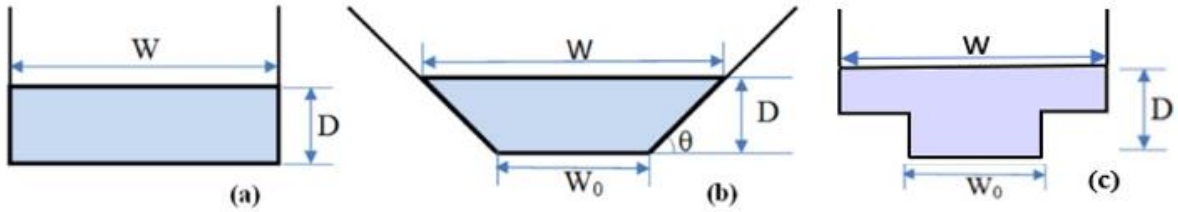

Figure 3-2 Three riverbed cross-sections, a rectangular (a), trapezoidal (b) and channel (c)

The discharge equation for a rectangular cross-section (Figure 3-2a) is as follows:

$$A = W * D \quad (5)$$

$$P_{wet} = W + 2D \quad (6)$$

$$Q = \frac{S^{1/2}}{n} \frac{(W*D)^{5/3}}{(W+2D)^{2/3}} \quad (7)$$

The discharge equation for a trapezoidal cross-section (Figure 3-2b) is as follows:

$$A = (W - D\tan\theta^{-1}) * D \quad (8)$$

$$P_{wet} = W + 2D\frac{1-\cos\theta}{\sin\theta} \quad (9)$$

$$Q = \frac{S^{1/2}}{n} \frac{(W*D-D^2\tan\theta^{-1})^{5/3}}{(W+2D\frac{1-cos\theta}{sin\theta})^{2/3}} \quad (10)$$

The discharge equation for a channel cross-section (Figure 3-2c) is as follows:
Main channel:

$$A = W_0 * D \quad (11)$$

$$P_{wet} = W_0 + 2 * \frac{1}{2} D = W_0 + D \quad (12)$$

$$Q = \frac{S^{1/2}}{n} \frac{(W_0*D)^{5/3}}{(W_0+D)^{2/3}} \quad (13)$$

Sides combined:

$$A = (W - W_0) * \frac{1}{2} D \quad (14)$$

$$P_{wet} = (W - W_0) + 2 * \frac{1}{2} D = (W - W_0) + D \quad (15)$$

$$Q = \frac{S^{1/2}}{n} \frac{(W-W_0) * \frac{1}{2}D)^{5/3}}{(W-W_0+D)^{2/3}} \quad (16)$$

The river planform above the water level in February 2000 is measured by satellites and displayed in the DEM, but can be very different from the current river planform. To minimize this difference, the cross-section of the river above SRTM water level is averaged every 2 km in the Flood Hazard Mapper. These cross-sections cover the main channel and the floodplain till a HAND-value of 20 meters above the water surface measured by the SRTM in February 2000.
The lower part of the Ayeyarwady River is a meandering and partly braided river from NyaungU till Pyay, which consists of channels separated by bars and islands. Especially during high floods water is diverted by the bars towards the banks, causing significant pressure on the riverbank. But for determining the roughness both the dry and wetted cross-section are needed. The shape of the bed profile displayed in the DEM is the dry river cross-section during SRTM measurement in February 2000. The wet part of the river cross-section is not measured, since it is under the water surface and therefore needs to be estimated.
As observed by Klaassen (1992), there is a clear limit to the period over which predictions can be made due to the planform changes in behaviour of a braided sand river with fine sand as bed and bank material. It is particularly difficult and expensive to collect and analyse data on large sand-bed rivers of depths from approximately 3 to 15 meter and mean annual discharges ≥ 500 m3/s (Holmes & Garcia, 2008). Therefore, the different Manning roughness coefficients for the riverbed *n*(wet) and the floodplain *n*(dry) are tested for the three shapes for wet profiles: Rectangle, Trapezoid and Channel.

3.3.2 Roughness of the riverbed and floodplain

For the third research question, different roughness coefficients are used for the riverbed and floodplain to better represent the resistance the water experiences when flowing into the floodplain. For natural river channels, the Manning coefficient depends on many factors, including riverbed roughness, cross-sectional geometry and channel sinuosity (Chow, 1959; George et al., 1989). When applying Manning's formula in hydraulic modelling, the greatest difficulty lies in the determination of the roughness coefficient *n*, as there is no exact method of selecting this value (Chow, 1959; George et al., 1989; Ghani et al., 2007).

In the Manning formula, when a flood exceeds bank-full stage, the roughness coefficient *n* should be changed to model the different flow conditions (Shaw et al., 2011). The bank-full discharge of a river cross-section can be determined by the discharge that the channel can convey when reaching the floodplain level. For determining the roughness of the riverbed, methods of Strickler (1923), Keulegan (1938), Limerinos (1970), Jarrett (1984) and Bathurst (1985) are commonly used, which depend on measurements for grainsize of the soil (Marcus et al., 2015). However, these methods require samples on many locations along the river, which makes it time-consuming and expensive to use for a quick scan analysis.
Other methods mainly depend on the characteristics of the riverbed and separate the riverbed from the floodplain for determining roughness, such as methods developed by Cowan (1956) and Chow (1959). The suggested Manning roughness coefficient for natural channels by Chow (1959) are shown in Table 3-1, where a simple distribution of channel characteristics is made.

Table 3-1 Suggested Manning n-values for natural channels (Chow, 1959)

Type of channel and description	Minimum	Normal	Maximum
Stream on plain			
Clean, straight, full stage, no rifts or deep pools	0.025	0.030	0.033
Same as above, but more stones and weeds	0.030	0.035	0.040
Clean, winding, some pools and shoals	0.033	0.040	0.045
Same as above, but more stones and weeds	0.035	0.045	0.050
Clean, winding, some pools and shoals, weeds and more stones	0.045	0.050	0.060

The suggested Manning roughness coefficient for the river floodplain are shown in Table 3-2, which mainly depends on the vegetation on the floodplain. Normally during flood events submerged vegetation on floodplains produces high resistance to flow and has a large impact on water levels in rivers (Fathi-Moghadam et al., 2011). However, in some cases peak flows during large flooding can be powerful enough to bend or remove weaker vegetation, although the vegetation may appear substantial (Phillips & Tadayon, 2006). This will have influence on the roughness, so for extreme floods it is expected that the roughness of the floodplain is slightly lower due to layover or removal of weaker vegetation. In this research, different Manning values for the roughness of the riverbed and floodplain are tested in the Flood Hazard Mapper.

Table 3-2 Suggested Manning roughness coefficients for floodplains (Chow, 1959)

3. Floodplains			
a. Pasture, no brush			
1.short grass	0.025	0.030	0.035
2. high grass	0.030	0.035	0.050
b. Cultivated areas			
1. no crop	0.020	0.030	0.040
2. mature row crops	0.025	0.035	0.045
3. mature field crops	0.030	0.040	0.050
c. Brush			
1. scattered brush, heavy weeds	0.035	0.050	0.070
2. light brush and trees, in winter	0.035	0.050	0.060
3. light brush and trees, in summer	0.040	0.060	0.080
4. medium to dense brush, in winter	0.045	0.070	0.110
5. medium to dense brush, in summer	0.070	0.100	0.160
d. Trees			
1. dense willows, summer, straight	0.110	0.150	0.200
2. cleared land with tree stumps, no sprouts	0.030	0.040	0.050
3. same as above, but with heavy growth of sprouts	0.050	0.060	0.080
4. heavy stand of timber, a few down trees, little undergrowth, flood stage below branches	0.080	0.100	0.120
5. same as 4. with flood stage reaching branches	0.100	0.120	0.160

The higher values of Manning's roughness coefficient for the floodplain undermine the rational use of one uniform Manning coefficient. Therefore, it is important that different roughness coefficients can be assigned based on characteristics of the riverbed and floodplain. The higher roughness of the floodplain will contribute to higher water levels during floods. The Manning coefficients for the riverbed and for the floodplain are estimates based on literature and local characteristics. A method often used to define different Manning values is the Cowan method, which quantifies components of roughness separately. The key components are formulated by Cowan (1956) and briefly described below:

$$n = (n_0 + n_1 + n_2 + n_3 + n_4)\, m_5$$

Where,
n_0 is a basic n-value for a straight, uniform and smooth channel,
n_1 is the adjustment factor for the effect of surface irregularity,
n_2 is the adjustment factor for the effect of variation in shape and size of the channel cross section,
n_3 is the adjustment factor for obstruction,
n_4 is the adjustment factor for vegetation,
m_5 is a correction factor for meandering channels

Cowan's method has been used in many studies, e.g. Chow (1959), George et al., (1989) and Soong et al., (2012) and is proven to be an effective method for determining Manning roughness. The Cowan method for channel is developed for streams with a hydraulic radius till 5 m. In this research, Cowan's method is therefore only used for determining the roughness of the floodplain, which is mainly depending on the roughness of the vegetation growing on the floodplain.

3.3.3 Comparison between stimulated and observed water levels

The results of both the current and new approach are compared to the observed water levels at the gauging stations. To determine the difference between the simulated and observed water levels, the water levels are compared by the Root Mean Square Error (RMSE), as used in studies of Wiele and Torizzo (2003) and Saleh et al., (2013). RMSE is commonly used in analysis to verify results and is used in this research to compare the observed water levels with the simulated water levels. The RMSE shows the difference between the simulated and observed water levels (for 11 different discharges evenly divided over the duration curves). The formula for calculating the RMSE between the simulated and observed water levels is as follows:

$$RMSE = \sqrt{\frac{\sum_{i=1}^{n}(\hat{y}_i - y_i)^2}{n}}$$

Where y_i is the observed water level from the derived Q-H relation of local measurement and $\hat{y}_i$ is the simulated water level by Flood Hazard Mapper either by the current or the new method. The gauging stations are compared, first to determine the shape of the bed profile and then different roughness coefficients for the riverbed and floodplain are compared.

The RMSE values between simulated and observed discharge are given for Manning's roughness coefficient for a wide range found in literature for a sandy river and cultivated floodplain. Different coefficients for the riverbed and floodplain are applied to compare water levels of the three profile shapes for the riverbed. The range that is tested is from a roughness of the riverbed between 0.030-0.040 s $m^{-1/3}$ and for the floodplain between 0.030-0.070 s $m^{-1/3}$ to determine the influence of the shape of the bed profile undependable of the chosen roughness coefficients.

3.4 Approach to generate flood inundation maps

For the last research question, the flood inundation maps are generated by the representative discharges derived from the duration curves for the period 1994-2017. The inundation maps show the flood-prone areas along the Ayeyarwady River. With these flood inundation maps, decision makers can determine whether certain areas are suitable for urban, industrial, or other developments. If a region is assigned where higher economic values are at stake, more detailed flood maps can be generated for a better analysis of the risk of flooding. The need for more detailed flood maps would arise, particularly for urbanized areas, where the value of economic activities as well as the population at risk of flooding is high. Although, people living in flood-prone areas are often to some degree protected against floods (Verwey et al., 2017), it is expected that many regions do suffer a flood safety deficit.

4 Data analysis: Determination of representative discharges

In this chapter, the data analysis of the local datasets from the Ayeyarwady River are described. First, the water level records based on local reference points are analysed and translated to water levels based on DEM height as used in the Flood Hazard Mapper. In section 4.2, the Q-H relation of the gauging stations are derived and the extended discharge series are analysed in section 4.3. Further, the duration curves are shown for a consistent record period 1994-2017 for all stations in section 4.4. At last, the representative discharges for the Lower Ayeyarwady River are determined in section 4.5.

4.1 Analysing water level records

The water level records are measured daily at the gauging stations and are therefore more reliable than the discharges series. The water level records are not measured with respect to Mean Sea Level (MSL), but with local reference points. From these local reference points, the water levels are translated to SRTM-DEM water levels as used in the Flood Hazard Mapper and estimated with respect to MSL, as described in Appendix A1. In this way, the water levels between different gauging stations can be compared. In this chapter, the measured water levels are compared, but first the historical maximum water levels are displayed against local danger levels.

4.1.1 Maximum water levels

The maximum water level of each of the gauging stations along the Ayeyarwady River is shown in Table 4-1, with corresponding flood duration during that flood event. The flood duration is defined as the number of consecutive days the measured water levels are above a local danger level. The danger levels are locally determined per gauging station based on historical experience with a safety margin around 20 cm before flooding (A. Commandeur local expert RHDHV). The danger levels are obtained from the local datasets of the DWIR and IWUMD in Myanmar and are all shown at local reference point. At this danger level, there is a high possibility that the river will flood parts of the city near that station. In Table 4-1, it can be observed that the area near station Sagaing was in danger of flooding/flooded for a total period of approximately 18 days during the longest recorded flood in 2004. The difference between local reference points and the SRTM references point are shown in Table 0-1 in Appendix A.1.

Table 4-1 Maximum water levels (local reference points) and flood duration for stations along the Ayeyarwady River

Station	**Characteristics of the maximum water level (local reference points)**					**Measuring period**
	Danger Level (m)	Max. WL (m)	Flood Duration	Above DL (m)	Year	Year
Myitkyina	12.00	14.01	3 days	2.01	2004	1966-2017
Katha	10.40	11.51	8 days	1.11	1979	1966-2017
Sagaing	11.50	12.73	18 days	1.23	2004	1966-2017
NyaungU	21.20	22.92	16 days	1.72	2016	1980-2017
Chauk	14.50	15.06	5 days	0.56	2016	1976-2017
Magway	17.00	18.92	16 days	1.92	2004	1994-2017
Aunglan	25.50	26.48	10 days	0.98	2004	1976-2017
Pyay	29.00	30.56	13 days	1.56	1974	1966-2017
Monywa	10.00	11.43	7 days	1.43	2015	1966-2017

4.1.2 Comparison of water levels between gauging stations

Myitkyina station is the most upstream station of the Ayeyarwady River and shows that the measured water levels change rapidly depending on the precipitation as shown in Figure 4-1. The water level changes less rapid for Katha station and is even smoother for Sagaing station. The water levels displayed are based on SRTM-DEM water levels, referenced in February 2000 as 0 m. The travel time of the flow is shown in July 2012 in Figure 4-1, where first high water levels are measured at Myitkyina than at Katha and at last at Sagaing. Increase water levels between Myitkyina and Katha, increase is limited between Katha and Sagaing.

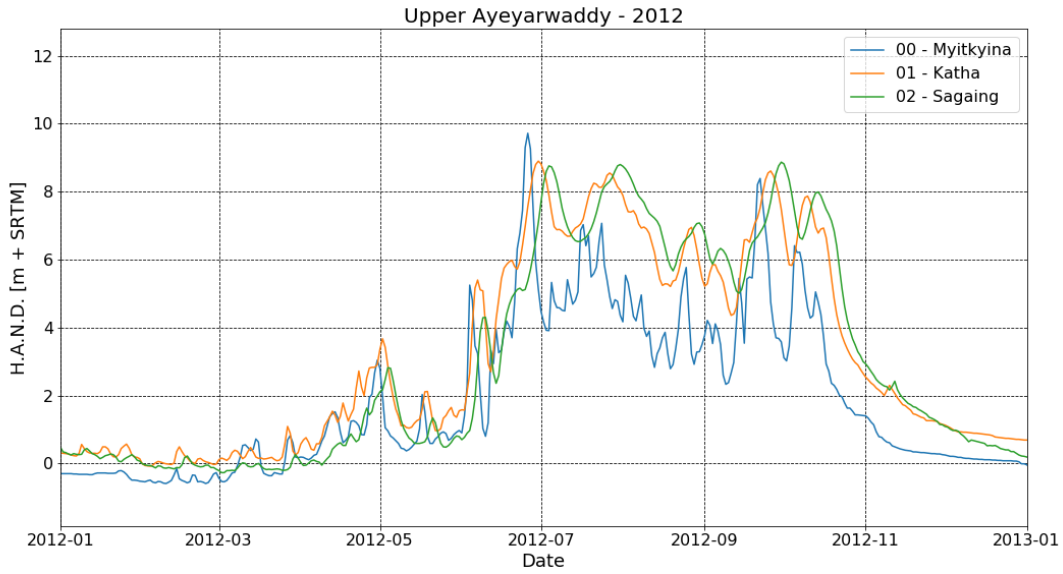

Figure 4-1 Water level measurements of the Upper Ayeyarwady in Height Above Nearest Drainage (HAND) in 2012

Comparing the SRTM-DEM water levels from gauge stations in the Lower Ayeyarwady in Figure 4-2, it shows that the patterns of the measurements are comparable. The same conclusion is drawn when comparing other record years. The only differences are found in the stage due to the changing river profile and the delay due to travel distance of the discharge waves with stations located more downstream. The results are as expected, since the stations in the Lower Ayeyarwady River are located relatively close to each other and are in the dry zone of Myanmar.

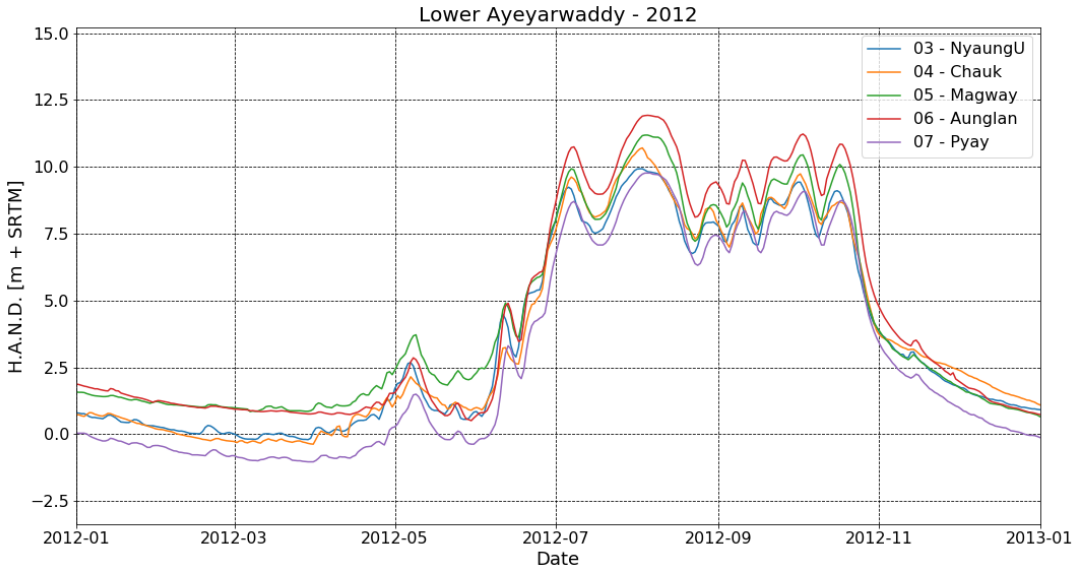

Figure 4-2 Water level measurements of the Lower Ayeyarwady in Height Above Nearest Drainage (HAND) in 2012

From these analyses, it is concluded that most runoff is from the Upper Ayeyarwady and the Chindwin River, whereas from the Lower Ayeyarwady water levels observed at gauging stations are comparable. The water levels of the Height Above Nearest Drainage at Pyay are lower compared to other stations, which is expected to be caused by erosion of the riverbed. The water level records of the gauging stations are displayed in Appendix A2.

4.2 Derived Q-H relation

For determining the derived Q-H relation or stage-discharge relationship, oblivious errors are removed from the recorded data, after which a power and parabolic function is calculated to determine the Q-H relation, as shown in Figure 4-3. The displayed Q-H relations do not suggest there is a floodplain present, which can be explained by a measuring period without high discharges and the smaller floodplains at the gauging station locations located near cities.

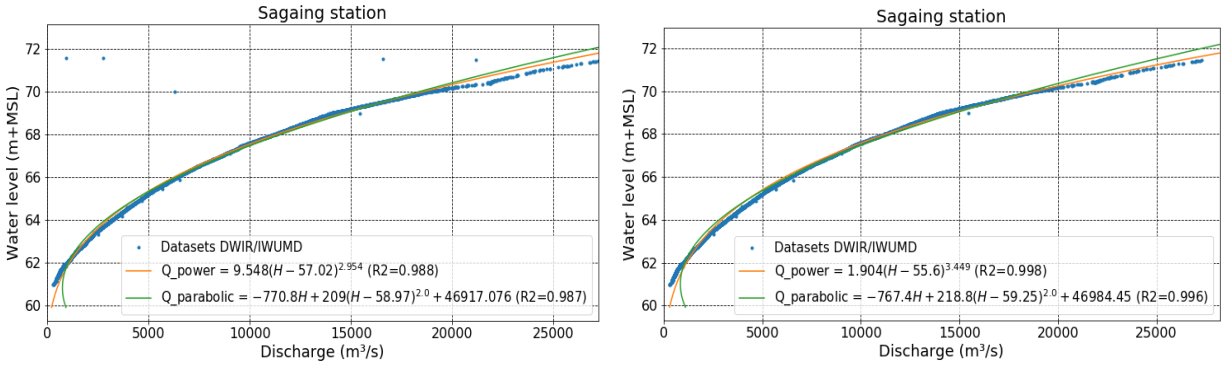

Figure 4-3 The initial Q-H relation (left) from the local datasets on Mean Sea Level (MSL) and the improved Q-H relation (right) for both the Power and Parabolic equation with corresponding coefficient of determination R^2 (Sagaing 1966-2014)

The Q-H relations derived for the DWIR and IWUMD data are often the same throughout the record period and are used to extend the record period or replace missing data. For the most commonly used power equation, the regression line shows R^2 values closer to the highest value of 1 at all stations. Because of the overall better performance of the power equation and the fact that the relation is more simplistic and

commonly used than the parabolic equation, it is used in this research to derive the Q-H relation of the gauging stations.

In the datasets, the derived Q-H relations are used to replace missing data and to extend the discharge series with the local water level measurements. The available discharge series are often of a shorter record period than the water level measurements, therefore the power equation for the Q-H relation is used for extending the discharge series. For each gauging station, the discharge data is extended and improved for the available period of water level measurements. The derived Q-H relations used for improving and extending the discharge series of the gauging stations are displayed in Appendix A.3 and the discharge series in Appendix A.4.

4.3 Analysing discharge series

The runoff delay between the stations as observed in Figure 4-1 and Figure 4-2 is further investigated by comparing the discharge series to the most downstream station Pyay. The comparison of the discharge series with station Pyay is to give an insight in the runoff delay between the gauging stations. In Figure 4-4, the discharges from gauging stations NyaungU and Pyay (located at the Lower Ayeyarwady River) are compared. This comparison shows, that there is not much increase in runoff between the station as the dots are mainly located around the central line. The higher discharges for Pyay during high water levels can be explained by lateral inflow, which includes groundwater flow, overland flow, or interflow.

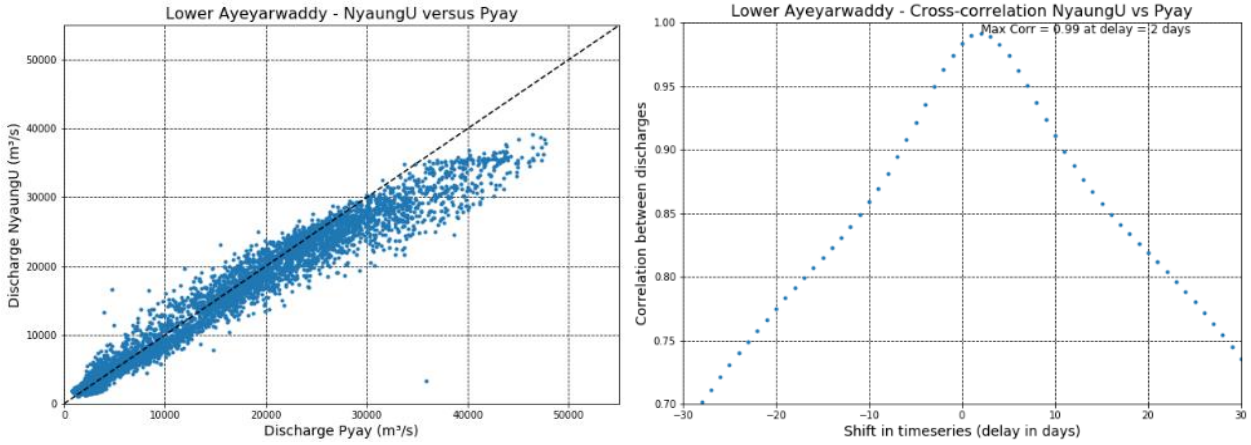

Figure 4-4 Comparison of discharges without delay between gauging stations NyaungU and Pyay (left) and the cross-correlation between discharges at NyaungU and Pyay in days (right)

The cross-correlation between the discharge of these gauging stations in Figure 4-4 (right) shows the maximum correlation that is found, based on the total discharge record. For the cross-correlation between the discharge series of station NyaungU and Pyay a maximum correlation of 0.99 is found for a delay of 2 days. Cross-correlations from the other gauging stations compared with Pyay show a similar pattern with high maximum correlations. This suggests that when more than one flooding occurs in a year, the runoff is not independent from each other. The station discharges are all compared to Pyay to show the delay in days as shown in Table 4-2. The lower maximum correlations at stations Myitkyina, Hkamti and Homalin are due to their locations upstream in a mountainous area, where river discharge increases and decreases faster in responds to rainfall. The distance between the upstream stations and downstream station is shown in the runoff delay in days compared to station Pyay.

Table 4-2 Maximum correlation between discharge at Pyay and the other gauging stations, corresponding delay and river length

Station	Maximum correlation	Delay (days)	River length (km)
Ayeyarwady River			
Myitkyina	0.88	11	1037
Katha	0.95	7	745
Sagaing	0.97	3	477
NyaungU	0.99	2	303
Chauk	0.98	1	262
Magway	0.99	1	157
Aunglan	0.99	0	63
Pyay	-	-	-
Chindwin River			
Hkamti	0.88	10	1123
Homalin	0.93	9	929
Mawlaik	0.96	6	714
Kalewa	0.97	5	653
Monywa	0.97	4	432

On average the peak discharge travels around 100 km/day, which means a flow rate around 1.2 m/s as determined from Table 4-2. Almost no delay is observed between gauging station NyaungU and Pyay, which means a rather steady discharge flow. Therefore, stationary discharges can be used to represent the discharges of the Lower Ayeyarwady River.

4.4 Flow duration curve

The discharge data is presented in flow duration curves and the water levels in water level duration curves. The water level duration curve in Figure 4-5 (left) shows the percentage of the time a water level at Sagaing station is exceeded, where the water level measurements are displayed in meters above the SRTM water level. The average water level at Sagaing station is 2.89 m above SRTM water level and water levels may differ up to 11.5 m between the lowest and highest recorded water level. To be able to compare the different gauging stations, the record period is taken for all stations between 1994 until 2017, since for all stations the data is complete and available for this period. The water level duration curves are shown in Appendix A.5 for all other gauging stations.

The flow duration curve in Figure 4-5 (right) shows the percentage of the time a discharge at Sagaing station is exceeded. For all stations, the average discharge is higher than the 50% discharge exceedance. This is due to the significantly higher discharges during the wet monsoon season. The SRTM discharge is the discharge as expected in February 2000 during the Shuttle Radar Topography Mission.

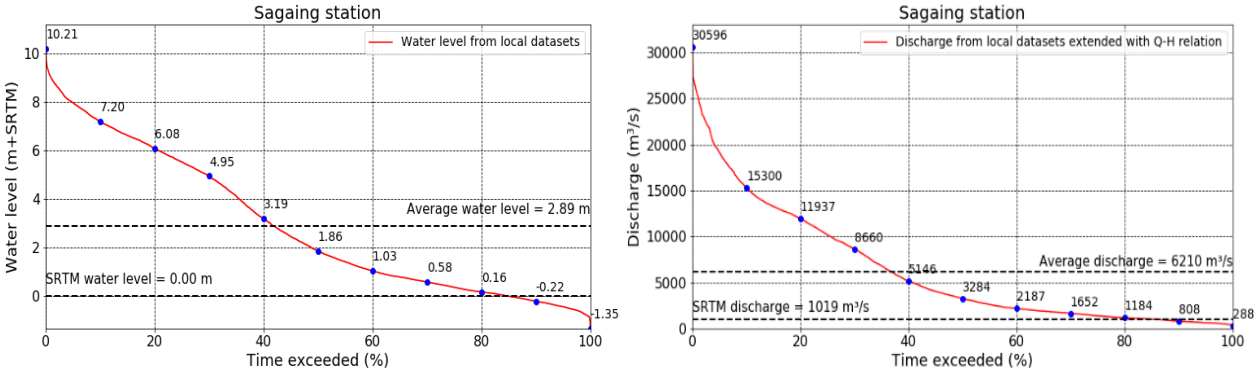

Figure 4-5 Percentage of the time a water level (left) or discharge (right) is exceeded at Sagaing station (1994-2017)

The Q exceedance for all other gauging stations can be found in Appendix A.6. The discharge exceedance percentages are used as discharge of the Lower Ayeyarwady River to simulate water levels in the Flood Hazard Mapper and compare them with observed water levels at these discharges.

4.5 Discharge of the Lower Ayeyarwady

The discharges of gauging stations located on the Lower Ayeyarwady River are used to generate representative discharges for testing the three river profile shapes and the Manning roughness coefficients. The Lower Ayeyarwady is used, since most of the discharge is already in the Ayeyarwady River. The drainage catchment comes for 87% upstream of NyaungU station, as the discharges in Figure 4-6 confirm. Further, the gauging stations at the Lower Ayeyarwady have a relatively constant slope and are well distributed over the river length.

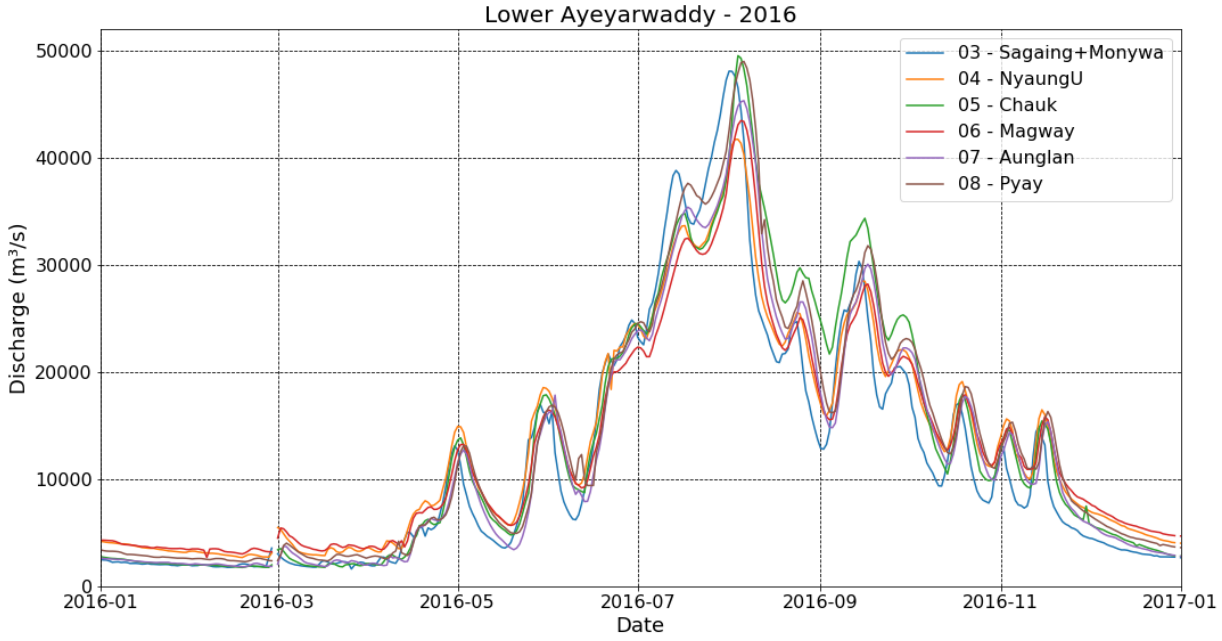

Figure 4-6 Discharge of the Lower Ayeyarwady gauging stations in 2016, when large flooding occurred along the Ayeyarwady River

4.5.1 The slope of the Lower Ayeyarwady

For the Lower Ayeyarwady, which contains gauging stations NyaungU, Chauk, Magway, Aunglan and Pyay, the shape of the bed profile and Manning roughness for the riverbed *n*(wet) and the floodplain *n*(dry) is determined. The approximate slope of the riverbed can be estimated from gradual changes in elevation over long distances (Julien, 2002). The average slope of the Lower Ayeyarwady, after the confluence with the Chindwin River, is estimated at 0.1 m/km based on the DEM. The slope corresponds to the water-surface elevation drop over the concerned river length. In the Flood Hazard Mapper, the smoothed slope (orange) derived by the SRTM-DEM is used, as displayed in Figure 4-7.

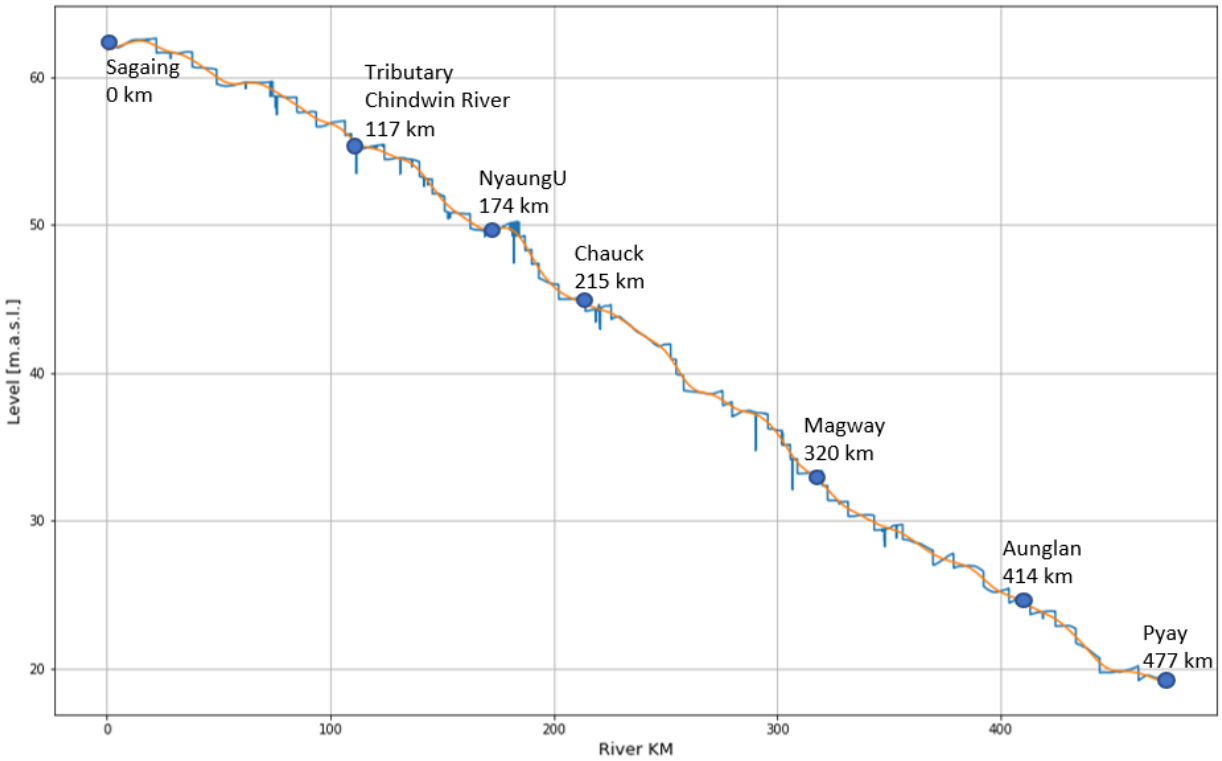

Figure 4-7 Measured water levels during the Shuttle Radar Topography Mission (SRTM) for the Lower Ayeyarwady from gauging station Sagaing till Pyay (blue) and the smoothed water levels (orange)

4.5.2 Generating representative discharge of the Lower Ayeyarwady

The reliability of the discharge records determined by a stage-discharge relationship of high and low discharges is questionable. Therefore, the discharge records of the gauging stations are compared by the discharges for exceedance percentages. The discharge values for different exceedance levels from 1994 till 2017 are compared in Table 4-3, derived from the duration curves shown in Appendix A.6. The average discharge at the exceedance percentages is compared for the stations in Table 4-4, where it is assumed that the discharge record of station Pyay has the most reliable discharge record. The reliability of the discharge at station Pyay is partly explained by its cross-section, which is relatively constant and without a floodplain.

Table 4-3 Comparison of exceedance of discharge between stations along the Lower Ayeyarwady River (1994-2017)

Station	Exceedance of discharge (m³/s)										
Ayeyarwady River	**0%**	**10%**	**20%**	**30%**	**40%**	**50%**	**60%**	**70%**	**80%**	**90%**	**100%**
NyaungU	42214	26578	22097	17143	9822	5845	4464	3622	3032	2472	1100
Chauk	47557	28413	21705	15933	9541	5630	3693	2484	1792	1316	378
Magway	44973	28423	22723	17337	10353	6732	5111	4194	3531	2881	2101
Aunglan	46124	27460	21947	16463	9817	4939	3375	2417	1840	1323	433
Pyay	48887	30093	23683	17627	9746	5760	4172	3319	2731	2248	807
Average	**45951**	**28193**	**22431**	**16901**	**9856**	**5781**	**4163**	**3207**	**2585**	**2048**	**964**

Table 4-4 Difference with the average discharge values for the exceedance levels of the Lower Ayeyarwady River (1994-2017)

Station	Difference with average discharge exceedance level (%)										
Ayeyarwady River	**0%**	**10%**	**20%**	**30%**	**40%**	**50%**	**60%**	**70%**	**80%**	**90%**	**100%**
NyaungU	-8%	-6%	-1%	1%	0%	1%	7%	13%	17%	21%	14%
Chauk	3%	1%	-3%	-6%	-3%	-3%	-11%	-23%	-31%	-36%	-61%
Magway	-2%	1%	1%	3%	5%	16%	23%	31%	37%	41%	118%
Aunglan	0%	-3%	-2%	-3%	0%	-15%	-19%	-25%	-29%	-35%	-55%
Pyay	6%	7%	6%	4%	-1%	0%	0%	3%	6%	10%	-16%

Further is assumed that the discharge between station NyaungU and Pyay should not decrease. So, for every gauging station located downstream the discharge should increase or remain unchanged compared to the station located upstream. The discharge at station Pyay is used as discharge for discharge exceedances between 40-100%. For the more important higher discharges with exceedances between 0-30% local discharges are chosen and interpolated between gauging stations. Table 4-5 presents the scores indicating how reliable the calculated discharges, based on discharge values in the duration curves. The (+) sign is when the assumption is met and the discharges are assumed possible, the (+/-) sign is when the assumptions is sometimes met and the discharge is questionable and the (-) sign is when the assumption is not met or the discharge is assumed not reliable.
First, for the representative discharges it is assumed that the derived Q-H relation from the data is reliable. Second, it has been checked whether subsequent stations show logical behaviour further downstream, the discharge on the same river reach should be higher going downstream. Third, the lower discharges are adjusted to the discharge at Pyay since the discharge fluctuations are highly doubtable and is the closest to the average discharge at those exceedance levels.

Table 4-5 Discharge exceedance values of the Lower Ayeyarwady compared to assumptions

Stations	Discharge exceedance categorised:		
	High (0-30%)	**Middle (40-60%)**	**Low (70-100%)**
NyaungU	+	+/-	+/-
Chauk	-	+/-	-
Magway	+	+/-	-
Aunglan	+/-	+/-	-
Pyay	+	+	+

Based on the reliability analysis of the station data, discharge scenarios are created for 0%-10%-…-90%-100% conditions along the Lower Ayeyarwady. The resulting discharges are presented in Table 4-6 and Figure 4-8. These discharges are used in this research to calculate water levels along the river stretch.

Table 4-6 Improved discharge values for different exceedance levels for stations along the Lower Ayeyarwady River (1994-2017), discharge shown in bold are not changed and discharges in cursive are assumed corrected

Stations	Exceedance of discharge (m³/s)										
	0%	10%	20%	30%	40%	50%	60%	70%	80%	90%	100%
NyaungU	**42214**	**26578**	**22097**	**17143**	*9746*	*5760*	*4172*	*3319*	*2731*	*2248*	*807*
Chauk	*43122*	*27481*	*22405*	*17239*	**9746**	**5760**	**4172**	**3319**	**2731**	**2248**	**807**
Magway	**44973**	**28423**	**22723**	**17337**	*9746*	*5760*	*4172*	*3319*	*2731*	*2248*	*807*
Aunglan	**46124**	*29234*	*23196*	*17480*	*9746*	*5760*	*4172*	*3319*	*2731*	*2248*	*807*
Pyay	**48887**	**30093**	**23683**	**17627**	**9746**	**5760**	**4172**	**3319**	**2731**	**2248**	**807**

The discharge shown in Figure 4-8 are the representative discharges for the Lower Ayeyarwady River, which are used as input for the Flood Hazard Mapper. The discharges at gauging stations are shown as squares for discharge values for different exceedance levels. The coloured lines show the representative discharges for different exceedance levels used to generate the water levels and flood inundation maps presented in chapter 5.

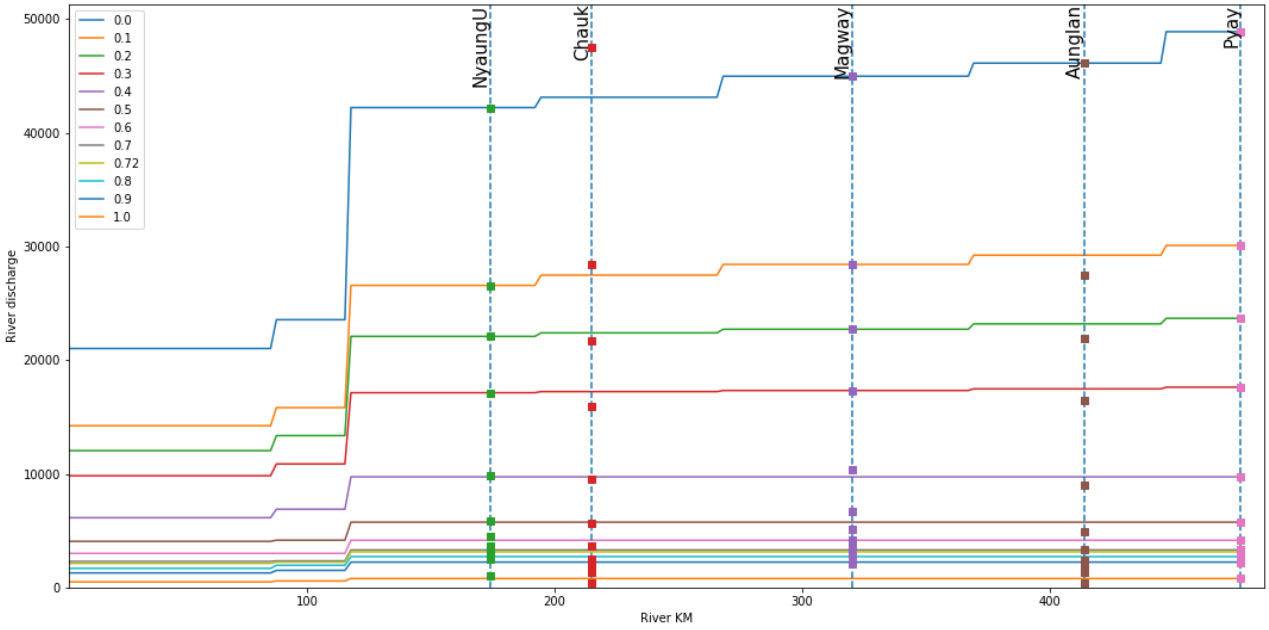

Figure 4-8 Discharge values for different exceedance levels along the Lower Ayeyarwady River are used as input in the Flood Hazard Mapper, with the original discharges from the datasets (squares) shown at exceedance for different exceedance levels

5 Results: Determination of inundation levels

Before determining inundation levels for different Manning roughness coefficients for the riverbed and the floodplain, first the shape of the bed profile is determined in section 5.1. The different Manning roughness coefficients for the riverbed and the floodplain are determined in section 5.2 by the characteristics of the riverbed and floodplain. In section 5.3, the simulated water levels by the Flood Hazard Mapper are compared with the observed water levels. Finally, the effect of the new approach for determining the inundation levels can be observed from flood inundation maps in section 5.4.

5.1 Shape of the bed profile

The ranges found in literature for Manning's roughness coefficient are applied on the three profile shapes of the riverbed shown in Figure 3-2. The range is tested for roughness coefficients between 0.030-0.040 s $m^{-1/3}$ for the riverbed and between 0.030-0.070 s $m^{-1/3}$ for the floodplain. To undependable of the roughness show the influence of the shape of the bed profile on the Root Mean Square Error (RMSE). The RMSE values display the difference in meters between the observed and calculated water levels for different occurrence intervals of discharges (0%-10%...100%).
The average RMSE is used to determine which cross-sectional shape should be used and what combination of roughness for the riverbed, *n*(wet), and floodplain, *n*(dry). The results are based on gauging stations along the Lower Ayeyarwady and is tested for river sections with a mild slope and large width to depth ratio. Pyay is not included since water levels are calculated with gauging station Pyay as reference level. In Table 5-1, for different Manning coefficient for the wet rectangular profile shape and dry profile by the DEM are water levels for representative discharges calculated and shown in RMSE values. Table 5-2 shows RMSE values for the wet trapezoidal profile shape and in Table 5-3 for the channel shape of the bed profile.

Table 5-1 Range of Manning coefficient for the wet rectangular profile and dry profile by the DEM, where the RMSE (Root Mean Square Error) of the water level is calculated in meters compared to the derived Q-H relation of gauging stations (1994-2017)

Shape_WetProfile	*n*(wet)	*n*(dry)	NyaungU	Chauk	Magway	Aunglan	Average RMSE
Rectangle	0.030	0.030	1.520	0.998	1.262	1.851	**1.408**
Rectangle	0.030	0.040	1.467	0.967	1.214	1.824	**1.368**
Rectangle	0.030	0.050	1.433	0.947	1.184	1.808	**1.343**
Rectangle	0.030	0.060	1.408	0.934	1.164	1.797	**1.326**
Rectangle	0.030	0.070	1.390	0.925	1.150	1.789	**1.313**
Rectangle	0.035	0.040	1.200	0.788	0.903	1.544	**1.108**
Rectangle	0.035	0.050	1.156	0.773	0.876	1.524	**1.082**
Rectangle	0.035	0.060	1.125	0.764	0.860	1.511	**1.065**
Rectangle	0.035	0.070	1.103	0.758	0.848	1.501	**1.052**
Rectangle	0.040	0.040	0.973	0.707	0.743	1.306	**0.932**
Rectangle	0.040	0.050	0.923	0.707	0.739	1.285	**0.913**
Rectangle	0.040	0.060	0.889	0.710	0.740	1.270	**0.902**
Rectangle	0.040	0.070	0.864	0.715	0.744	1.260	**0.896**

Table 5-2 Range of Manning coefficient for the wet trapezoidal profile and dry profile by the DEM, where the RMSE (Root Mean Square Error) of the water level is calculated in meters compared to the derived Q-H relation of gauging stations (1994-2017)

Shape_WetProfile	*n*(wet)	*n*(dry)	NyaungU	Chauk	Magway	Aunglan	Average RMSE
Trapezoid	0.030	0.030	1.049	0.487	0.681	1.330	**0.887**
Trapezoid	0.030	0.040	0.756	0.402	0.466	1.048	**0.668**
Trapezoid	0.030	0.050	0.547	0.470	0.526	0.861	**0.601**
Trapezoid	0.030	0.060	0.397	0.577	0.675	0.733	**0.595**
Trapezoid	0.030	0.070	0.300	0.683	0.822	0.646	**0.613**
Trapezoid	0.035	0.040	0.569	0.485	0.531	0.840	**0.606**
Trapezoid	0.035	0.050	0.346	0.641	0.758	0.650	**0.599**
Trapezoid	0.035	0.060	0.226	0.797	0.985	0.541	**0.637**
Trapezoid	0.035	0.070	0.240	0.935	1.180	0.493	**0.712**
Trapezoid	0.040	0.040	0.424	0.609	0.690	0.681	**0.601**
Trapezoid	0.040	0.050	0.224	0.815	1.003	0.515	**0.639**
Trapezoid	0.040	0.060	0.250	1.001	1.275	0.470	**0.749**
Trapezoid	0.040	0.070	0.387	1.162	1.503	0.501	**0.888**

Table 5-3 Range of Manning coefficient for the wet channel profile and dry profile by the DEM, where the RMSE (Root Mean Square Error) of the water level is calculated in meters compared to the derived Q-H relation of gauging stations (1994-2017)

Shape_WetProfile	*n*(wet)	*n*(dry)	NyaungU	Chauk	Magway	Aunglan	Average RMSE
Channel	0.030	0.030	1.561	1.084	1.321	1.899	**1.466**
Channel	0.030	0.040	1.509	1.055	1.274	1.874	**1.428**
Channel	0.030	0.050	1.475	1.037	1.246	1.858	**1.404**
Channel	0.030	0.060	1.451	1.025	1.227	1.847	**1.387**
Channel	0.030	0.070	1.433	1.016	1.213	1.839	**1.375**
Channel	0.035	0.040	1.252	0.897	0.984	1.605	**1.185**
Channel	0.035	0.050	1.209	0.884	0.959	1.587	**1.160**
Channel	0.035	0.060	1.180	0.875	0.944	1.574	**1.143**
Channel	0.035	0.070	1.158	0.870	0.933	1.564	**1.131**
Channel	0.040	0.040	1.037	0.829	0.845	1.385	**1.024**
Channel	0.040	0.050	0.990	0.828	0.840	1.364	**1.005**
Channel	0.040	0.060	0.957	0.830	0.840	1.350	**0.995**
Channel	0.040	0.070	0.934	0.834	0.843	1.340	**0.988**

The average RMSE value of the rectangle, trapezoid and channel are compared. The figures show that the trapezoidal profile shape performs significantly better than the channel or rectangular shape. The trapezoidal profile shape also depends on its bed percentage, where for different roughness coefficients a bed width of 40% of the total width is used for the Lower Ayeyarwady River. The trapezoidal profile is further used as the unknown wetted river section for determining the roughness coefficients. The cross-sections derived by SRTM-DEM data with a trapezoid profile shape are shown in Appendix A.1, including the satellite images of the gauging locations.

5.2 Roughness of riverbed and floodplain

The methods used for the roughness coefficients of the riverbed and the floodplain are from Chow and Cowan, as described in section 3.2.3. These methods show different Manning values than currently used in the Flood Hazard Mapper. Chow's method for a clean river without rifts or deep poles gives the riverbed a Manning roughness of 0.030 s $m^{-1/3}$ (normal) and 0.033 s $m^{-1/3}$ (maximum), as shown in Table 3-1. Land use maps from Myanmar are used to determine the main vegetation on the floodplain of the Ayeyarwady River. Unfortunately, due to the year of the DEM and land use maps not overlapping and the rapid profile changes of the Ayeyarwady River, this could not be implemented in the model. However, the land use maps showed that the floodplain mainly consist of agricultural areas, as confirmed by satellite images. For the floodplain of the Lower Ayeyarwady, the main vegetation during the yearly monsoon flooding are mature rice paddy fields, as described in Appendix B.2. In Table 3-2, the main floodplain vegetation for cultivated areas is mature row crops, which show Manning between 0.035 s $m^{-1/3}$ (normal) and 0.045 s $m^{-1/3}$ (maximum) for cultivated areas of the floodplain. The roughness of the floodplain for mature row crops by Cowan's method give Manning's roughness coefficients between 0.035-0.058 s $m^{-1/3}$, as shown in Table 5-4.

Table 5-4 Cowan method for floodplain roughness of the Lower Ayeyarwady

Cowan method: Floodplain roughness		**Description**	**Range of roughness *n* (s m-1/3)**		
n0	Floodplain material	Sandy soils	0.024		
n1	Surface irregularity	Slightly irregular shape a few rises and dips	0.001 - 0.005		
n2	Variation floodplain cross-section	Not applicable	0.000		
n3	Relative effect of obstruction	A few scattered obstructions, less than 5% of the floodplain flow area	0 - 0.004		
n4	Amount of vegetation	Grass and/or weeds with the flow one to two times the height of the vegetation	0.010 - 0.025		
m5	Degree of meandering	Not applicable	1		
Manning's *n*	Total	*n* = (n0+n1+n2+n3+n4)*m5	minimum	normal	maximum
			0.035	0.047	0.058

In the current approach used in the Flood Hazard Mapper, the roughness of the riverbed called *n*(wet) and the floodplain called *n*(dry) are the same value, for the Lower Ayeyarwady between 0.030-0.035 s $m^{-1/3}$ depending on the slope. Whereas in the approach with different roughness coefficients for the riverbed and floodplain, there are two values. The Manning roughness coefficients of the Lower Ayeyarwady River are shown in Table 5-5 for both methods. The minimum roughness coefficients are not included, since the vegetation is fully growing during the yearly monsoon flooding.

Table 5-5 Range of Manning roughness coefficients used for the Lower Ayeyarwady River

Method	**Roughness riverbed *n*(wet)**		
Currently used	minimum	normal	maximum
	0.030	**0.033**	**0.035**
Chow	minimum	normal	maximum
	~~0.025~~	**0.030**	**0.033**

Method	**Roughness floodplain *n*(dry)**		
Chow	minimum	normal	maximum
	~~0.025~~	**0.035**	**0.045**
Cowan	minimum	normal	maximum
	~~0.035~~	**0.047**	**0.058**

For the new approach with different roughness coefficients for the riverbed and floodplain, the RMSE values for Chow and Cowan's method are shown in Table 5-6. These values all use the trapezoidal shape for the unknown bed profile and the DEM for the known river cross-section. Both approaches for roughness perform better as compared with using a single roughness coefficient for the riverbed and floodplain, as currently used in the Flood Hazard Mapper. However, Cowan's method for roughness of the floodplain depends on the interpretation of the reader, which makes Cowan's method for determination of the roughness less ambiguous to use. The average Root Mean Square Error of the current method is between 0.61 and 0.87 meter compared to observed water levels for the discharge values for different exceedance levels, whereas the method of Chow and Cowan have simulated water levels closer to the observed water levels of gauging stations located along the Lower Ayeyarwady.

Table 5-6 The RMSE (Root Mean Square Error) of the water level is calculated in meters compared to the observed water levels gauging stations

Method	WetProfile	Wbed	*n*(wet)	*n*(dry)	NyaungU	Chauk	Magway	Aunglan	Average
Currently used	Trapezoid	40%	0.030	0.030	1.144	0.487	0.633	1.195	**0.865**
	Trapezoid	40%	0.033	0.033	0.946	0.399	0.437	0.958	**0.685**
	Trapezoid	40%	0.035	0.035	0.820	0.400	0.406	0.809	**0.609**
Chow used for riverbed and floodplain	Trapezoid	40%	0.030	0.035	0.960	0.381	0.436	0.990	**0.691**
	Trapezoid	40%	0.030	0.045	0.662	0.384	0.437	0.677	**0.540**
	Trapezoid	40%	0.033	0.035	0.872	0.383	0.399	0.876	**0.633**
	Trapezoid	40%	0.033	0.045	0.559	0.471	0.561	0.547	**0.535**
Cowan used for floodplain	Trapezoid	40%	0.030	0.047	0.611	0.407	0.480	0.626	**0.531**
	Trapezoid	40%	0.030	0.058	0.371	0.570	0.757	0.409	**0.527**
	Trapezoid	40%	0.033	0.047	0.506	0.505	0.621	0.496	**0.532**
	Trapezoid	40%	0.033	0.058	0.262	0.703	0.948	0.297	**0.553**
	Trapezoid	40%	0.035	0.047	0.446	0.572	0.717	0.422	**0.539**
	Trapezoid	40%	0.035	0.058	0.213	0.787	1.068	0.259	**0.582**

The average RMSE values in Table 5-6 show that on average the RMSE value of the water levels can be improved by 7 till 33 cm, compared to the current implementation. It should be noted that this improvement is tested for the best fitting shape of the bed profile.

.

5.3 Water levels in the Lower Ayeyarwady

The water levels in the Lower Ayeyarwady River are calculated based on the trapezoidal river profile and the approach for implementing roughness. The discharge values for different exceedance levels shown in Table 4-6 are used as discharge in the Flood Hazard Mapper. The water levels shown in Figure 5-1 are simulated from Pyay station and match the observed water levels at Pyay. Further, the water levels observed at gauging stations are shown as squares for discharge values for different exceedance levels.

The Manning roughness coefficients for the current approach are between 0.030-0.035 s $m^{-1/3}$ for the Lower Ayeyarwady. To compare the water levels an average Manning value of 0.033 s $m^{-1/3}$ for riverbed and floodplain is chosen (average roughness with this slope). Figure 5-1 (A) shows that for high discharge exceedances the water level is estimated lower than observed water levels at gauging stations. The results of the new approach have low Manning roughness coefficients of n(wet) = 0.030 s $m^{-1/3}$ for the riverbed and n(dry) = 0.045 s $m^{-1/3}$ for the floodplain. Figure 5-1 (B) shows that for high discharge exceedances the water level is estimated closer to the measured water levels at the gauging stations. The results of the new approach have high Manning roughness coefficients of n(wet) = 0.033 s $m^{-1/3}$ for the riverbed and n(dry) = 0.058 s $m^{-1/3}$ for the floodplain. For the high roughness coefficients, the simulated water levels are closer to the observed water levels, as shown in Figure 5-1 (C).
For the current approach, the simulated water levels are underestimated compared to the observed water levels at the gauging stations. For the low roughness coefficient of the floodplain, the simulated water levels are already closer to measured water levels at gauging station. It can be observed that the water levels calculated by the Flood Hazard Mapper at some locations differ from corresponding water levels from local data. High water levels suggest that the river cross-section is smaller at those locations, as can be observed between Magway and Aunglan. For the high roughness coefficient of the floodplain, it can be observed that simulated water levels close to measured water levels and only overestimated at station Chauk and Magway. The effect these water levels have on the flood inundations maps of the Lower Ayeyarwady River is discussed in section 5.5.

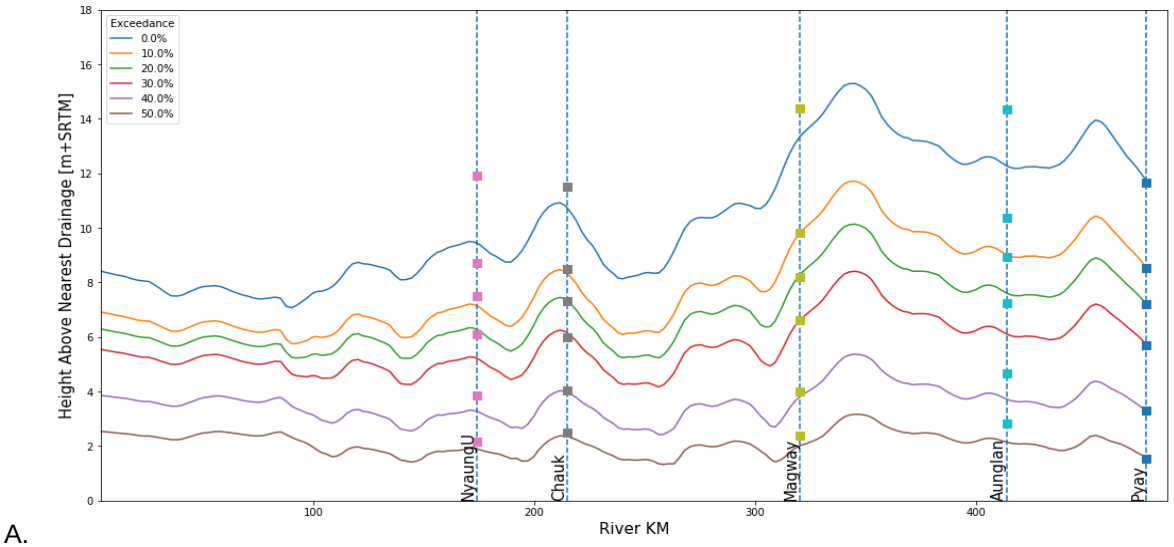

A.

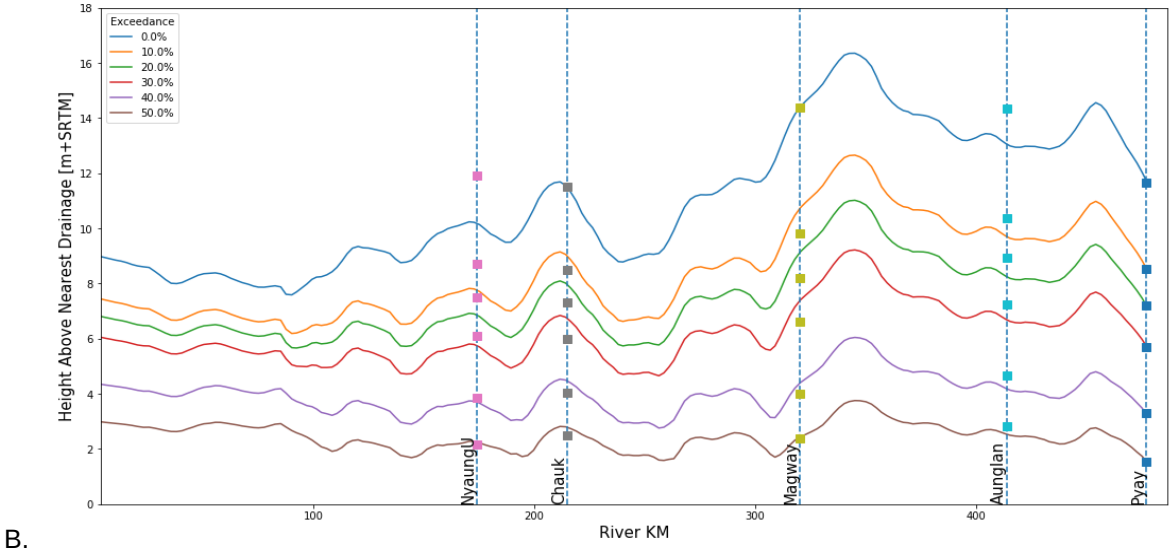

B.

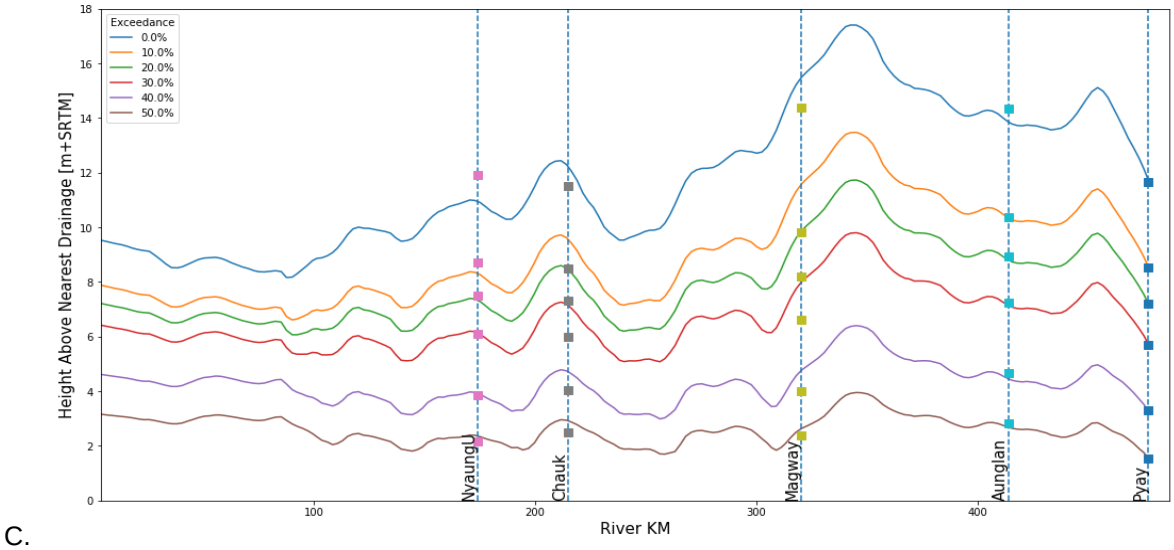

C.

Figure 5-1 Water level in meters above SRTM-DEM for the Lower Ayeyarwady with the measured water levels (squares) at the shown exceedance percentage. A. Current average used n = 0.033. B. Low values new approach with n(dry) = 0.030 and n(wet) = 0.045. C. High values new approach with n(dry) = 0.033 and n(wet) = 0.058.

5.4 Flood inundation maps

The flood inundation maps are generated for representative discharges levels for the period 1994-2017 to show the flood-prone areas along the Lower Ayeyarwady River. Section A in Figure 5-2 shows some small villages (red circles) located on the other side of the river of the city NyaungU. The houses here have some protection against floods by being located on higher grounds, although most are in danger of flooding starting at a 10% discharge exceedance. The extend a flood depends on the exceedance percentage and the roughness as shown in sections B, C and D in Figure 5-2. The roughness coefficients used have visible influence on inundation levels, where it can make the difference being flooded or remaining dry.

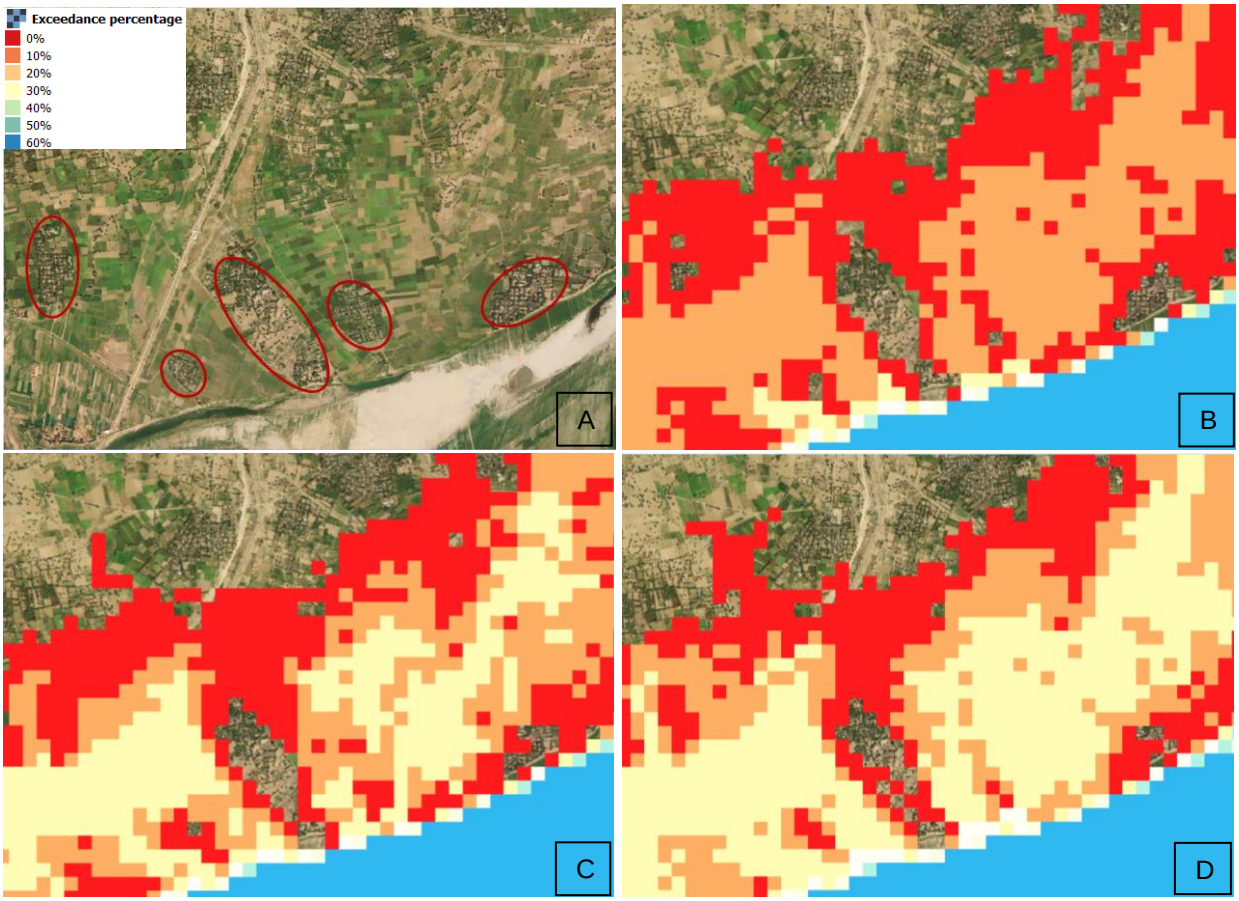

Figure 5-2 Example of an inundation map of the Flood Hazard Mapper with the exceedance percentage of the duration curve. Where the location of the river is blue and the flooded areas yellow to red depending on the exceedance percentage. Figure A. is a satellite image, B. single Manning roughness *n* = 0.033, C. different Manning values for the riverbed n= 0.030 and floodplain *n* = 0.045 and D. different Manning values for the riverbed *n* = 0.033 and floodplain *n* = 0.058

The flood inundation maps shown of the Lower Ayeyarwady River are the results of the Flood Hazard Mapper based on DEMs of Myanmar, a trapezoidal profile shape and chosen Manning roughness coefficients. The flood inundation maps show the average roughness of 0.033 s $m^{-1/3}$, as currently used in the Flood Hazard Mapper and the roughness for the riverbed *n*(wet) = 0.033 s $m^{-1/3}$ and floodplain *n*(dry) = 0.058 s $m^{-1/3}$.

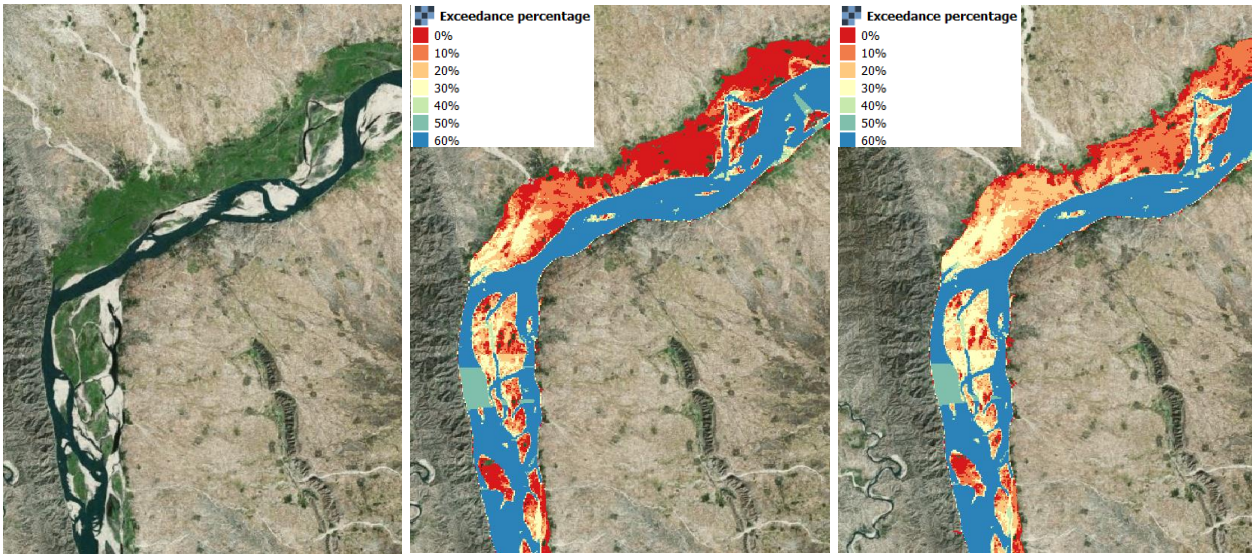

Figure 5-3 Inundation map at gauging station NyaungU with the exceedance percentage of the duration curve, single roughness *n* = 0.033 (middle) and different Manning values for the riverbed *n*(wet) = 0.033 and floodplain *n*(dry) = 0.058 (right)

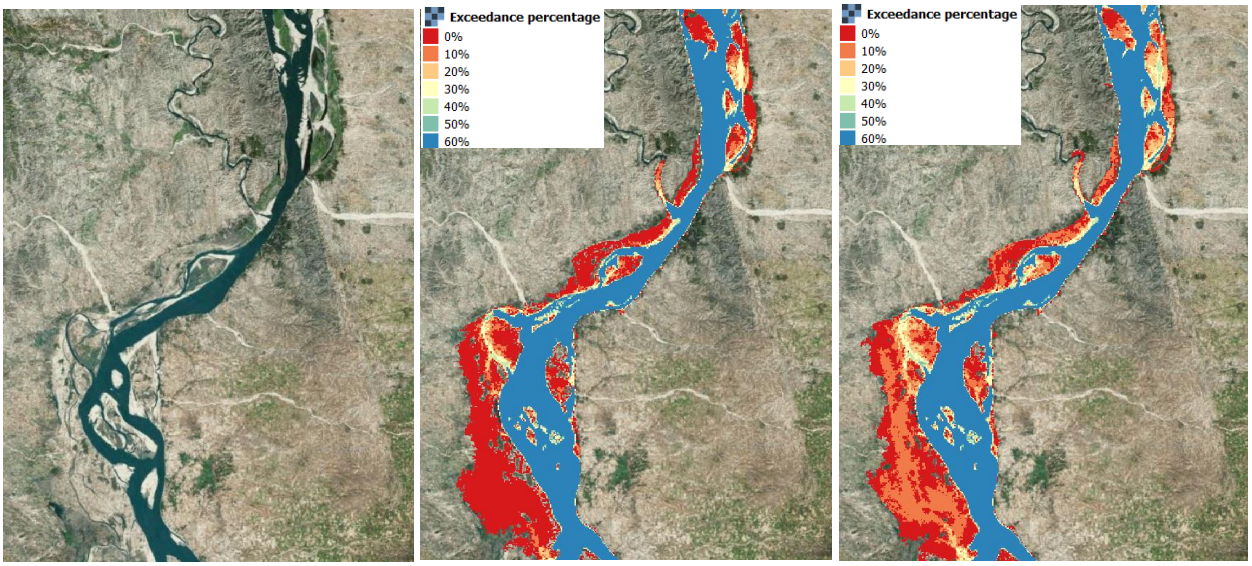

Figure 5-4 Inundation map at gauging station Chauk with the exceedance percentage of the duration curve, single roughness *n* = 0.033 (middle) and different Manning values for the riverbed *n*(wet) = 0.033 and floodplain *n*(dry) = 0.058 (right)

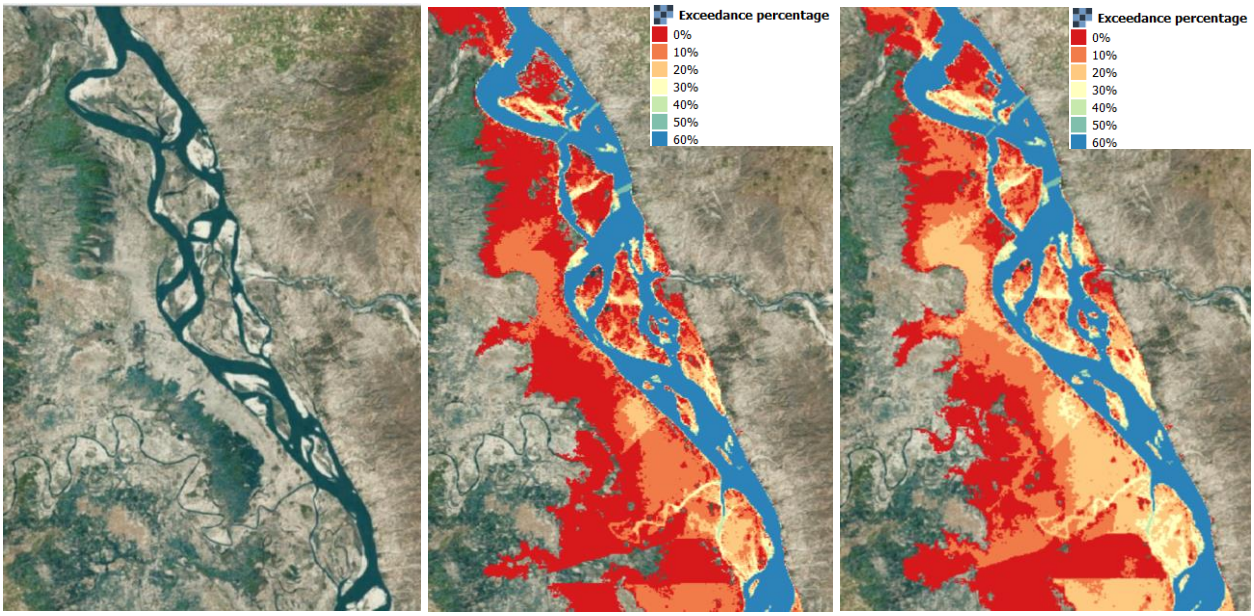

Figure 5-5 Inundation map at gauging station Magway with the exceedance percentage of the duration curve, single roughness *n* = 0.033 (middle) and different Manning values for the riverbed *n*(wet) = 0.033 and floodplain *n*(dry) = 0.058 (right)

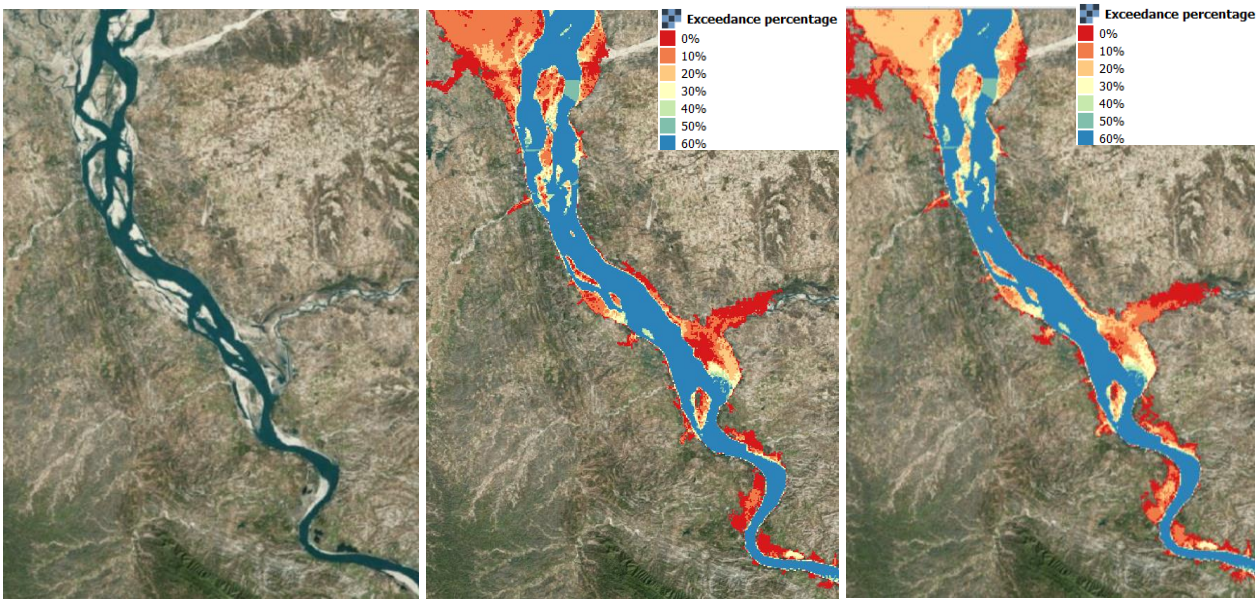

Figure 5-6 Inundation map at gauging station Aunglan with the exceedance percentage of the duration curve, single roughness *n* = 0.033 (middle) and different Manning values for the riverbed *n*(wet) = 0.033 and floodplain *n*(dry) = 0.058 (right)

The differences between the roughness approaches can be observed in inundation maps, where for the higher floodplain roughness lighter colours indicate that the area is flooded more frequently. It can also be observed that the total area of flooding slightly increases for different Manning coefficients, due to new areas that are beginning to flood at the lowest exceedance percentage. Separate roughness for the riverbed and floodplain has a visible influence on inundation maps, which mostly effects the frequency with which the floodplain of the Ayeyarwady is flooded becoming higher. The current approach causes the flood inundated area to be smaller than measured water levels at gauging stations would suggest. The new approach shows inundation levels closer to measured water levels at gauging stations, which would suggest that larger areas along to Lower Ayeyarwady can be inundated and also more frequent than currently implemented in the Flood Hazard Mapper.

6 Discussion

In the discussion, the representative discharges obtained from the data analysis, the shape of the bed profile and the roughness implementation in the Flood Hazard Mapper are discussed. First, the approach to determine representative discharges is discussed in section 6.1. Second, the approach to determine inundation levels is discussed in section 6.2. In the last section 6.3, the generation of flood inundation maps in the Flood Hazard Mapper is discussed.

6.1 Approach to determine representative discharge

The prediction of a model is only as accurate as the input data used to run the model, since poor input data will result in poor predictions. Also, the model used for simulating the water levels is determinative. Since the stage-discharge relationship can be derived, but it is unknown which datasets are used to determine these relations. Therefore, it is important to understand difficulties than can be found related to determining these relations. There can be uncertainties in the measurements for the stage-discharge relationship, especially for the low and high discharges. Stage-discharge relationships usually change with time, which is especially the case in alluvial and braided sand-bed rivers as the Ayeyarwady River. These changes occur either gradually or abruptly, due to scour and silting in the channel and moving sand dunes. For determining the representative discharges assumptions are made to account for these differences.

The changes in the river cross-section mainly depend on bed material size and flow velocities occurring. The profile changes are different between stations and through time, which makes profile measuring difficult and expensive. The changing roughness due to different bed forms has also an influence on the Q-H relation as derived from local data. Furthermore, when considering that gauging stations are heterogeneously and unevenly distributed, the calibration and validation of the Flood Hazard Mapper is an even more challenging task. However, it is especially relevant to make use of measurements, since a developing country as Myanmar has limited resources for flood protection.

6.2 Approach to determine inundation levels

The DEM used in the Flood Hazard Mapper does not display the wetted river profile during the SRTM measurement. The shape of the bed profile is therefore estimated by three different shapes. The profile shape is important for the total cross-section of the river and has influences on the simulated water levels in the Flood Hazard Mapper. The Ayeyarwady River is a large sand-bed river, which makes it difficult and expensive to collect and analyse data due to continuous profile changes. In the Flood Hazard Mapper, the bed profiles shapes for the river are an assumption, which mainly depends on the discharge during SRTM measurement. The SRTM measurement in February 2000 was during the dry season with very low discharges. However, DEM data during low river discharge is not always available for a river basin, which makes the reliability depend on the discharges of other catchments. Therefore, the uncertainty surrounding the to be determined river cross-section increases strongly, when available DEMs are not created at moments with low discharges.

Manning's roughness coefficients for the riverbed found in Chow's method are in the same range as currently implemented in the Flood Hazard Mapper. However, Manning's roughness coefficients for the floodplain is for both Chow's and Cowan's method higher than currently assigned. The roughness of the floodplain is taken as constant for the Ayeyarwady River from gauging station NyaungU till Pyay. Further, it should be considered that Cowan's method for roughness of the floodplain depends on the interpretation of the reader, which makes Cowan's method for determination of the roughness less ambiguous to use in the Flood Hazard Mapper compared to Chow's method. Finally, the representative discharges that are used to

compare the simulated water levels for the shape of the bed profile and the roughness are determined on only 11 representative discharges.

6.3 Approach to generate flood inundation maps

In a 1D hydrological model, floodplains are often not represented very well, since it is difficult to simulate overlapping cross-sections. Translation of water levels from a 1D model into flood inundation maps requires some effort to spread simulated water levels towards the floodplains. The delineation of flood inundation areas is a critical issue according to Samela et al., (2018), where practical difficulties in countries with limited data available can make complete achievement a challenge.

The flood inundation maps show for some areas sudden changes in height by the DEM, as shown by the green colour in the riverbed indicating a sudden higher elevation for that area in Figure 5-3. However, since high-accuracy coverage of DEM data (with elevation errors less than 1 m) is limited, so hydrologic modelling at regional or larger scales uses DEM data obtained by space borne sensors. The DEM data currently has a grid cell size adjusted to 90 x 90 meter for Myanmar. For covering elevation of a flat floodplain, the DEM data is not that precise. Therefore, it performs better on a hilly or mountainous terrain, because elevation differences are larger and the effect of an error due to accuracy less significant. High spatial resolution is a key factor for flood mapping, which is a limitation of using satellite data especially in urban areas. Therefore, the Flood Hazard Mapper is better to use for large scale areas instead of urbanised areas, where higher resolution than 90 x 90 meter is needed, since the roof height can be taken as mistake instead of the ground elevation.

7 Conclusion and recommendations

The conclusion recaps the results of this research and gives answers to the research questions as described in section 1.4. The questions are used to answer the main question of this research. Finally, the recommendations for further development of the Flood Hazard Mapper for quick scan basin scale flood analysis are described.

7.1 Conclusion

1. *Based on local datasets on water levels and derived discharges, which representative discharges through the river system of the Ayeyarwady River can be used?*

Analyses of discharge and water level series gave insight in the river system of the Ayeyarwady River. The water level records are measured daily at the gauging stations and are considered more reliable than the derived discharges series. The data analyses display the overall quality of the water levels and discharges records in the datasets and are used for determining representative discharges in the Flood Hazard Mapper. From the data analysis, it is found that the stage-discharge relationship is less reliable for extreme high and low discharges. This is indicated by the differences that are found in the duration curves, when compared between the gauging stations. The lower reliability for high discharges can be explained by flood events not happening frequently enough in the period the Q-H relation was determined, or lack measurements during the flood events. The lower reliability during low discharges can be explained by the static measurement of water levels in the sandy Ayeyarwady River, not considering scour and silting in the channel and moving sand dunes through time.
The duration curves are used to evenly distribute the representative discharges and are corrected for by the assumption that discharge at downstream gauging stations is expected higher than upstream. The representative discharges are used as input in the Flood Hazard Mapper to compare the shape of the bed profile and the Manning roughness coefficients of the riverbed and floodplain by comparing the simulated water levels of and the observed water levels at gauging stations.

2. *What is the influence of the profile shape of the unknown bed profile of the river cross-section?*

In the previous version of the Flood Hazard Mapper, the shape of the bed profile of the river is determined by the measured river width in the Digital Elevation Model (DEM), which is translated into a water depth using a width-to-depth ratio and assumes a rectangular shape. Furthermore, Manning roughness coefficients for the river are estimated between 0.030 – 0.050 s $m^{-1/3}$, based on the slope derived from the DEM.
In this research, the profile shape of the unknown bed profile of the river cross-section is tested for a rectangular, trapezoidal and channel shape for a wide range in Manning roughness coefficients. The results show that the best wetted profile to use for the Lower Ayeyarwady River is the trapezoidal shape. The trapezoidal shape performs significantly better than the rectangular and channel shape, where the roughness needs to be significantly higher than what literature suggests for this type of river and floodplain. For the unknown bed profile by the DEM in the Flood Hazard Mapper, a trapezoidal shape shows most realistic outcomes compared to measured water levels of the Lower Ayeyarwady River. The results show that the bed profile shape of the unknown part of the river cross-section is important, since it influences the simulated water levels.

3. *Which representative Manning's roughness coefficients for the riverbed and floodplain should be used for the Lower Ayeyarwady River?*

To determine representative Manning's roughness coefficients for the riverbed and floodplain of the Lower Ayeyarwady River, roughness coefficients found in literature by Chow and Cowan are used. The result for the Lower Ayeyarwady River show that the Manning roughness coefficient for the riverbed named '*n(wet)*' should be between 0.030-0.033 s $m^{-1/3}$ based on Chow's roughness coefficients, which corresponds with the roughness 0.030-0.035 s $m^{-1/3}$ as currently implemented in the Flood Hazard Mapper. However, the Manning roughness coefficient for the floodplain named '*n*(dry)' should be between 0.045-0.058 s $m^{-1/3}$ according to Chow's and Cowan's method, which is significantly higher than previous between 0.030-0.035 s $m^{-1/3}$. The results in this research show that using separate roughness coefficients for the riverbed and floodplain, significantly decreases the Root Mean Square Error (RMSE) between the simulated and observed water levels and therefore improves the outcome of the model.

4. *What is the effect of different roughness coefficients for the riverbed and floodplain on generated water levels and flood inundation maps by the Flood Hazard Mapper?*

The advantages of the new approach are that the wetted profile is defined and the different roughness coefficients for the riverbed and floodplain are given in the Flood Hazard Mapper. Roughness is especially an important factor for simulating water levels at locations with low slopes and large floodplains. The outcome of one roughness value for both riverbed and floodplain, as currently used in the Flood Hazard Mapper, is compared to different roughness coefficients for the riverbed and floodplain.
The Root Mean Square Error (RMSE) is significantly lower for different roughness coefficients of the riverbed and floodplain than the currently implemented roughness coefficient for the river. The RMSE values in Table 5-6 are between 0.87-0.61 meters on average for the current approach, compared to 0.53-0.55 meter on average for different roughness coefficients. So, the average RMSE of the water levels exceedance can be improved by 7 till 33 cm by using different roughness coefficients for the riverbed and floodplain.
The new approach shows water levels significantly closer to observed water levels at gauging station along the Lower Ayeyarwady River in Figure 5-1. This new approach causes the flood inundated area to be closer to the observed water levels at gauging stations, which would suggest that larger areas along to Lower Ayeyarwady can be inundated during flooding and also more frequent than currently implemented in the Flood Hazard Mapper.

The main question of this research is: *"Can the Flood Hazard Mapper, for basin scale river flood risk analysis, be improved by implementing roughness for the riverbed and floodplain and/or by determined bed profile shape for the Ayeyarwady River in Myanmar?"*

Based on the results of the case study on the Lower Ayeyarwady River, the Flood Hazard Mapper will improve by implementing different roughness coefficients for the riverbed and floodplain. The average RMSE of the water levels will improved by 7 till 33 cm compared to observed water levels at gauging stations along the Lower Ayeyarwady River. However, according to the results of this research the choice in the river profile shape of the unknown part of the river cross-section is also important, where the average RMSE of the water levels exceedance can be improved by 30 till 60 cm compared to observed water levels at gauging stations along the Lower Ayeyarwady River.
This research shows that it is important to make a separation between the roughness of the riverbed and floodplain. For the Lower Ayeyarwady River it is found that the Manning roughness coefficient *n* from literature for the riverbed between 0.030-0.033 s $m^{-1/3}$ is in the same range as currently implemented in the Flood Hazard Mapper. Whereas, the roughness coefficient of the floodplain is between 0.045-0.058 s $m^{-1/3}$ (1,5 till 2 times higher). This study shows that it is important to determine the shape of bed profile the

unknown part of the river cross-section when using a DEM. The results show that the use of a trapezoidal shape of the river bed and a separated Manning coefficient for the river bed and floodplains, with a higher value for the floodplains, reduced the root mean square error between the measured and simulated water levels compared to the current model, suggesting that more accurate flood inundation maps are produced for the Ayeyarwady River in Myanmar.

7.2 Recommendations

Form the results of this research, it is recommended to implement different roughness coefficients for the riverbed and the floodplain for the Ayeyarwady River as well as for other rivers. Second, it is recommended to use a trapezoidal shape of the bed profile for the unknown river cross-section in the DEM for sandy rivers with similar characteristics as the Lower Ayeyarwady. This research shows that a trapezoidal profile shape significantly improves the water level outcomes of the Flood Hazard Mapper compared to measured water level. Applying different roughness coefficients for the riverbed and floodplain, especially matter for extreme discharges/floods in the Flood Hazard Mapper. The recommendation of the shape of the bed profile is based on data from the Ayeyarwady River and is recommended to first be tested before implemented for other river basins in the Flood Hazard Mapper.

Further, it is recommended for the Ayeyarwady River to research the joint probability of the Chindwin River and the upper part of the Ayeyarwady. At this location, the likelihood of two flood events occurring together at the same point in time (joint probability) can be calculated. This event is recommended for further research, since it will affect downstream flooding of the Ayeyarwady River. Furthermore, it is important to notice that short discharge waves are normally flattened when flowing into the floodplains, which is not represented yet in the Flood Hazard Mapper.

It is recommended to Royal HaskoningDHV to further improve the Flood Hazard Mapper by comparing outcomes with other models, as well as with data from different river basins around the world. This will contribute to further development of the Flood Hazard Mapper and help further calibration and validation, before the tool is used for other river basins for which no or limited data are available.

Finally, it is recommended to Directorate of Water Resources and Improvement of River Systems (DWIR) and the Irrigation and Water Utilization Management Department (IWUMD) in Myanmar to improve some stage-discharge relationships of gauging stations along the Ayeyarwady River. First, the relation at station Chauk should be changed, since both for high discharges as low discharges there are large difference with other stations along the Ayeyarwady River. Further, for station Magway low discharges are too high and for station Aunglan the low discharges are too low compared to the other stations.

References

Aquastat. (2011). *Irrigation in Southern and Eastern Asia in figures*. Rome. Retrieved from http://www.fao.org/3/i2809e/i2809e.pdf

Aung, L. L., Zin, E. E., Theingi, P., Elvera, N., Aung, P. P., Han, T. T., … Skaland, R. G. (2017). *Myanmar Climate Report*. Department of Meteorology and Hydrology Myanmar, Ministry of Transport and Communications, Government of the Republic of the Union of Myanmar; Norwegian Meteorological Institute, Norway.

Baldassarre, G. Di, Schumann, G., Bates, P. D., Freer, J. E., Di, G., Schumann, G., … Freer, J. E. (2010). Flood-plain mapping : a critical discussion of deterministic and probabilistic approaches probabilistic approaches, *6667*. https://doi.org/10.1080/02626661003683389

Berends, K. D., Warmink, J. J., & Hulscher, S. J. M. H. (2018). Environmental Modelling & Software Efficient uncertainty quantification for impact analysis of human interventions in rivers. *Environmental Modelling & Software*, *107*, 50–58. https://doi.org/10.1016/j.envsoft.2018.05.021

Boulomytis, V. T. G., Zuffo, A. C., Dalfré Filho, J. G., & Imteaz, M. A. (2017). Estimation and calibration of Manning's roughness coefficients for ungauged watersheds on coastal floodplains. *International Journal of River Basin Management*, *15*(2), 199–206. https://doi.org/10.1080/15715124.2017.1298605

Braca, G. (2014). Stage-discharge relationships in open channels: Practices and problems, (October).

Chavoshian, A., Ishidaira, H., Takeuchi, K., & Yoshitani, J. (2007). Hydrological modeling of large-scale ungauged basin case study of Ayeyarwady (Irrawaddy) Basin, Myanmar. *Paper Presented at the HRSD 2007 Conference in Conjunction with the 15th Regional Steering Committee Meeting for UNESCO-IHP Southeast Asia and the Pacific.* Retrieved from http://pwweb1.pwri.go.jp/eng/activity/pdf/reports/ali.071116.pdf

Cole, R. A. J., Johnston, H. T., & Robinson, D. J. (2003). The use of flow duration curves as a data quality tool. *Hydrological Sciences Journal*, *48:6*. https://doi.org/10.1623/hysj.48.6.939.51419

Cowan, W. L. (1956). *Estimating hydraulic roughness coefficients: Agricultural Engineering*.

Daleles, C., Donato, A., Adriana, L., Vianei, J., Hodnett, M. G., Tomasella, J., & Waterloo, M. J. (2008). HAND, a new terrain descriptor using SRTM-DEM: Mapping terra-firme rainforest environments in Amazonia. *Remote Sensing of Environment*. https://doi.org/10.1016/j.rse.2008.03.018

Davies, R. (2016). Myanmar – Floods Affect Almost Half a Million People. Retrieved March 1, 2019, from http://floodlist.com/asia/myanmar-floods-affect-half-million-august-2016

Disse, M. (2018). Uncertainties in hydrodynamic moddeling. Retrieved February 15, 2019, from https://courses.edx.org/courses/course-v1:RWTHTUMx+FRMx+3T2017/courseware/f1890df20fdb4090914c04bfecf85bc5/1b09ec9577e041beb9e6189073469fab/1?activate_block_id=block-v1%3ARWTHTUMx%2BFRMx%2B3T2017%2Btype%40vertical%2Bblock%404fc93630c20b4f16ac2aba2a57866f3

Domeneghetti, A., Tarpanelli, A., Grimaldi, L., Brath, A., & Schumann, G. (2018). Flow Duration Curve from Satellite : Potential of a Lifetime SWOT Mission. *Remote Sensing*, *10*. https://doi.org/10.3390/rs10071107

Ettritch, G., Hardy, A., Bojang, L., D, C., Bunting, P., & Brewer, P. (2018). Enhancing digital surface models for hydraulic modelling using flood frequency detection. *Remote Sensing of Environment*, *217*, 506–522. https://doi.org/10.1016/J.RSE.2018.08.029

Fathi-Moghadam, M., Kashefipour, S., Ebrahimi, N., & Emamgholizadeh, M. (2011). Physical and Numerical Modeling of Submerged Vegetation Roughness in Rivers and Flood Plains. *Journal of Hydrologic Engineering*, (November), 858–864. https://doi.org/10.1061/(ASCE)HE.1943-

5584.0000381

Finnegan, N. J., Roe, G., Montgomery, D. R., & Hallet, B. (2005). Controls on the channel width of rivers : Implications for modeling fluvial incision of bedrock. *Geology*, *33*(3), 229–232. https://doi.org/10.1130/G21171.1

Food and Agriculture Organisation of the United Nations. (2015). FAO in emergencies: Myanmar. Retrieved February 5, 2019, from http://www.fao.org/emergencies/countries/detail/en/c/326208/

Furuichi, T., Win, Z., & Wasson, R. J. (2009). Discharge and suspended sediment transport in the Ayeyarwady River , Myanmar : Centennial and decadal changes, (April), 1631–1641. https://doi.org/10.1002/hyp

George, J., Archement, J. R., & Schneider, V. R. (1989). Guide for Selecting Manning's Roughness Coefficients for Natural Channels and Floodplains United States Geological Survey Water-supply Paper, *2339*, 39. https://doi.org/Report No. FHWA-TS-84-204

Ghani, A. A., Zakaria, N. A., Kiat, C. C., Ariffin, J., Hasan, Z. A., & Abdul Ghaffar, A. B. (2007). Revised equations for manning's coefficient for sand-bed rivers. *International Journal of River Basin Management*, *5*(4), 329–346. https://doi.org/10.1080/15715124.2007.9635331

Holmes, R. R., & Garcia, M. H. (2008). Flow over bedforms in a large sand-bed river : A field investigation Flow over bedforms in a large sand-bed river : A field investigation Ecoulements sur des configurations de lits sableux de grands fleuves : investigation en nature. *Journal of Hydraulic Research*, *46*(3), 322–333. https://doi.org/10.3826/jhr.2008.3040

ICEM. (2018). *Ayeyarwady intergated river basin management project (AIRBMP): Executive summary for ESIA of subproject 1*.

International Federation of Red Cross and Red Crescent Societies. (2017). *Final Report Myanmar : Floods*.

Julien, P. Y. (2002). *River Mechanics*. Cambridge: Cambridge University Press.

Kennedy, E. J. (1984). Techniques of Water-Resources Investigations of the United States Geological Survey; Discharge ratings at gaging stations. In *Applications of Hydraulics*.

Kim, J.-S., Lee, C.-J., Kim, W., & Kim, Y.-J. (2010). Roughness coefficient and its uncertainty in gravel-bed river. *Water Science and Engineering*, *3*(2), 217–232. https://doi.org/10.3882/j.issn.1674-2370.2010.02.010

Kim, J., Kim, W., & Kim, J. P. (2015). Discharge Estimation in a Backwater Affected River Junction Using HPG. *Journal of Water Rescources Planning and Hydraulic Engineering*, *4*(2), 205–210. https://doi.org/10.5963/JWRHE0402011

Klaassen, G. J. (1992). Planform changes of a braided river with fine sand as bed and bank material. *5th International Symposium on River Sedimentation*.

Luo, T., Maddocks, A., Iceland, C., Ward, P., & Winsemius, H. (2015). World Resources Institute: World's 15 Countries with the Most People Exposed to River Floods. Retrieved September 21, 2018, from https://www.wri.org/blog/2015/03/world's-15-countries-most-people-exposed-river-floods

Luo, X., Li, H., Leung, L. R., Tesfa, T. K., Getirana, A., & Papa, F. (2017). Modeling surface water dynamics in the Amazon Basin using MOSART-Inundation v1.0 : impacts of geomorphological parameters and river flow representation. *Geoscientific Model Development*, *10*, 1233–1259. https://doi.org/10.5194/gmd-10-1233-2017

Mander, R. J. (1978). Aspects of unsteady flow and variable backwaters. *Hydrometry: Principles and Practice*, *1*(1).

Marcus, W. A., Roberts, K., Harvey, L., & Tackman, G. (1992). An Evaluation of Methods for Estimating Manning's n in Small Mountain Streams. *Mountain Research and Development*, *12*(3), 227.

https://doi.org/10.2307/3673667

Marg, O. P., & Khas, H. (1999). *How to establish stage discharge rating curve*. New Delhi, India.

Maswood, M., & Hossain, F. (2016). Advancing river modelling in ungauged basins using satellite remote sensing : the case of the Ganges – Brahmaputra – Meghna basin Advancing river modelling in ungauged basins using satellite remote sensing : the case of the Ganges – Brahmaputra – Meghna b. *International Journal of River Basin Management*, *14*(1), 103–117. https://doi.org/10.1080/15715124.2015.1089250

MIMU. (2016). Myanmar Information Management Unit: Monsoon flooding 2016. Retrieved March 1, 2019, from http://themimu.info/emergencies/floods-2016

Nobre, A. D., Cuartas, L. A., Hodnett, M., Rennó, C. D., Rodrigues, G., Silveira, A., … Saleska, S. (2011). Height Above the Nearest Drainage - a hydrologically relevant new terrain model. *Journal of Hydrology*, *404*(May), 13–29. https://doi.org/10.1016/j.jhydrol.2011.03.051

Nomden, H. G. (2018). *Assignment description: Further development Quick Scan tool for river basin scale flood risk analysis*. Royal Haskoning DHV, Amersfoort.

Notti, D., Giordan, D., Caló, F., Pepe, A., Zucca, F., & Galve, J. P. (2018). *Potentiality and Limitations of Open Satellite Data for Flood Mapping*. Research Institute for Geo-Hydrological Protection, Torino, Italy. https://doi.org/10.20944/preprints201807.0624.v1

Patro, S., Chatterjee, C., Mohanty, S., Singh, R., & Raghuwanshi, N. (2009). Flood Inundation Modeling using MIKE FLOOD and Remote Sensing Data, (May 2014). https://doi.org/10.1007/s12524-009-0002-1

Petersen-Øverleir, A. (2006). Modelling stage — discharge relationships affected by hysteresis using the Jones formula and nonlinear regression. *Hydrological Sciences Journal*, *51*(3), 365–388. https://doi.org/10.1623/hysj.51.3.365

Phillips, J. V, & Tadayon, S. (2006). *Selection of Manning ' s Roughness Coefficient for Natural and Constructed Vegetated and Non- Vegetated Channels , and Vegetation Maintenance Plan Guidelines for Vegetated Channels in Central Arizona: Scientic Investigations Report 2006 – 5108*.

Rai, R. K., Upadhyay, A., Sarkar, S., Upadhyay, A. M., & Singh, V. P. (2009). GIUH Based Transfer Function for Gomti River Basin of India. *Journal of Spatial Hydrology*, *9,*(2), 24–50.

Saleh, F., Ducharne, A., Flipo, N., Oudin, L., & Ledoux, E. (2013). Impact of river bed morphology on discharge and water levels simulated by a 1D Saint-Venant hydraulic model at regional scale. *Journal of Hydrology*, *476*, 169–177. https://doi.org/10.1016/j.jhydrol.2012.10.027

Samela, C., Albano, R., Sole, A., & Manfreda, S. (2018). A GIS tool for cost-effective delineation of flood-prone areas. *Computers , Environment and Urban Systems*, *70*, 43–52. https://doi.org/10.1016/j.compenvurbsys.2018.01.013

Schellekens, J. (2018). *Wflow Documentation*. Detares, Delft.

Schumann, G., Matgen, P., Hoffmann, L., Hostache, R., Pappenberger, F., Pfister, L., & Carlo-based, M. (2007). Deriving distributed roughness values from satellite radar data for flood inundation modelling, 96–111. https://doi.org/10.1016/j.jhydrol.2007.06.024

Sharma, S. K., Kwak, Y., Kumar, R., & Sarma, B. (2018). Analysis of Hydrological Sensitivity for Flood Risk Assessment. *International Journal of Geo-Information*, *7,*(51), 1–17. https://doi.org/10.3390/ijgi7020051

Shaw, E. M., Beven, K. J., Chappell, N. A., & Lamb, R. (2011). *Hydrology in Practice; Fourth edition*. New York: Spon Press.

Sichangi, A. W., Wang, L., Yang, K., Chen, D., Wang, Z., Li, X., … Kuria, D. (2016). Remote Sensing of Environment Estimating continental river basin discharges using multiple remote sensing data sets.

Remote Sensing of Environment, *179*, 36–53. https://doi.org/10.1016/j.rse.2016.03.019

Soong, D. T., Prater, C. D., Halfar, T. M., & Wobing, L. A. (2012). *Manning's Roughness Coefficients for Illinois Streams Data Series 668*. Illinois Department of Natural Resources–Office of Water Resources.

Strahler, A. N. (1957). Quantitative Analysis of Watershed Geomorphology. *EOS, Transactions American Geophysical Union*, *38*, 913–920. Retrieved from http://dx.doi.org/10.1029/TR038i006p00913

Te Chow, V. (1959). *Open-channel hydraulics*. McGraw-Hill Book Company.

Than, H. H. (2012). Flood Risk Management in Chindwin River Basin (Myanmar). Retrieved from https://www.unece.org/fileadmin/DAM/env/documents/2015/WAT/03Mar_19-20_Geneva/presentations/Session_1_Presentation_Htay_Htay_V2_EN.pdf.pdf

Torbick, N., Chowdhury, D., Salas, W., & Qi, J. (2017). Monitoring Rice Agriculture across Myanmar Using Time Series Sentinel-1 Assisted by Landsat-8. https://doi.org/10.3390/rs9020119

United Nations Office for Disaster Risk Reduction. (2015). *The Human Cost of Weather Related Disasters 1995-2015*.

Utrecht University. (2018). PCRaster software for evironmental modelling. Retrieved November 12, 2018, from http://pcraster.geo.uu.nl/pcraster_courses/how-to-subscribe/

Van Huijgevoort, M. H. J., Tetzlaff, D., Sutanudjaja, E. H., & Soulsby, C. (2016). Using high resolution tracer data to constrain water storage, flux and age estimates in a spatially distributed rainfall-runoff model. *Hydrological Processes*, *30,*(25), 4761–4778. https://doi.org/10.1002/hyp.10902

Verwey, A., Kerblat, Y., & Chia, B. (2017). *Flood Risk Management at River Basin Scale : The need to adopt a proactive approach*. The World Bank Group: Urban Floods Community of Practice (UFCOP).

Vogel, R. M., & Fennessey, N. M. (1994). Flow-Duration Curves. *Journal of Water Rescources Planning and Management*, *120*(4), 485–503.

Warmink, J. J., Straatsma, M. W., & Huthoff, F. (2012). The effect of hydraulic roughness on design water levels in river models. *Comprehensive Flood Risk Management*, 157–164.

Wiele, S. M., & Torizzo, M. (2003). *A Stage-Normalized Function for the Synthesis of Stage-Discharge Relations for the Colorado River in Grand Canyon , Arizona*. Tucson, Arizona.

Yamazaki, D., Ikeshima, D., Tawatari, R., Yamaguchi, T., O'Loughlin, F., Neal, J. C., … Bates, P. D. (2017). A high-accuracy map of global terrain elevations. *Geophysical Research Letters*, 5844–5853. https://doi.org/10.1002/2017GL072874

Zin, W. W., Kawasaki, A., Takeuchi, W., Mar, Z., & Tin, L. (2018). Flood Hazard Assessment of Bago River Basin , Myanmar Flood Hazard Assessment of Bago River Basin , Myanmar, (February). https://doi.org/10.20965/jdr.2018.p0014

Appendix A Hydrological data

A.1 Translation of gauge height to MSL and SRTM-DEM water level

The Digital Elevation Model (DEM) used in the Flood Hazard Mapper is based on the Shuttle Radar Topography Mission (SRTM) between 11-22 February 2000. In the case study Myanmar, the month February falls within the dry season with low river discharges, which means that the river floodplain and some parts of the river cross-section are observed. At the locations of the gauging station, the measured water levels from the local dataset in 17 February 2000 is used. The measured height of the water level by radar read from the DEM is compared with the measured water level at the gauging stations. In this way, a reference level based on SRTM measurement is obtained, which is used to estimate the Mean Sea Level (MSL) for the measured water level records. The translation from local reference points to SRTM water level is illustrated in Figure 0-1. The coordinates of these gauging stations are displayed in Google Earth, which is loaded in QGIS interface used to display the Flood Hazard Mapper. In this way, the water levels at the measurement location are compared at the same location.

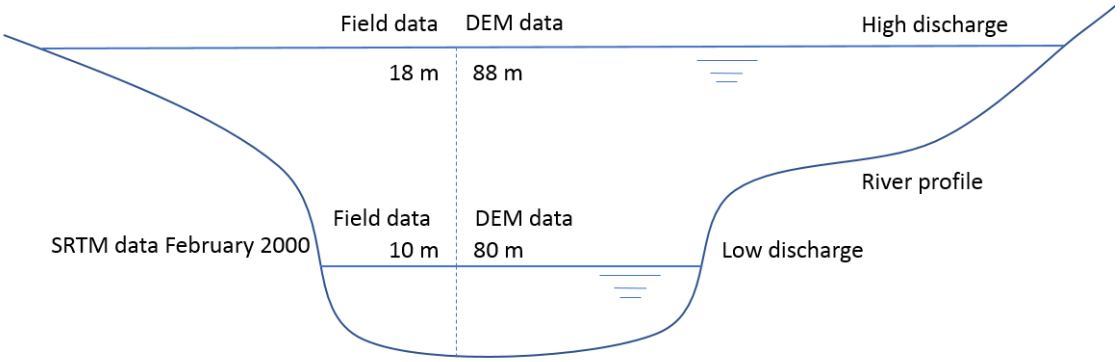

Figure 0-1 Translation from the measured water levels at gauging stations compared to water level and topography measured during the Shuttle Radar Topography Mission (SRTM) in the Digital Elevation Model (DEM) of Myanmar

The water level difference of the gauging stations is used to correct the water levels to DEM height as used in the model and to an estimated Mean Sea Level. To be able to use the measured water levels in the Flood Hazard Mapper, the water levels are adjusted to the water level of the DEM with the use of Table 0-1.

Table 0-1 Water level at stations along the Ayeyarwady River measured with SRTM-DEM (Shuttle Radar Topography Mission) data

Water level at stations along the Ayeyarwady River during SRTM date (17 February 2000)			
Station	SRTM-DEM data	Locally measured data	Difference
Ayeyarwady River	Water Level (m)	Water Level (m)	Water level (m)
Myitkyina	130.13	1.92	128.21
Katha	87.57	1.55	86.02
Sagaing	62.02	2.52	59.50
NyaungU	49.71	1.02	48.69
Chauk	45.02	3.56	41.46
Magway	33.25	4.54	28.71
Aunglan	24.28	12.15	12.13
Pyay	19.4	18.08	1.32
Chindwin River			
Monywa	67.56	1.74	65.82

The measured daily water levels from the period 1966-1986 (DWIR) and 1980-2017 (IWUMD) are combined and used to replace missing measurements of the discharge record shown in Figure 0-2.

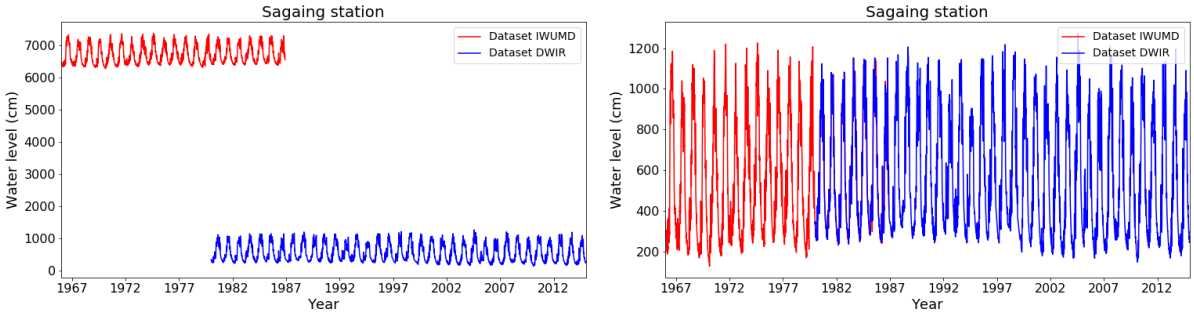

Figure 0-2 Daily measured water levels from the Directorate of Water Resources and Improvement of River Systems (DWIR) from 1966-1986 and the Irrigation and Water Utilization Management Department (IWUMD) from 1980-2017 (left) corrected for difference in height (right)

For these stations, both SRTM-DEM water levels and the measured water levels are available. By subtracting the difference, all daily water level measurements are adjusted for the DEM height in February 2000. In this way a discharge recorded from 1966 till 2017 is derived as shown in Figure 0-3. The result in Figure 0-3 shows the water level above the DEM height in the Flood Hazard Mapper.

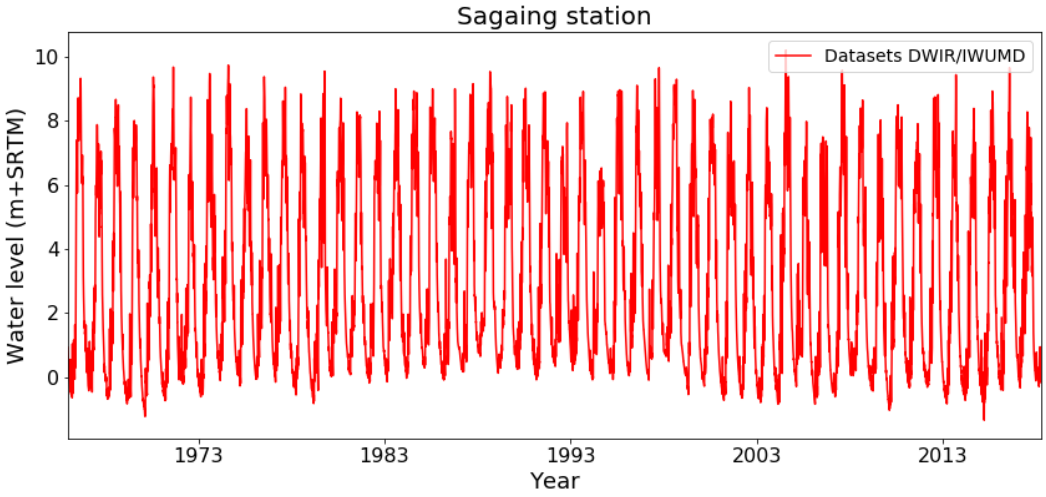

Figure 0-3 Daily water level measurements from local datasets combined for the period 1966-2014 adjusted to the SRTM-DEM water level in the Flood Hazard Mapper as 0 m in February 2000

With the water level at the same SRTM data (17 February 2000), the water level is adjusted to Mean Sea Level (MSL). The adjusted water levels for each gauging station can be found in Appendix 0.

A.2 Water levels

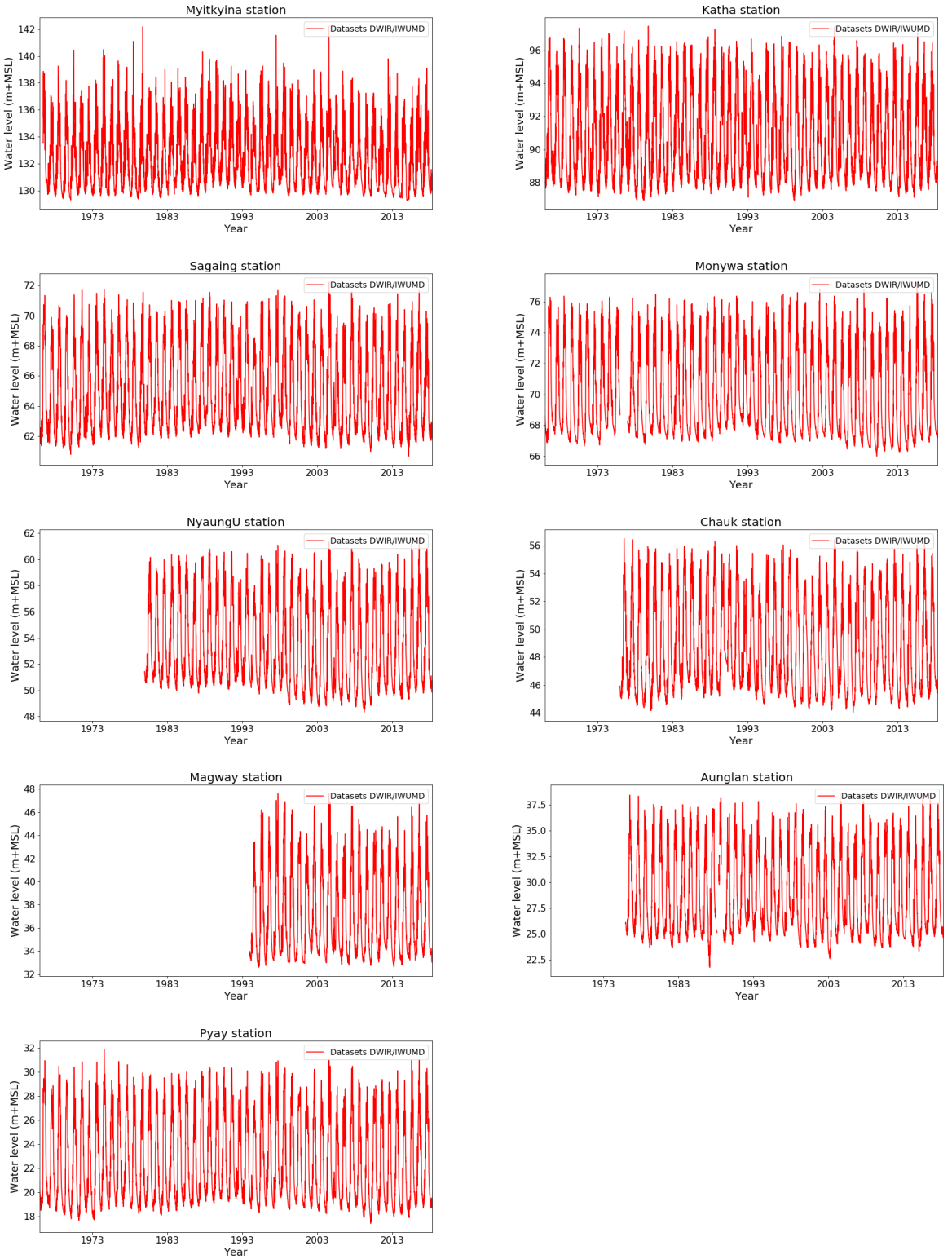

Figure 0-4 Daily water level measurements from local datasets combined for the period 1966-2014 adjusted to the Mean Sea level (MSL) by using the SRTM-DEM data (February 2000)

A.3 Q-H relations

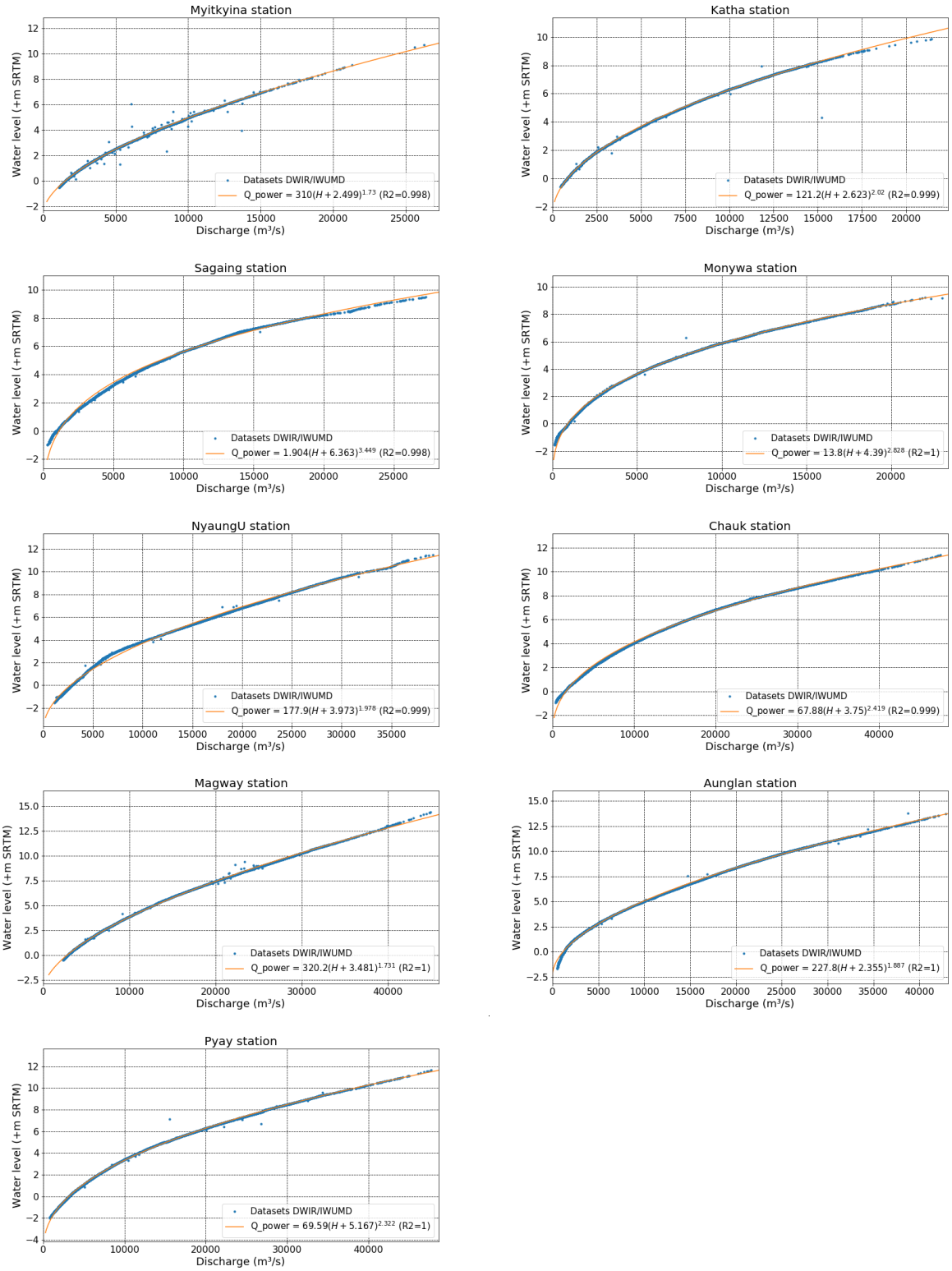

Figure 0-5 The derived Q-H relation and the Power equation with corresponding coefficient of determination R^2 for each gauging

A.4 Hydrological discharges

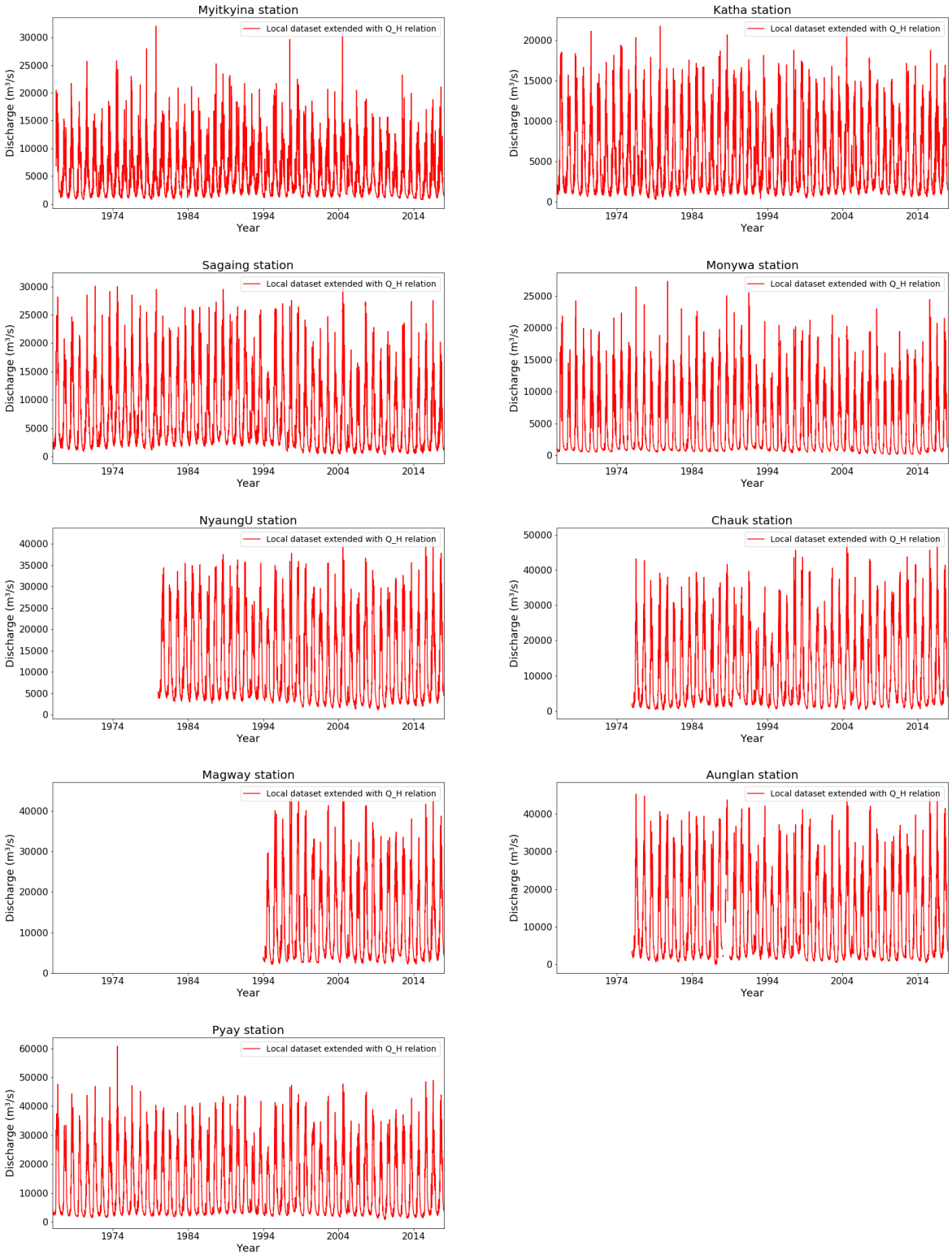

Figure 0-6 The discharge series of each station, extended with the water level measurements and the power equation from derived Q-H relation

A.5 H Exceedance

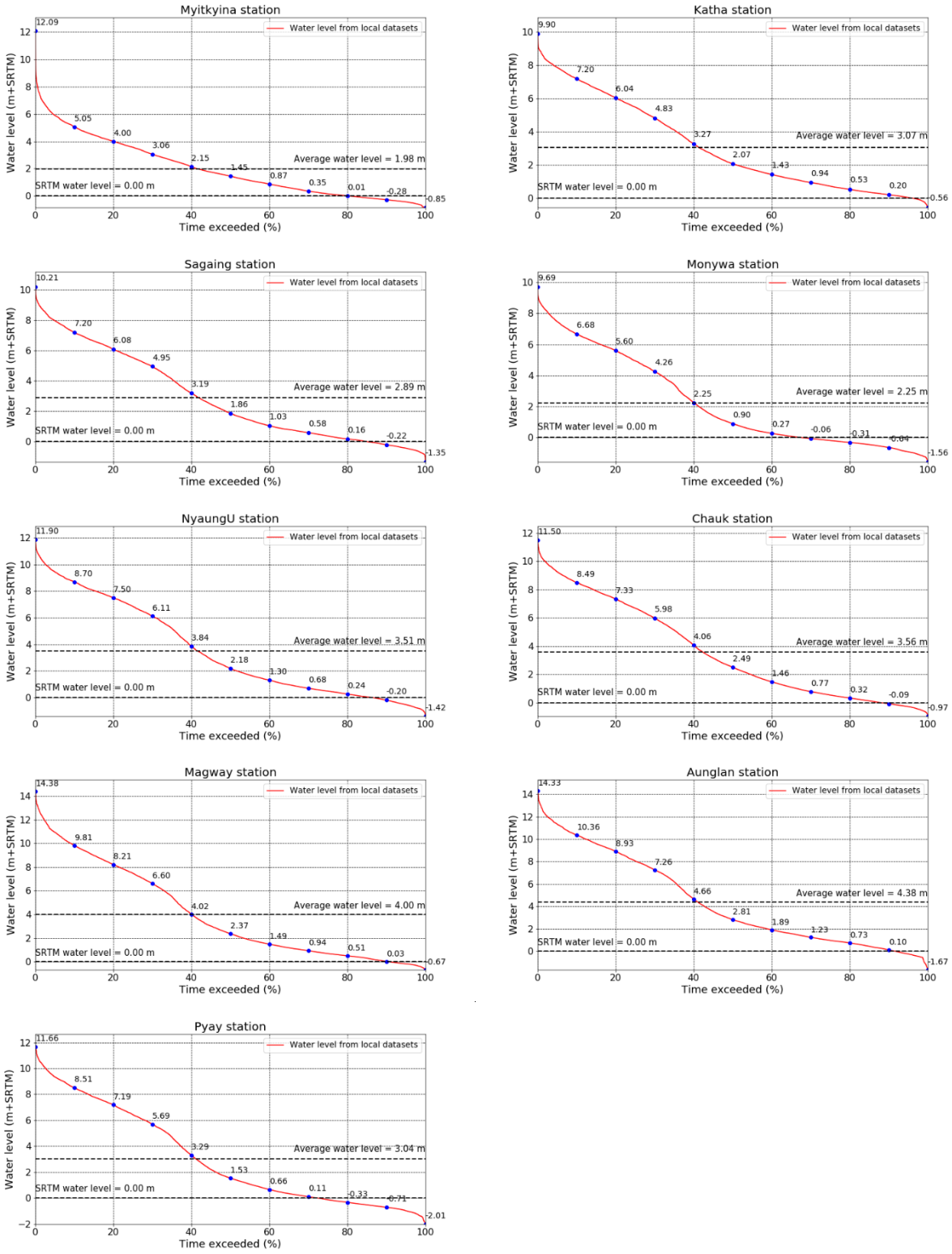

Figure 0-7 Percentage of the time a water level from local measurements is exceeded for each gauging station (1994-2017)

A.6 Q Exceedance

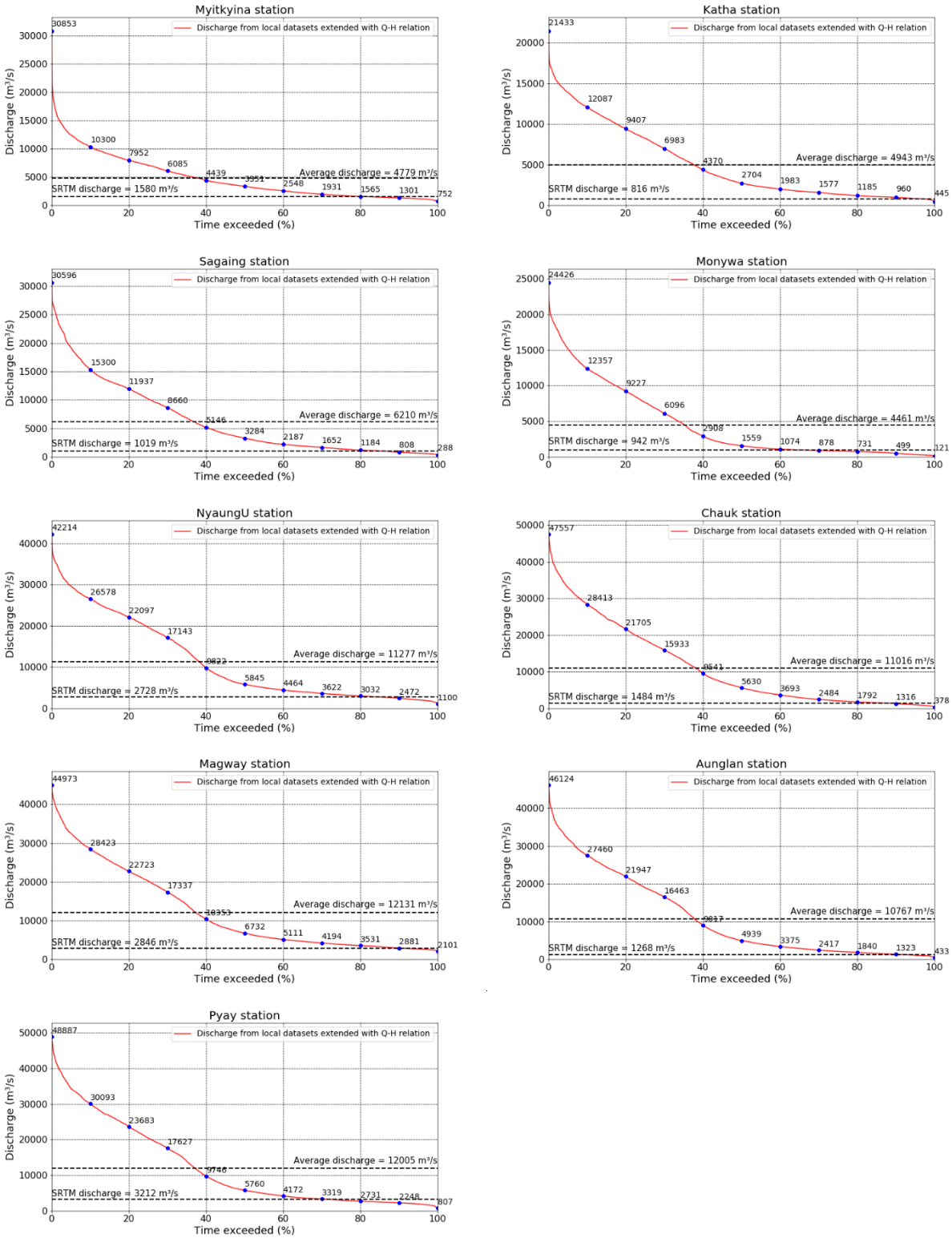

Figure 0-8 Percentage of the time a discharge from local measurements is exceeded for each gauging station (1994-2017)

A.7 Distribution between the Ayeyarwady and the Chindwin

The discharge distribution between the Chindwin and the Ayeyarwady River is determined for every year at the location of the gauging stations. The water balance between the average discharge from the Ayeyarwady and the Chindwin branch is shown in Figure 0-9. These percentages are estimated for the local dataset as well as for the Wflow model outcomes in the Flood Hazard Mapper. The percentages can slightly change between depending on the rainfall events or between the monsoon and the dry and hot season.

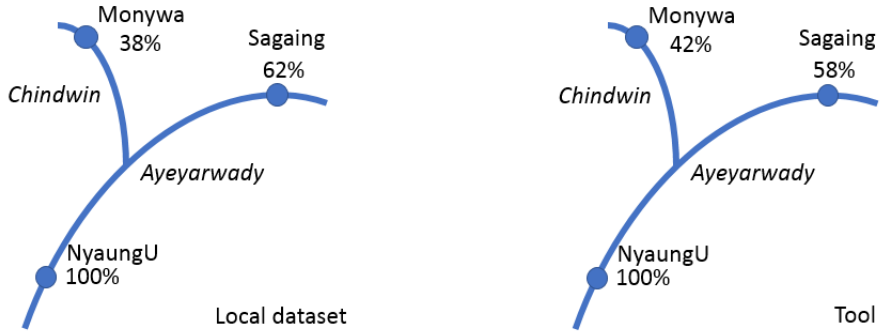

Figure 0-9 Water balance of the Chindwin and the Ayeyarwady determined for the local measurements of the gauging stations and the average discharge derived from the Flood Hazard Mapper

Including the discharge of the Upper Ayeyarwady at Sagaing station with the discharge of the Chindwin River at Monywa station displays the green line in Figure 0-10. Where the river length between Sagaing and Monywa station till NyaungU station is comparable. The difference between NyaungU station during extreme discharges is partly explained by the flooding that occurs in the area in between the stations and the difficulties in determining high flow discharges. Errors caused by incorrect water level data and Q-H relations tend to occur at low or high flows due to problems with the station construction or instrumentation faults (Cole et al., 2003). Thus, these discharges are likely to cause the true flow range to be exceeded, either above or below.

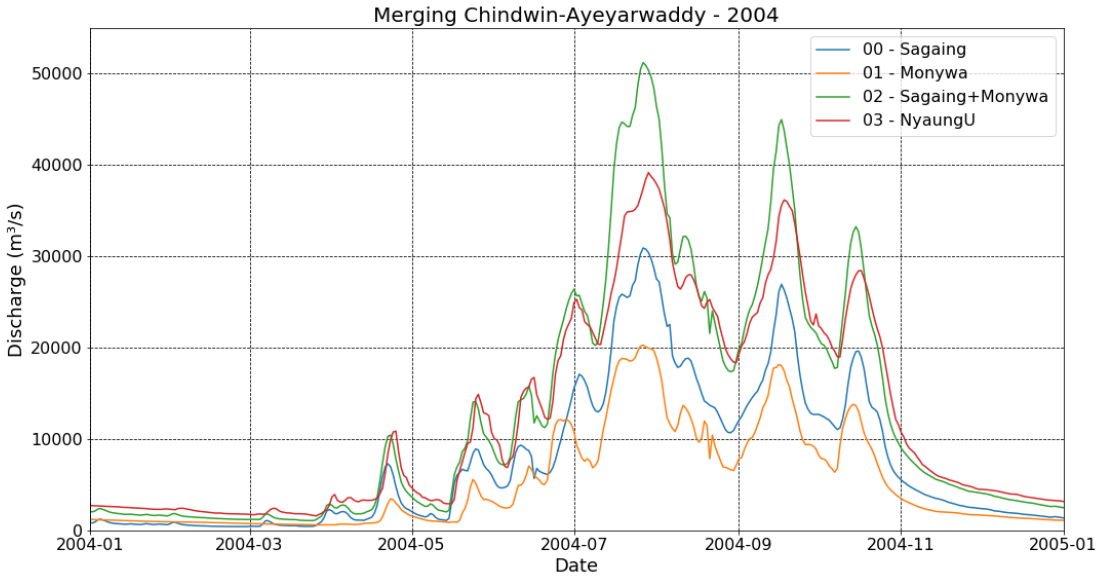

Figure 0-10 Merging of the Chindwin and the Upper Ayeyarwady during a large flood in 2004

The discharge of the Upper Ayeyarwady (station Sagaing) and the Chindwin (station Monywa) in 2004 is shown in Figure 0-10, which is compared with the discharge at NyaungU station. The discharges of gauging

stations in Figure 0-11 follows the expected discharge at NyaungU station. Although, during high discharge, the combined discharge coming from station Sagaing and Monywa seems to be higher than the discharge at NyaungU station.

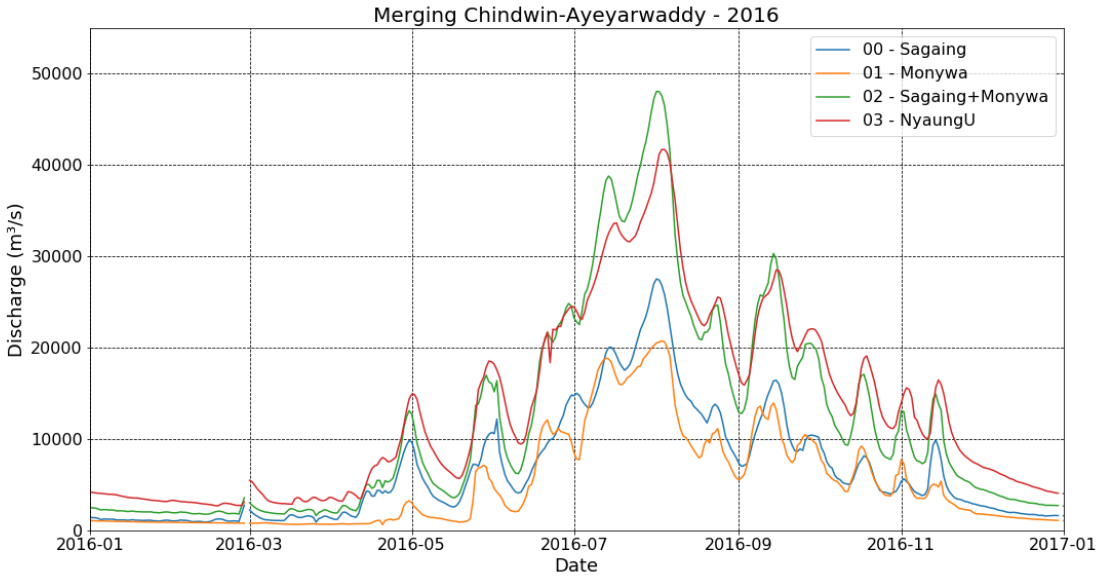

Figure 0-11 Merging of the Chindwin and the Upper Ayeyarwady River during a large flood in 2016

Appendix B Implementation of roughness

B.1 Simulated river cross-sections at gauging stations

A cross-section profile is determined from the DEM, by the total number of cells calculated for every HAND value. All cells in the DEM along the Ayeyarwady River are accumulated per altimeter till HAND value of 20 m. The averaged cross-sections are generated very 2 km of river, with a cell size of MERIT DEM data of 90 x 90 meter. For generating the cross-sections, the total number of cells within the river length of 2 km per HAND meter is multiplied by the cell size and then divided to the area. So, even with mid-channel bars, the river the generated averaged cross-section would have a flat surface of the riverbed. Because of the constant change of the riverbed and floodplain, the averaged cross-section displays the estimated river width per meter of HAND through time.

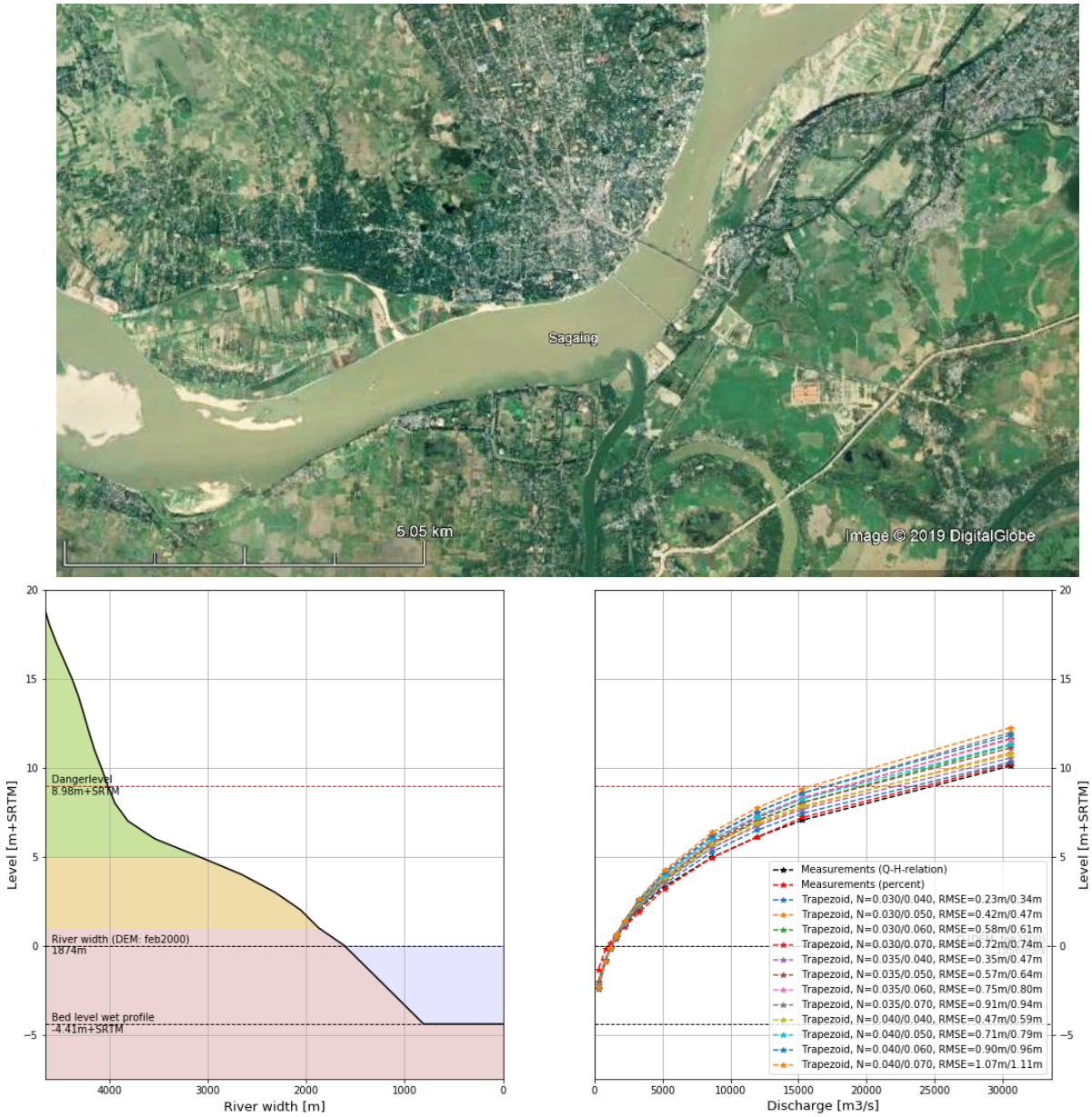

Figure 0-1 Satellite image of the river profile of the Ayeyarwady River at gauging station Sagaing on 30-12-2018 and the modelled cross-section with a trapezoidal shape with the derived Q-H relations for different Manning roughness coefficients

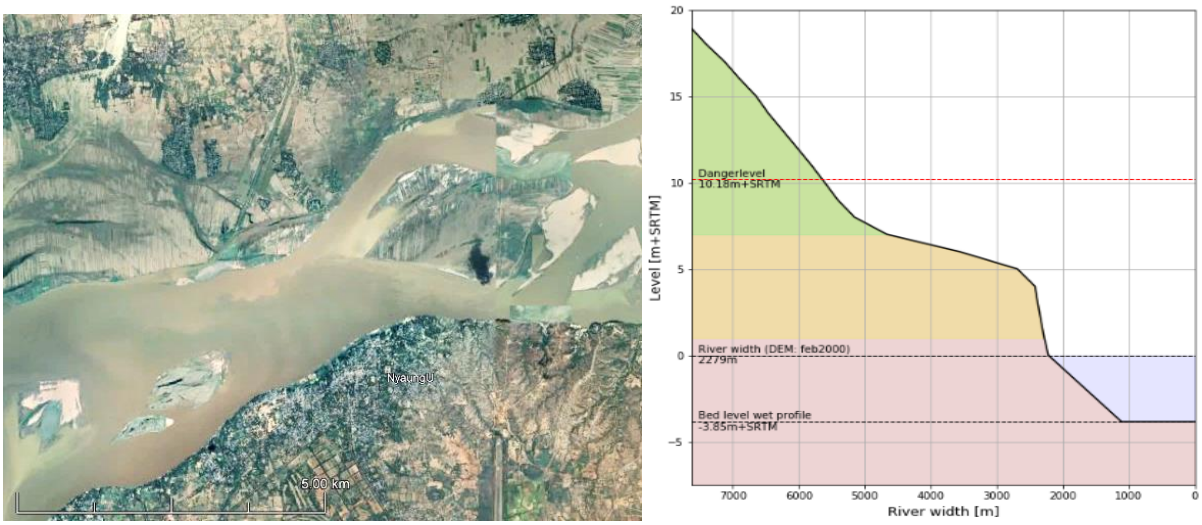

Figure 0-2 River profile of the Ayeyarwady River at gauging station NyaungU on 01-10-2018 and the modelled cross-section

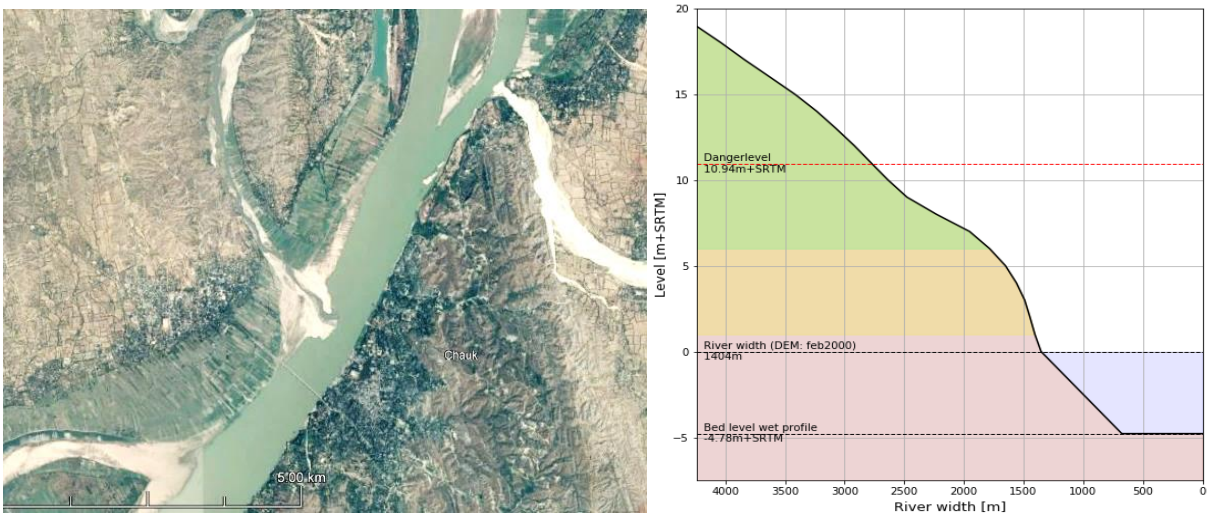

Figure 0-3 River profile of the Ayeyarwady River at gauging station Chauk on 03-02-2017 and the modelled cross-section

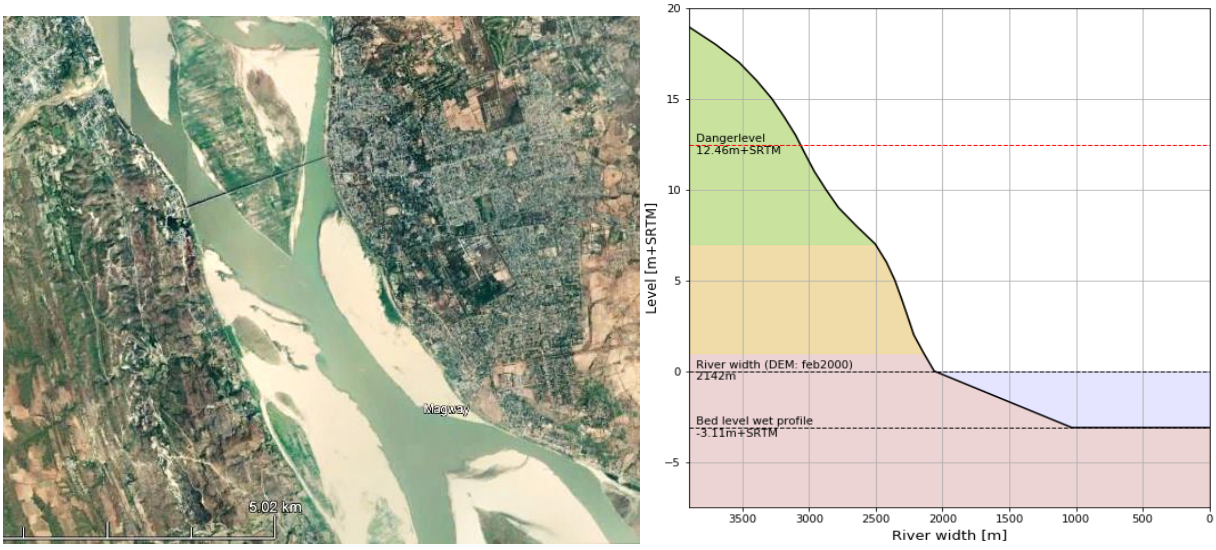

Figure 0-4 River profile of the Ayeyarwady River at gauging station Magway on 11-1-2018 and the modelled cross-section

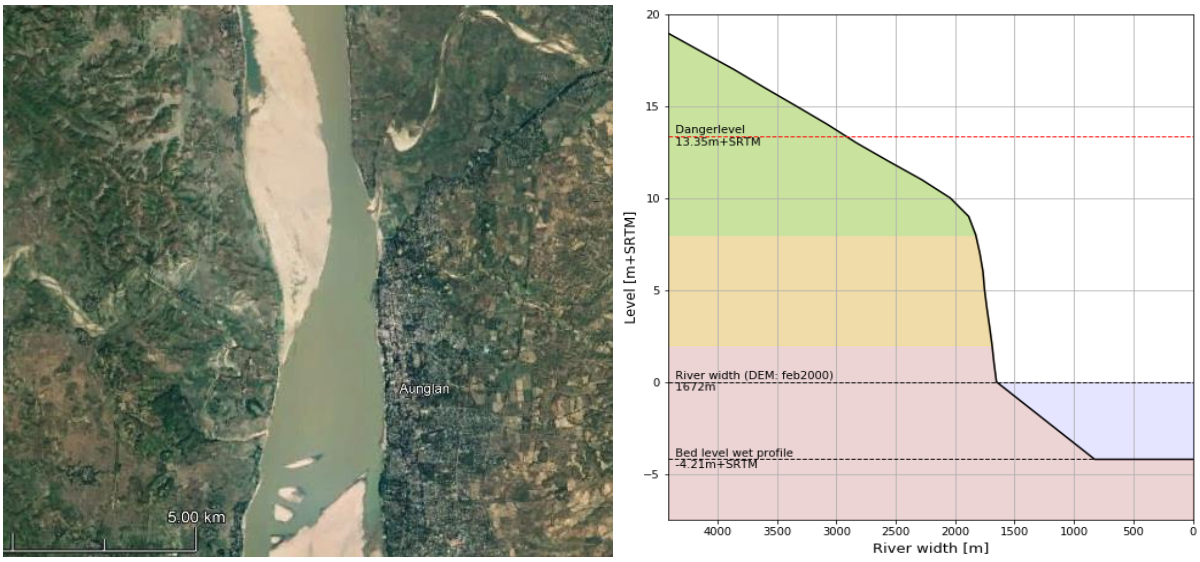

Figure 0-5 River profile of the Ayeyarwady River at gauging station Magway on 09-01-2017 and the modelled cross-section

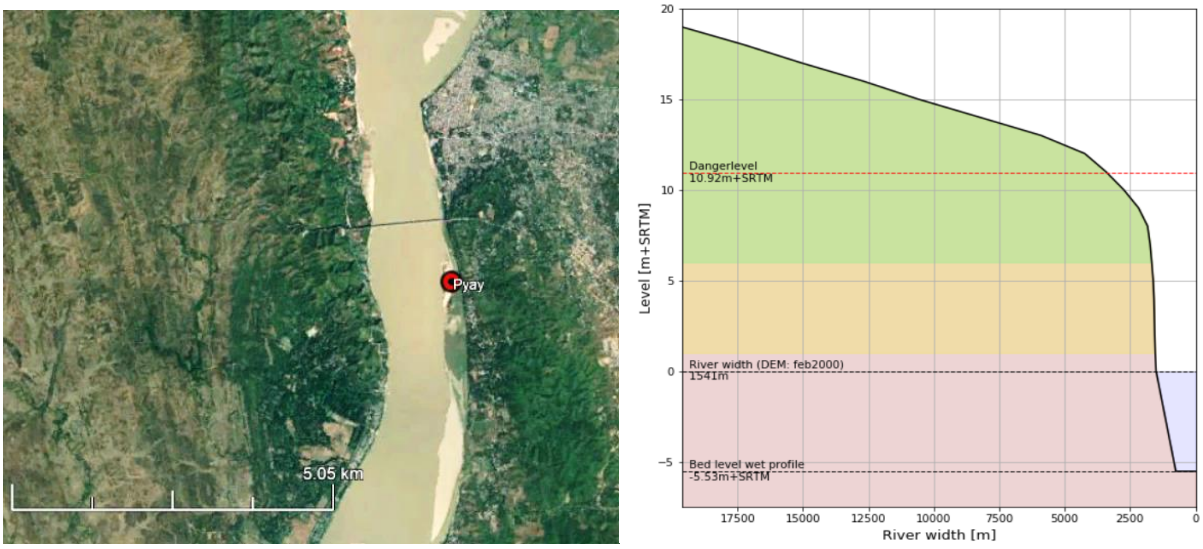

Figure 0-6 River profile of the Ayeyarwady River at gauging station Pyay on 18-012-2018 and the modelled cross-section

B.2 Floodplain Vegetation

Myanmar is historically seen a top rice producer. The main crop growth in Myanmar is still rice, which occupies over million acres each year. The agriculture sector in Myanmar accounts for 50% till 60% of Gross Domestic Product and supports upward of 70% of the labour force (Food and Agriculture Organisation of the United Nations, 2015). Typically, the main rice crop is sowed between May to early June, grows until September, and is mostly harvested during November with some regions trailing into December harvests (Torbick et al., 2017). There can exist some local variability, but the majority (>75%) of rice is produced during the main wet season in Myanmar. In 2006 rice was cultivated on 6.54 million ha comprising 4.90 million ha in the rainy season and 1.64 million ha in the dry season (Aquastat, 2011). In the dry season, a second rice crop can potentially be sowed during November with harvest by May the following year. Other crops as maize, potatoes, wheat and rotation crops can be grown outside of the main rice season.

Figure 0-7 Myanmar rice crop calendar (Food and Agriculture Organisation of the United Nations, 2015)

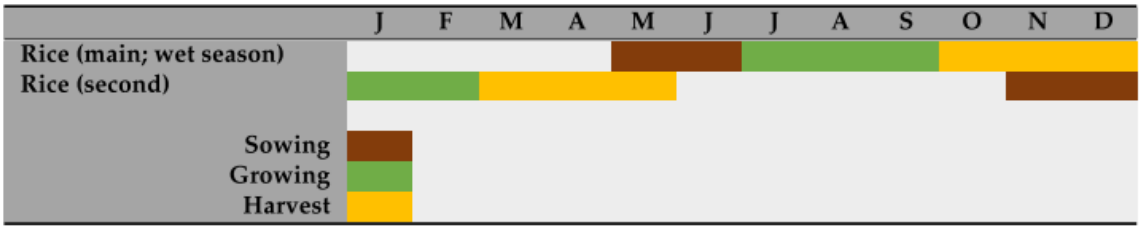

A land use cover map fusing Sentinel-1, Landsat-8 OLI, and PALSAR-2 were integrated and classified using a random forest algorithm. Time series phenological analyses of the dense Sentinel-1 data were then executed to assess rice information across all of Myanmar (Torbick et al., 2017). On this map, it is clearly variable that mainly rice is planted on the floodplains of the Ayeyarwady River during the wet season.

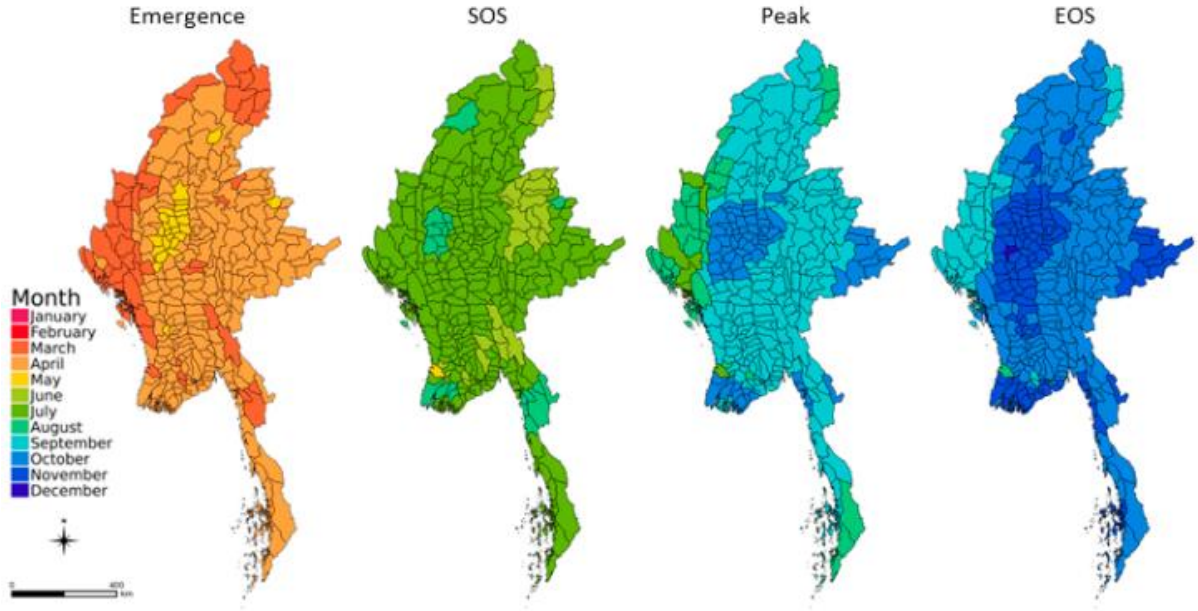

Figure 0-8 Rice crop calendar during the main wet season crop detected from Sentinel-1 showing mean A. Emergence, B. Start-of-season (SOS), C. peak and D. End-of-season (EOS) scaled to administrative units for Myanmar (Torbick et al., 2017)

Because of this the roughness of the floodplain depends on the height of rice during peak which is between 0.6-1.0 m. Therefore, Manning's roughness coefficient for mature row crops as floodplain vegetation is used.